The role of the pentose phosphate pathway in TMPyP4 resistance and the telomere uncapping response

Elizabeth Joan Andrew

Thesis submitted to Newcastle University for the degree of Doctor of Philosophy

September 2012

Institute for Ageing and Health
School of Biomedical Sciences
Newcastle University

Abstract

G-quadruplex stabilising ligands are of interest as potential anti-cancer drugs. G-quadruplexes are folded DNA structures which can form in guanine-rich regions of DNA or RNA, and stabilisation of these structures at telomeres can result in the inhibition of telomerase activity. In this thesis, *Saccharomyces cerevisiae* was used as a model to examine the *in vivo* cellular response to treatment with the G-quadruplex stabilising ligand TMPyP4. The findings indicate that the pentose phosphate pathway (PPP) is key for resistance to TMPyP4, since the absence of PPP genes resulted in increased sensitivity to treatment with the ligand. However, the TMPyP4-sensitivity exhibited by *ppp*Δ strains is most likely due to oxidative stress caused by the photosensitivity of the porphyrin. There are also potential links between PPP activity, the response to uncapped telomeres and the DNA damage response (DDR). The *cdc13-1* mutant strain, in which the telomere binding protein Cdc13 is defective, was used to explore these connections. Here, I demonstrate that deletion of key PPP genes results in suppression of the temperature-sensitive growth phenotype of *cdc13-1*. In addition, the activity of the enzyme which catalyses the initial step of the oxidative phase of the PPP, Zwf1, increases in *cdc13-1* strains. Studies of Zwf1 activity in strains arrested in late anaphase and G_1, however, suggest that the increase in Zwf1 activity is due to the phase of the cell cycle in which the strains are arrested, rather than the DDR. The work described here demonstrates that the PPP is intrinsically linked to the response to a variety of cellular stresses. Due to its role in the Warburg effect, a metabolic shift observed in tumour cells, examination of PPP function is important not only for the study of normal tissues but also immortal cancer cells, and lessons in budding yeast can lead to important insights.

Dedication

For my grandad, Bernard Codd (1932 – 2006).

Acknowledgements

I have been most fortunate in the past four years to have had the opportunity to work alongside some of the most interesting, dedicated, fun, intelligent and accommodating people I have ever known. And so I would first like to thank all of the members of the Lydall lab, past and present, for their companionship and encouragement throughout my PhD. Particular thanks are extended to Alan Leake for his assistance in the lab through media and plate preparations, and cleaning all of the glassware I managed to get through over the course of my project!

The genome-wide screens detailed in Chapter 3 were carried out in collaboration with Stephanie Merchan and Conor Lawless of the Lydall Lab, and Darren Wilkinson of the School of Mathematics and Statistics at Newcastle University. I would like to thank them all for their input into this work. I would also like to thank Peter Banks for his assistance with the robotic procedures associated with the screens, and Pharminox Ltd for supplying the RHPS4.

Obviously enormous thanks go to my supervisor Professor David Lydall, who has been an incredible source of support, wisdom and scientific knowledge over the past four years. I am extremely grateful that he gave me the opportunity to carry out my PhD in his lab and for his continued encouragement as I finish my project and work towards my future career. I would also like to thank Dr. Daryl Shanley for his advice and support as my secondary supervisor, and for his guidance with my Masters.

Thanks also go to all of my friends, both in Newcastle and further afield, to my brother, Ben, and to my boyfriend Tim, who has been superbly patient and supportive. Lastly I would like to thank my parents for their phenomenal, unwavering and unending support. I could not have achieved this without them. Thank you.

Table of Contents

List of figures

List of tables

Abbreviations

bp – base pair

C-rich – cytosine-rich

CSM – complete synthetic medium

DAPI – 4’,6-diamidino-2-phenylindole

DDR – DNA damage response

DHE – dihydroethidium

DSB – double strand break

FD – fitness differential

FFD – final fitness differential

GO – gene ontology

G-rich – guanine-rich

HU – hydroxyurea

HR – homologous recombination

kb – kilobases

MDP – maximum doubling potential

MDR – maximum doubling rate

NHEJ – non-homologous end joining

ORF – open reading frame

PPP – pentose phosphate pathway

PQS – putative quadruplex sequence

QFA – quantitative fitness analysis

ROS – reactive oxygen species

rpm – revolutions per minute

SDL – single deletion library

SGD – *Saccharomyces* genome database

ssDNA – single-stranded DNA

YEPD – yeast extract/peptone/dextrose

yfg – your favourite gene

YMC – yeast metabolic cycle

Budding yeast nomenclature

TKL1	Wild type gene
*tkl1*Δ	Null allele
Tkl1	Protein encoded by wild type gene
cdc13-1	Mutant allele
*ppp*Δ	Null allele of pentose phosphate pathway gene

1 Introduction

1.1 Telomeres

1.1.1 The structure and function of telomeres

The linear nature of eukaryotic chromosomes can result in replication and degradation issues in the terminal regions. These problems are circumvented by the presence of telomeres, which are found at the ends of all linear chromosomes and which protect against damage to genomic integrity (Blackburn, 1991). Telomeres are nucleoprotein structures, composed of both DNA and proteins, both of which play important roles in the protection of genomic stability. Telomeric DNA acts as a buffer, protecting coding DNA further away from the end of the chromosome from degradation (Blackburn, 1991). This degradation is a phenomenon called the end replication problem, the result of the fallibility of the DNA replication machinery, which occurs every time the cell undergoes replication and division (Olovnikov, 1973; Watson, 1972; Olovnikov, 1971).

The proteins which bind to or interact with telomeric DNA aid a second function of telomeres: the prevention of recognition of the ends of chromosomes as double strand breaks (DSBs) (di Fagagna et al., 2004; Nugent et al., 1998). The resemblance of the terminal regions of linear chromosomes to DSBs means that without the protection afforded by telomere binding proteins, specific DNA damage responses and double strand break repair processes can be activated. Homologous recombination (HR) repairs DSBs by using similar or identical DNA, usually a sister chromatid, as a template for repair (Kim et al., 2005; Frank-Vaillant and Marcand, 2002; Szostak et al., 1983). Non-homologous end joining (NHEJ), on the other hand, does not require a homologous template to repair the break and instead carries out the repair by directly ligating the broken ends together (Kim et al., 2005; Frank-Vaillant and Marcand, 2002; Szostak et al., 1983). Since the ends of linear chromosomes resemble double strand breaks, many of the same components are involved in both the repair of DSBs and the processing of the telomere end (Nugent et al., 1998).

Whereas prokaryotes commonly encode their genome on circular chromosomes (and thereby evade the end replication problem), the majority of eukaryotic chromosomes are linear. The basic telomere function is conserved between most eukaryotic species; however, there is variation between species in the composition of the DNA element of the structure and the proteins associated with it (Figure 1.1). The multiple repeat sequences of which all telomeres are composed are guanine-rich, and most telomeres end in a single-stranded 3' overhang (Henderson and Blackburn, 1989). However, significant variation is present between species in sequence structure, repeat number and the length of the telomere. In *Homo sapiens* telomeres are composed of the hexameric DNA sequence $TTAGGG_{(n)}$, a sequence conserved among vertebrates (Meyne et al., 1989; Moyzis et al., 1988). In yeast, such as the budding yeast *Saccharomyces cerevisiae*, the telomere is formed instead from multiple $TG_{1\text{-}3}$ repeats (Greider and Blackburn, 1985; Szostak and Blackburn, 1982). Not all eukaryotic species use these repeating elements as telomeres; the fruit fly *Drosophila melanogaster* instead uses the retrotransposons HeT-A and TART to combat NHEJ and chromosomal instability (Biessmann and Mason, 1994; Levis et al., 1993; Biessmann et al., 1992).

The 3' overhang found at the end of most eukaryotic telomeres provides a substrate for telomerase binding, which may also have a role in recombination-dependent telomere maintenance (Wang and Blackburn, 1997; Lingner and Cech, 1996; Henderson and Blackburn, 1989). In some species, this 3' overhang can fold back on itself and invade the corresponding strand to create a loop. This loop is found at the termini of telomeres of a broad range of species, such as *Pisum sativum* (peas), *Trypanosoma brucei* (a flagellate protozoan) and humans, and is known as the 't-loop' (Cesare et al., 2003; Muñoz-Jordán et al., 2001; Griffith et al., 1999). It is thought that this loop structure provides an extra level of protection and that this protection can be increased further by the presence of structures known as 'd-loops' (Griffith et al., 1999).

As well as differences in telomeric structure, there is also interspecies variation in telomere length. For instance, telomeres in humans can be very long (from around 15kb at birth) (Shay and Wright, 2005). In contrast, yeast telomeres are amongst the shortest found, at 300±75bp (Wellinger et al., 1993). The length of the 3' overhang

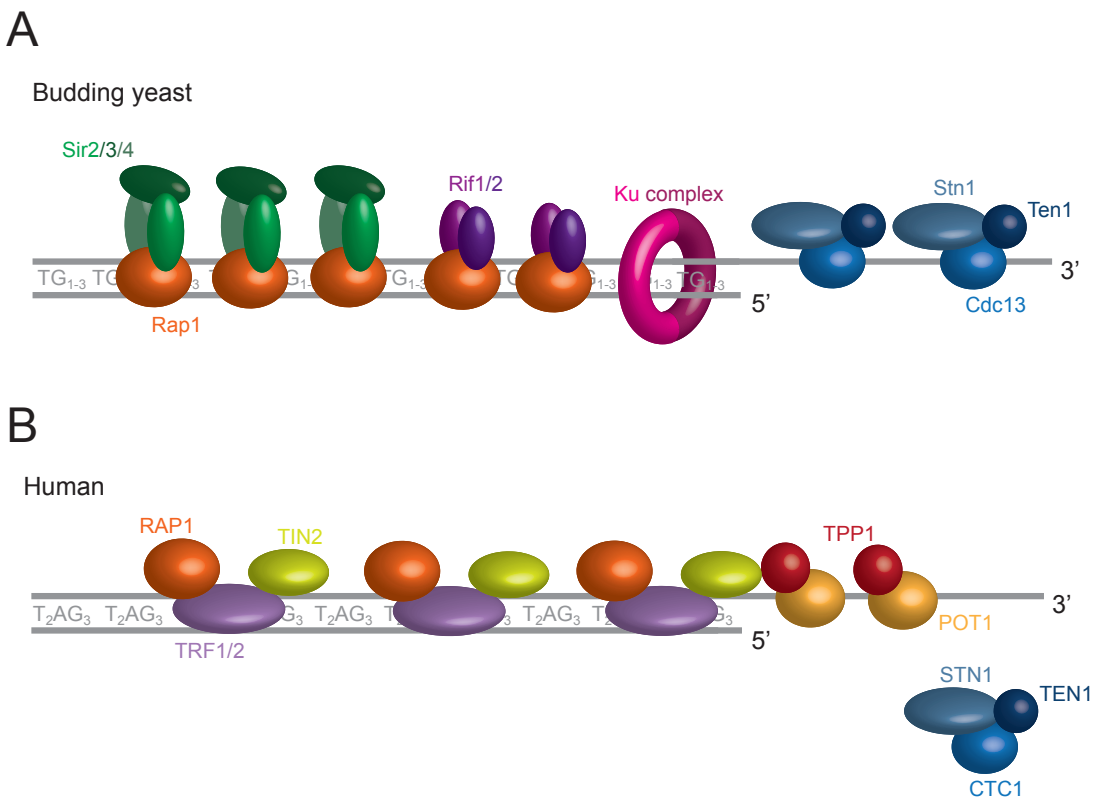

Figure 1.1: The structure of yeast and human telomeres
(a) The nucleoprotein structure of telomeres in yeast. The 3' overhang at the termini of chromosomes is bound by the CST complex; Cdc13 and the Cdc13-interacting factors Ten1 and Stn1. The heterodimeric Ku complex (Yku70/80) interacts with the double-stranded region at the terminus of the telomere. Rap1 binds to double-stranded telomeric sequences and interacts with Rif1 and Rif2, which regulate telomere length. Rap1 also recruits the Sir2, Sir3 and Sir4 proteins present in the subtelomeric region. **(b)** The nucleoprotein structure of telomeres in humans. Three proteins resembling those in the yeast CST complex (CTC1, STN1 and TEN1) form a complex which associates with a fraction of telomeres. The 3' overhang at the terminus of chromosomes is bound by POT1 and TPP1. The double stranded region of human telomeres is bound by TRF1 and TRF2. TRF1 recruits TIN2 and TRF2 recruits Rap1 to the telomere, and TIN1 interacts with TPP1, tethering the single-stranded and double-stranded regions together and forming the six-protein Shelterin complex. Colour and shape of the proteins in the figure represents homology (if any) between the yeast and human forms. Adapted from Jain & Cooper (2010) and Auriche et al. (2008).

at the end of the telomere and regulation of overhang length also varies. In yeast, the length of the 3' overhang is affected by the cell cycle and in S phase it can stretch from anywhere between 50 bp and 100 bp in length (Wellinger et al., 1993). In mammalian systems, the 3' overhang is present throughout the cell cycle (Makarov et al., 1997; McElligott and Wellinger, 1997).

Adjacent to telomeric repeats at the ends of most (but not all) *S. cerevisiae* yeast chromosomes are regions known as Y' elements (Walmsley et al., 1984; Chan and Tye, 1983). These elements are formed from 6500 bp repeat sequences, and up to 4 tandem copies of these repeats make up the element. Another subtelomeric repeat, the X sequence, is found at the end of all *S. cerevisiae* chromosomes. This has little sequence similarity or homology with the Y' element. Variation between Y' element number and X element length is demonstrated between chromosome ends. There can also be variable numbers of telomeric repeats between Y' and X elements, and between tandem copies of the Y' element (Louis and Haber, 1991; Walmsley et al., 1984). The Y' and X elements both contain ARSs (autonomously replicating sequences), which most likely function as chromosomal replication origins (Chan and Tye, 1983). The replication origins found in Y' and X elements are densely packed together (around 6.5 kb apart), indicating potential co-regulation, and perhaps a role in ensuring the initiation of replication at telomeres (Chan and Tye, 1983). Within the *Saccharomyces* genus, the Y' elements are conserved; however, between species the hybridisation pattern of the telomeric sequences differs. Nevertheless, the closely related species can still mate and generate viable spores, suggesting that this change in telomeric sequence does not affect the conservation of telomeric function (Chan and Tye, 1983).

1.1.2 Telomerase and the elongation of telomeres

The 'end replication problem' refers to the shortening of the chromosome upon DNA replication (Figure 1.2). It was independently described by Watson (Watson, 1972) and Olovnikov (Olovnikov, 1973; Olovnikov, 1971) to explain the phenomenon of DNA loss upon the replication of linear chromosomes as a result of the fallibility of the DNA replication machinery. During DNA replication, a 5' to 3' polymerase is employed to generate newly synthesised strands of DNA and this

polymerase, as indicated, can only operate in the 5' to 3' direction. This means that one strand of the chromosome can be replicated without disruption (known as the leading strand) and using just one primer. However, replication of the complementary strand can only be carried out in smaller sections, producing segments of DNA called Okazaki fragments. This is known as lagging strand synthesis and it requires multiple primers bound to the parent strand.

Following replication, the primers are removed and through the action of the DNA polymerase, the gaps are filled in. However, removal of the terminal primer at the end of the lagging strand results in a 5' gap and a 3' overhang. In the absence of telomerase, the result is a shortening of the chromosome which occurs each time the DNA replicates and the cell divides. Since no primer removal occurs at the terminal end of the leading strand, the chromosome end is left blunt. In order for telomere protection through the binding of capping proteins to occur, a 3' overhang needs to be present; therefore, this blunt end requires processing (Figure 1.2). Without capping proteins, the end of the chromosome would be recognised as a double strand break (DSB) and initiate a DNA damage response (di Fagagna et al., 2003). To combat this, the C-rich strand at the blunt end is degraded by nucleases, such as the MRX (Mre11-Rad50-Xrs2) complex in budding yeast and the MRN (Mre11-Rad50-Nbs1) complex in humans, leaving a G-rich overhang which can then be bound by ssDNA telomere binding proteins (Faure et al., 2010).

The shortening which occurs due to the end replication problem can be circumvented by the action of the enzyme telomerase. The 3' telomeric overhang is bound by capping proteins such as Cdc13 in yeast and the TRF complex in humans (Smogorzewska and de Lange, 2004; Hughes et al., 2000; Lin and Zakian, 1996; Nugent et al., 1996). These proteins recruit telomerase to the ssDNA overhang and through the action of the reverse transcriptase, the 3' strand is elongated. This means that an additional primer can bind to the elongated 3' overhang, facilitating the action of the 5' to 3' polymerase, which fills in the gap on the lagging strand and prevents the loss of DNA due to the end replication problem. A 3' overhang still remains, which is bound by telomere capping proteins and prevents recognition of the chromosome end as a DSB.

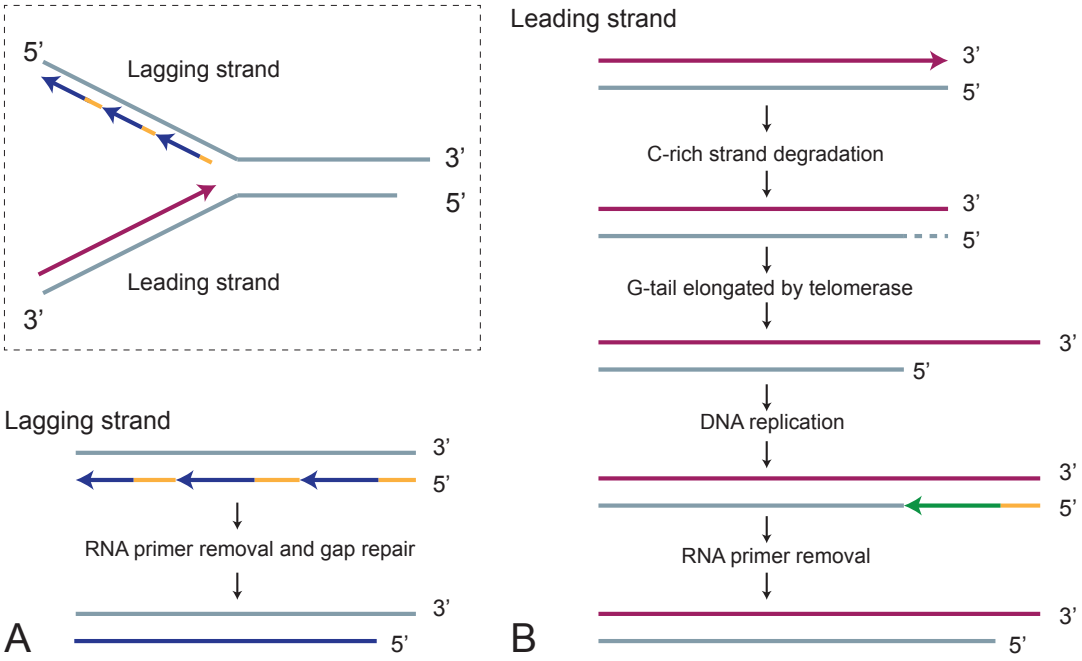

Figure 1.2: The end replication problem and 3’ overhang generation
(a) Following DNA replication the removal of RNA primers leaves a 5’ gap at the end of the lagging strand. **(b)** The blunt end which results from leading strand synthesis is processed to generate the 3’ overhang necessary for telomere protection. Adapted from (Vega et al., 2003)

Composed of several subunits, the highly conserved reverse transcriptase telomerase uses an RNA template complementary to the nascent telomeric repeat sequence to elongate the 3' overhang at the terminus of the telomere (Feng et al., 1995). In *S. cerevisiae*, this essential RNA template is called *TLC1*. *TLC1* RNA is AC-rich, producing a TG-rich DNA elongation (Singer and Gottschling, 1994). The other yeast telomerase subunits are Est1, Est2 and Est3. *EST2* encodes the subunit of telomerase which provides reverse transcriptase activity and along with *TLC1* forms the catalytic core of telomerase (Lingner et al., 1997b). Est1 and Est3 on the other hand are dispensable for telomerase catalytic activity *in vitro* and instead play regulatory roles. For instance, Est1 provides a link between the 3' end of ssDNA and the catalytic core of telomerase, and loss of Est1 leads to a progressive reduction in telomere length (Qi and Zakian, 2000; Evans and Lundblad, 1999; Lingner et al., 1997a; Lundblad and Szostak, 1989). This link occurs through binding of Est1 to the ssDNA binding protein Cdc13 (also known as Est4), an interaction which is regulated negatively by Stn1 and positively by the Ku complex (Grandin et al., 2000; Qi and Zakian, 2000; Evans and Lundblad, 1999). The interaction between Est1 and Cdc13 is essential for telomerase activity, as it recruits telomerase to chromosomal ends. The role of Est3 in the function of telomerase is yet to be defined, as it is not required for catalysis *in vitro*; however, *in vivo* it is required for telomere replication (Lingner et al., 1997a).

There is homology between yeast and human telomerase subunits; for example, the human orthologue of the RNA template subunit *TLC1* is known as TERC, or hTR (Feng et al., 1995). Est2, which has reverse transcriptase activity, is similar to TERT (or hTERT) in humans (Nakamura et al., 1997). hEST1a and hEST1b are Est1-like proteins found in humans which have also been shown to associate with telomeres (Reichenbach et al., 2003; Snow et al., 2003). However, no homologue of Est3 has yet been found. Telomerase in humans is only expressed in gametes, stem cells, and stem cell niches, and not in somatic cells, which have significantly shorter telomeres (Kim et al., 1994; De Lange et al., 1990). Despite the absence of telomerase in somatic human cells, a lack of correctly functioning telomerase in humans is associated with the disorder known as Cri du chat, which most commonly occurs following mutation of the catalytic subunit TERT (Zhang et al., 2003; Bryce et al., 2000; Niebuhr, 1978).

Telomerase activity is regulated by interactions with the telomere binding proteins. Through interactions with the Est1 subunit, the *S. cerevisiae* ssDNA binding protein Cdc13 mediates recruitment of telomerase to the 3' overhang at the terminus of the telomere (Hughes et al., 2000; Qi and Zakian, 2000; Lin and Zakian, 1996; Nugent et al., 1996). Cdc13 also mediates the recruitment of telomerase to double strand breaks (DSBs) as part of its role in a process called 'telomere healing' (Zhang and Durocher, 2010; Bianchi et al., 2004). This recruitment results in the production of a *de novo* telomere within the chromosome, and can lead to a loss of coding DNA in the distal arm of the chromosome (Bianchi et al., 2004). Due to the loss of genomic DNA, this method of double-strand break repair is extreme, and is possibly an effort to combat a double strand break which cannot be repaired by the usual methods. Telomerase activity can also be regulated by the Ku complex. Ku interacts with the *TLC1* subunit of telomerase throughout the cell cycle, an interaction which is lessened following telomere replication (Fisher et al., 2004; Stellwagen et al., 2003). In the absence of the Ku complex, the associations of Est2 and Est1 with the telomere are affected, and so a model is proposed where the Ku complex recruits inactive telomerase to the telomere in G_1 and promotes its activity late in S phase (Fisher et al., 2004).

1.1.3 The role of telomere binding proteins

Telomeres are bound by multiple binding proteins to form the nucleoprotein structure. These proteins have numerous roles in the protection of the telomere, telomere length maintenance and telomere positioning. In addition to its role in recruitment of telomerase, Cdc13 is also involved in preventing telomere degradation by exonucleases such as Exo1 (Zubko et al., 2004; Maringele and Lydall, 2002). In the absence of telomere capping, this degradation leads to activation of DNA damage response pathways and, ultimately, cell cycle arrest (Garvik et al., 1995). The capping of telomeres by Cdc13 is regulated by interactions with Stn1 and Ten1, which promote and prevent Cdc13 binding to the telomere respectively, and the three form the CST complex (Petreaca et al., 2007; Petreaca et al., 2006; Chandra et al., 2001; Grandin et al., 2001; Grandin et al., 2000).

Cdc13, along with Ten1 and the telomere capping protein Stn1, forms part of the CST complex (Grandin et al., 2000). Loss of Cdc13 is lethal; however, overexpression of *STN1* can provide telomere capping in the absence of Cdc13 (Petreaca et al., 2007; Petreaca et al., 2006). Stn1 and Ten1 also play essential roles in the regulation of telomere length. Stn1 negatively regulates telomerase activity by competing with Est1 for binding with Cdc13 (Chandra et al., 2001). Ten1, on the other hand, promotes the interaction between Cdc13 and telomerase, potentially through disrupting the efforts of Stn1 to displace Est1 (Chandra et al., 2001; Grandin et al., 2001). The N-terminus of Cdc13 is essential for the activity of the capping protein, as it interacts with other binding proteins (Hughes et al., 2000). Telomere capping also occurs through the binding of the Ku complex. This heterodimeric ring, which is composed of Yku70 and Yku80, binds to the double stranded region distal to the terminus of the chromosome (Milne et al., 1996). The Ku complex is involved in telomere length homeostasis, nuclear localisation of telomeres and telomeric silencing via interactions with Sir proteins (Martin et al., 1999; Boulton and Jackson, 1998; Boulton and Jackson, 1996a; Boulton and Jackson, 1996b). As mentioned previously in the chapter, the Ku complex interacts with the telomerase subunit *TLC1* throughout the cell cycle (Fisher et al., 2004; Stellwagen et al., 2003). The complex also potentially regulates the recruitment of Est1 and Est2 to the telomere, and subsequently the activity of telomerase in S phase (Fisher et al., 2004; Stellwagen et al., 2003). Like Cdc13, the Ku complex also plays a role in the repair of double strand breaks in relocating to the site of DSBs and promoting repair through non-homologous-end-joining (NHEJ) (Smith and Jackson, 1999; Boulton and Jackson, 1996a; Boulton and Jackson, 1996b; Mages et al., 1996). In humans, the six-protein complex Shelterin also protects chromosomal ends against DNA damage response activation and activity (Palm and de Lange, 2008; De Lange, 2005). There is little conservation of the Shelterin subunits in yeast; the only subunit which is present in *S. cerevisiae* is Rap1, which binds telomeric DNA directly, instead of depending on TRF2 for its telomeric localisation (Li and De Lange, 2003; Li et al., 2000) (Figure 1.1). In yeast, Rap1 associates with Rif1 and Rif2 to form a complex which binds telomeric double-stranded DNA repeats and inhibits NHEJ and telomere elongation by telomerase (Marcand et al., 2008; Levy and Blackburn, 2004; Marcand et al., 1997).

Homologues of both Cdc13 and the Ku complex are present at the telomeres in humans. POT1 encodes the functional homologue of Cdc13, with both proteins containing the OB-fold domains important for binding ssDNA and interacting with other binding proteins (Theobald and Wuttke, 2004). POT1 and Cdc13 play similar roles in capping the telomere and protecting chromosomal ends; however, a link between POT1 and the recruitment of telomerase in humans is less well known. The presence of POT1 alone does not increase telomerase activity, although in the absence of POT1, telomere elongation is reduced (Colgin et al., 2003). And the processivity of telomerase is increased when POT1 binds to TPP1, though the method by which this occurs is unclear (Wang et al., 2007). The Ku complex is also conserved in humans. The human form of the Ku complex, which is composed of the subunits Ku70 and Ku80 (equivalent to Yku70 and Yku80 in yeast respectively), plays similar roles to its yeast counterpart, primarily facilitating NHEJ (Smith and Jackson, 1999). DSBs in mammalian systems are predominantly repaired using this method.

Due to their importance in the protection of telomeres, experiments involving Cdc13 and the Ku complex can reveal aspects of telomere regulation, protection and function, and the response that occurs when capping is defective. However, as mentioned above, *CDC13* is essential and its deletion causes the rapid accumulation of ssDNA at telomeres, cell cycle arrest and cell death (Zubko et al., 2004; Garvik et al., 1995; Lydall and Weinert, 1995). Nevertheless, its function and role in telomere capping can be studied through the use of the temperature-sensitive mutant *cdc13-1*. This mutant form is deficient in capping at temperatures over 26^{o}C, though it can still recruit telomerase (Nugent et al., 1996; Garvik et al., 1995). Telomere uncapping in *cdc13-1* leads to cell cycle arrest in G_2-M. The role of the Ku complex at the telomere can also be studied using the temperature-sensitive null mutant *yku70*Δ (Barnes and Rio, 1997; Feldmann et al., 1996). In contrast to *cdc13-1*, telomere uncapping occurs at the higher temperature of around 36^{o}C in *yku70*Δ strains. Uncapping brought about by temperature sensitivity in both strains results in the initiation of DNA damage responses. Using a combination of techniques, such as gene deletion and overexpression studies, the response to telomere uncapping can be studied in these strains.

1.1.4 Telomeres, DSBs and the DNA damage response (DDR)

The dysfunction or loss of telomeric binding proteins leads to the initiation of the DNA damage response (DDR). Uncapping caused by loss of Cdc13 function at telomeres or the absence of Yku70 leads to exposure of the terminus of the chromosome This is recognised as a double strand break (DSB), and the response to uncapped telomeres resembles the response to DSBs with a few key exceptions. Following the detection of a DSB, the MRX (Mre11-Rad50-Xrs1) complex binds to and processes the break, generating a 3' overhang (D'Amours and Jackson, 2002). However, if the MRX complex is absent ssDNA may still be generated, though this generation is delayed (Diede and Gottschling, 2001). The 3' ssDNA is possibly generated in the absence of the MRX complex by Exo1, a 5' to 3' exonuclease. The 3' overhang at the break is bound by the RPA complex and recognised by ATR (in humans) or Mec1 and Ddc2 (in yeast), which recruit HR proteins to the break (Zou and Elledge, 2003). The Ddc1-Rad17-Mec3 complex (the 9-1-1 complex in humans) is loaded onto DNA by the Rad24/Rfc2-5 (replication factor C-like complex with Rad24) clamp loader and enhances Mec1-dependent checkpoint activation (Majka et al., 2006). Rad9, along with the activities of Rad53 and Chk1, transmits the DNA damage signal which results in cell cycle arrest at G_2-M (Sweeney et al., 2005; Gilbert et al., 2001).

The response to telomere uncapping differs from the response to double strand breaks in that MRX does not play a role in resection of the C-rich strand to generate a 3' overhang; rather, the MRX complex may play more of a protective role in telomere capping (Foster et al., 2006; Tsukamoto et al., 2001). Following a shift of *cdc13-1* strains to restrictive temperatures, the uncapped telomere is detected as a DSB with a short 3' overhang (Figure 1.3). The initial step of the response to uncapping is the loading of the Ddc1-Mec3-Rad17 sliding clamp by Rad24/Rfc2-5 (Green et al., 2000; Venclovas and Thelen, 2000). This clamp, along with a helicase, processes the telomere, producing a substrate which is recognised by the Mec1/Rad53/Dun1-dependent checkpoint pathway (Maringele and Lydall, 2002). Exo1 (possibly along with another, unknown, nucleases) processes the telomere further still, leaving a 3' overhang (Maringele and Lydall, 2002). This long ssDNA overhang initiates the Rad9/Mec1/Chk1- and Pds1-dependent checkpoint pathway (Maringele and Lydall, 2002). These two checkpoint pathways initiate a signalling

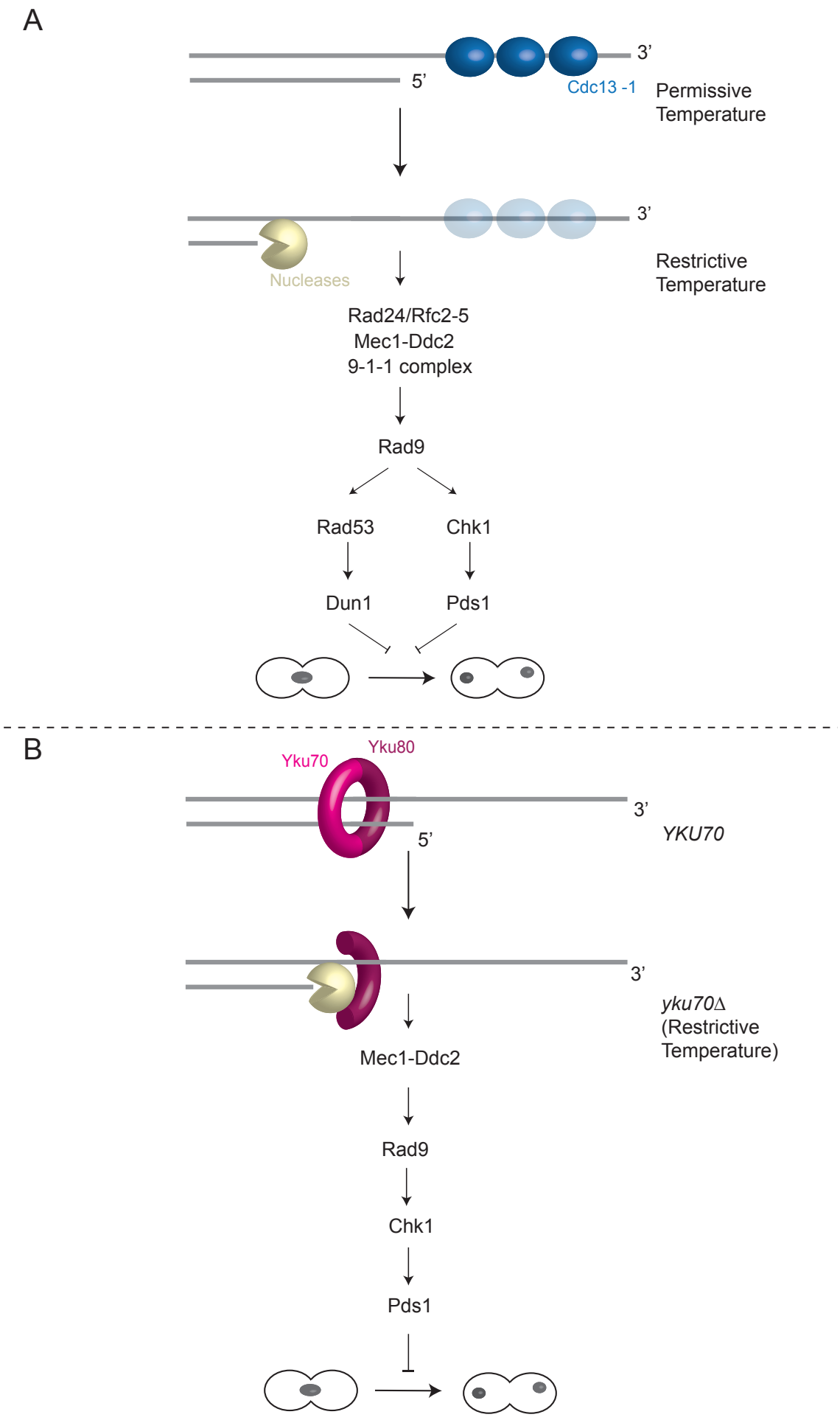
A
3'
5'
Cdc13 -1
Permissive Temperature
3'
Nucleases
Restrictive Temperature
Rad24/Rfc2-5
Mec1-Ddc2
9-1-1 complex
Rad9
Rad53
Chk1
Dun1
Pds1
B
Yku70
Yku80
3'
5'
YKU70
3'
yku70Δ
(Restrictive Temperature)
Mec1-Ddc2
Rad9
Chk1
Pds1

Figure 1.3: Telomere uncapping and the DNA damage response

(a) Following a shift to restrictive temperature, telomere capping in *cdc13-1* strains is defective and leads to the generation of a long single-stranded 3'overhang. The presence of this overhang initiates the Mec/Rad53/Dun1-dependent and Rad9/Mec1/Chk1- and Pds1-dependent checkpoint pathways and leads to cell cycle arrest. **(b)** A shift to restrictive temperature in *yku70*Δ strains leads to the generation of a 3' overhang, the activation of the Rad9/Mec1/Chk1- and Pds1-dependent checkpoint pathway and cell cycle arrest (Maringele and Lydall, 2002).

cascade, prompting cell cycle arrest in G_2-M.

In *yku70*Δ strains the response to telomere uncapping due to a dysfunctional Ku complex involves similar processes – the uncapped telomere is recognised as a DSB, the 3' ssDNA overhang is extended and the 5' strand is processed by the exonuclease Exo1 (Maringele and Lydall, 2002). However, there are differences between the response to telomere uncapping in *cdc13-1* strains and the response to uncapping in *yku70*Δ strains. For instance, following telomere uncapping in *yku70*Δ strains, Rad24 and the Ddc1/Mec3/Rad17 sliding clamp are not required for Exo1 recruitment and the Mec1/Rad53/Dun1-dependent checkpoint pathway is not initiated, although it has been shown that Rad53 is activated at 37^{o}C at very low levels in *yku80*Δ mutants (Maringele and Lydall, 2002; Teo and Jackson, 2001). However, Exo1 is still recruited to the uncapped telomere and the 3' overhang produced by the activity of the exonuclease activates the Rad9/Mec1/Chk1- and Pds1-dependent pathway (Figure 1.3) (Maringele and Lydall, 2002). In addition to regulating the transcription of downstream effectors, the DNA damage response also regulates activity at the uncapped telomere. Exo1 activity at unprotected telomeres is inhibited by its checkpoint-dependent phosphorylation, mediated by Rad17, Rad24, Rad9, Rad23 and Mec1 (Morin et al., 2008). This potentially limits ssDNA production at uncapped telomeres, which therefore limits DNA damage checkpoint activation and so acts as a negative feedback loop (Morin et al., 2008).

1.1.5 The DDR and nucleotide production

Downstream of the Rad53 and Chk1 pathways are various effectors of the DNA damage response and it is the change in activity of these effectors which results in an arrest in cell division. The downstream DNA damage response is widespread and varied, and can affect the transcription of a number of genes. Some of the effectors of Dun1 and Pds1 include transcription factors and transcriptional repressors, which regulate the genome-wide transcriptional response to telomere uncapping. For instance, activation of Dun1 leads to an alteration in ribonucleotide reductase (RNR) activity through a variety of pathways and processes (Elledge et al., 2005; Reichard, 1988). Upon activation as part of the DNA damage response, Dun1 phosphorylates the transcriptional repressor Crt1, which prevents the transcription of genes that

encode the RNR subunits (Huang et al., 1998; Huang and Elledge, 1997; Zhou and Elledge, 1993). This targets the transcriptional repressor for degradation and allows expression of *RNR2*, *RNR3* and *RNR4*, and leads to an increase in RNR transcript concentration (Fu et al., 2008).

RNR activity is also regulated by Dun1 via the degradation of Sml1 (Zhao and Rothstein, 2002). Sml1 binds to the large subunit of ribonucleotide reductase, Rnr1, and suppresses activity of the enzyme (Zhao et al., 2000; Chabes et al., 1999; Zhao et al., 1998). Dun1 phosphorylates Sml1, targeting it for degradation and allowing RNR to catalyse the conversion of ribonucleotides to the deoxyribonucleotides, which are in turn used in the synthesis of DNA. In addition to transcriptional changes and degradation of inhibitors, RNR activity is also promoted through the redistribution of Rnr2 and Rnr4, which move from the nucleus to the cytoplasm (An et al., 2006). This redistribution is mediated by the Mec1/Rad53/Dun1 checkpoint kinase pathway and occurs in response to DNA damage, including when *cdc13-1* cells are shifted to non-permissive temperatures (Yao et al., 2003). Therefore, as part of the DNA damage response there is a robust stimulation of RNR production and activity via the increased expression of RNR subunits and the removal of suppression by Sml1.

1.1.6 Longevity and cancer

A lack of telomerase activity in cells, either due to mutation or lack of expression (such as seen in human somatic cells) can lead to progressive telomere shortening upon cell division due to the end replication problem (as discussed in Chapter 1.1.2) (Harley et al., 1990). In 1973, Olovnikov proposed that the shortening of telomeres eventually results in cell death, and that this shortening may play a role in the entry of cells into a senescent state (Olovnikov, 1973). All human cells possess the ability to produce telomerase, but not all express the necessary genes for its synthesis. Only embryonic cells and stem cells express telomerase, allowing them to divide repeatedly without shortening of the telomeres (Wright et al., 1996). Somatic cells, in contrast, do not express telomerase and so lose a terminal fragment of telomeric DNA upon each cell division. The telomere is finite, which means that once the telomere has been lost, the coding DNA is exposed to degradation. At this point, the

cell reaches its replicative limit, stops dividing and enters senescence. Studies into ageing have investigated whether the telomeres found in cells of elderly subjects are shorter than those of their younger counterparts and found that, in the majority, this is the case (Allsopp et al., 1992; Harley et al., 1990). Additionally, telomeres from patients with premature ageing syndromes appear to be far shorter than those of people of the same age without the disease (Blasco, 2005). However, there can be a large amount of heterogeneity between the subjects with regards to the original length of the telomeres, which subsequently affects telomere length even after several cell divisions (Allsopp et al., 1992).

The concept of the role of telomere shortening in ageing originated from tissue culture experiments, in which human fibroblast cells only divide a certain number of times, and then ceased to divide further. The Hayflick Limit is the number of times a cell can divide before entering a senescent state (Hayflick and Moorhead, 1961). This 'limit' is named after the scientist who, upon studying human fibroblast cell cultures *in vitro*, discovered that cells have a finite replicative capacity. It is thought that this number of divisions is linked to telomere shortening, and that once the telomere reaches a critical length, the Hayflick Limit has been reached. Human fibroblast cells can undergo ~60 population doublings *in vitro* before entering senescence – a highly stable state (Figure 1.4). At this stage, the cell cycle is arrested by tumour suppressors such as p53 and retinoblastoma (RB) protein (Artandi and DePinho, 2000; Hara et al., 1991; Shay et al., 1991). If the functionality of these tumour suppressors is compromised (for example by tumour viruses) the checkpoint is bypassed and cells can divide once more, with the capacity for division limited to around 20-30 divisions. This stage is known as 'crisis' and is accompanied by a high spontaneous mutation rate. Any spontaneous mutations in the DNA are not dealt with because of a lack of cell cycling and dysfunction of the associated checkpoints which usually protect the cell from damage. These mutations can lead to the expression of proteins not typically expressed in normal cells and this means that telomerase can potentially be expressed in these cells in crisis. This is rare, occurring in about 1 in 10 million human cells (Wright and Shay, 1992). New telomerase activity can lead to the elongation of critically short telomeres and the resumption of cell division. If a random mutation leads to the activation of telomerase, the cells can exit the crisis state and become 'immortal', dividing indefinitely and unchecked.

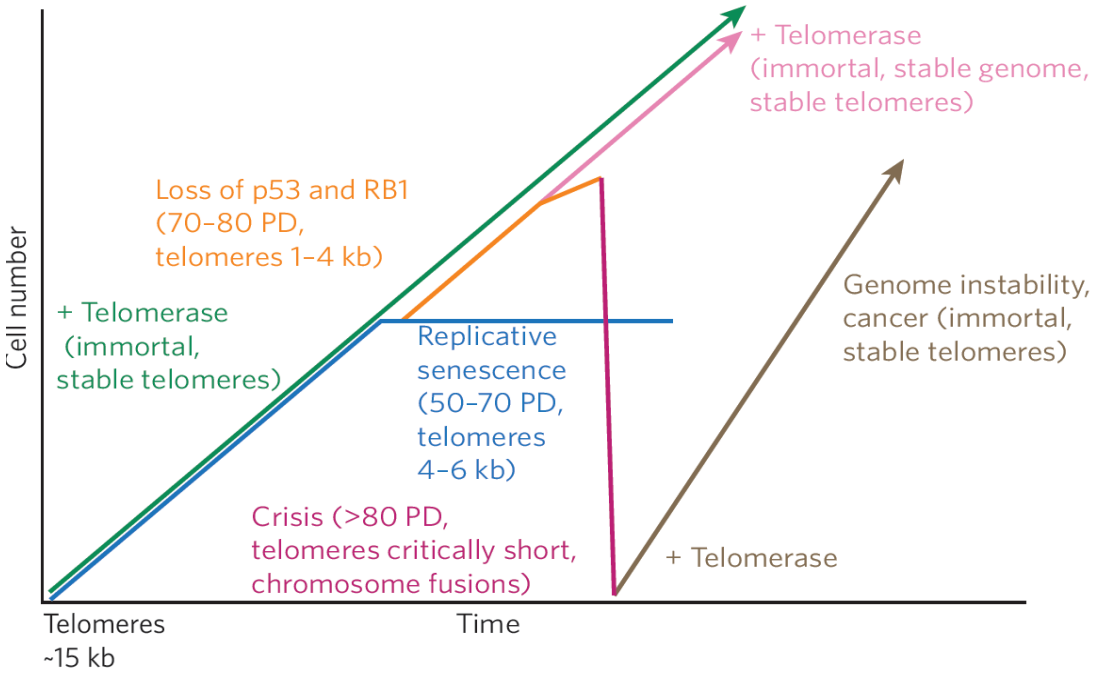

Figure 1.4: Replicative capacity, replicative senescence and cancer
Human somatic cells have a finite replicative capacity (between 60-80 population doublings in culture) due to telomere shortening. Telomeres shorten until they reach a critcal length between 4-6kb and cell-cycle arrests irreversibly (blue line). Cells can continue to divide indefinitely if telomerase is activated before senescence (green). If the p53 and RB1 pathways are suppressed then cells continue to divide (orange). Telomerase activation before end protection is lost prevents genomic instability (light pink); otherwise the complete loss of end protection results in telomeric crises, cell death and genomic instability (dark pink). The accumulation of mutation means that activation of telomerase at this point results in clones carrying multiple mutations with the ability to escape cell death, and these cells are predisposed to oncogenic transformation. PD indicates population doublings. Taken from Verdun and Karlseder (2007).

This is one of the proposed mechanisms for the proliferation of cancerous cells and the initiation of tumour growth (Harley et al., 1994).

Telomerase is commonly a target for anti-cancer drugs. When activity of the reverse transcriptase is prevented in the immortal cells found in tumours, the spread of cancerous cells can be slowed or even stopped (Hahn et al., 1999). Most of these drugs target hTERT (the human equivalent of yeast Est2) due to its catalytic activity (Shay and Wright, 2006). However, a number of compounds are under investigation as potential anti-cancer drugs due to their ability to inhibit telomerase via alternative mechanisms. Ligands which bind to and stabilise nucleic acid structures known as G-quadruplexes have been shown to prevent the action of telomerase and are effective against cancer cell lines (Mikami-Terao et al., 2009; Mikami-Terao et al., 2008; Leonetti et al., 2004; Neidle and Read, 2000; Kim et al., 1994).

1.2 G-quadruplexes

1.2.1 G-quadruplex structure and location

Due to the chemical structure of nucleotides, hydrogen bonds can form between the bases which make up DNA and RNA. Bonding between bases can lead to the formation of complex structures within nucleic acid sequences. Guanine (Figure 1.5a) is a derivative of purine and forms a pair with cytosine through three hydrogen bonds. However, multiple guanines can also bind together, forming structures such as G-quartets and G-quadruplexes. A G-quartet in DNA and RNA is formed when four guanine bases in close proximity interact through Hoogsteen hydrogen bonding, forming a planar structure (Williamson et al., 1989; Gellert et al., 1962). The stacking of several G-quartets together results in the formation of a higher structure known as a G-quadruplex (Williamson et al., 1989). The presence of a cation (for example potassium) within the central channel of this quadruplex can stabilise the structure (Figure 1.5b) (Guschlbauer et al., 1990). The structure of the G-quadruplex is dependent on the number of consecutive guanine bases (Figure 1.5c, adapted from (Guo, 2008)). For instance, a quadruplex formed from a single strand where four distinct runs of guanine bases are in close proximity is called an intramolecular quadruplex (Wang and Patel, 1994; Williamson et al., 1989). Conversely, a tetramolecular quadruplex is formed from four individual strands containing a single run of guanines (Wang and Patel, 1993; Sen and Gilbert, 1988). Bimolecular quadruplexes are formed from two separate guanine-rich strands (Kang et al., 1992; Sundquist and Klug, 1989). Other bases, such as thymine, are able to form equivalent quartet structures; however, they are significantly less stable and cannot form the channels required for the stabilising cation (Balasubramanian et al., 2011).

A sequence which holds the potential to form a quadruplex is known as a putative quadruplex sequence (PQS). Huppert & Balasubramanian (2005) identified a rule for PQS prediction based on primary DNA sequence for investigating the prevalence of PQSs within the genome. The research lead to the proposition of the Folding Rule - '*A sequence of the form* $d(G_{3+}N_{1-7}G_{3+}N_{1-7}G_{3+}N_{1-7}G_3)$ *will fold into a quadruplex under near-physiological conditions*' – in which N is any base (including guanine)

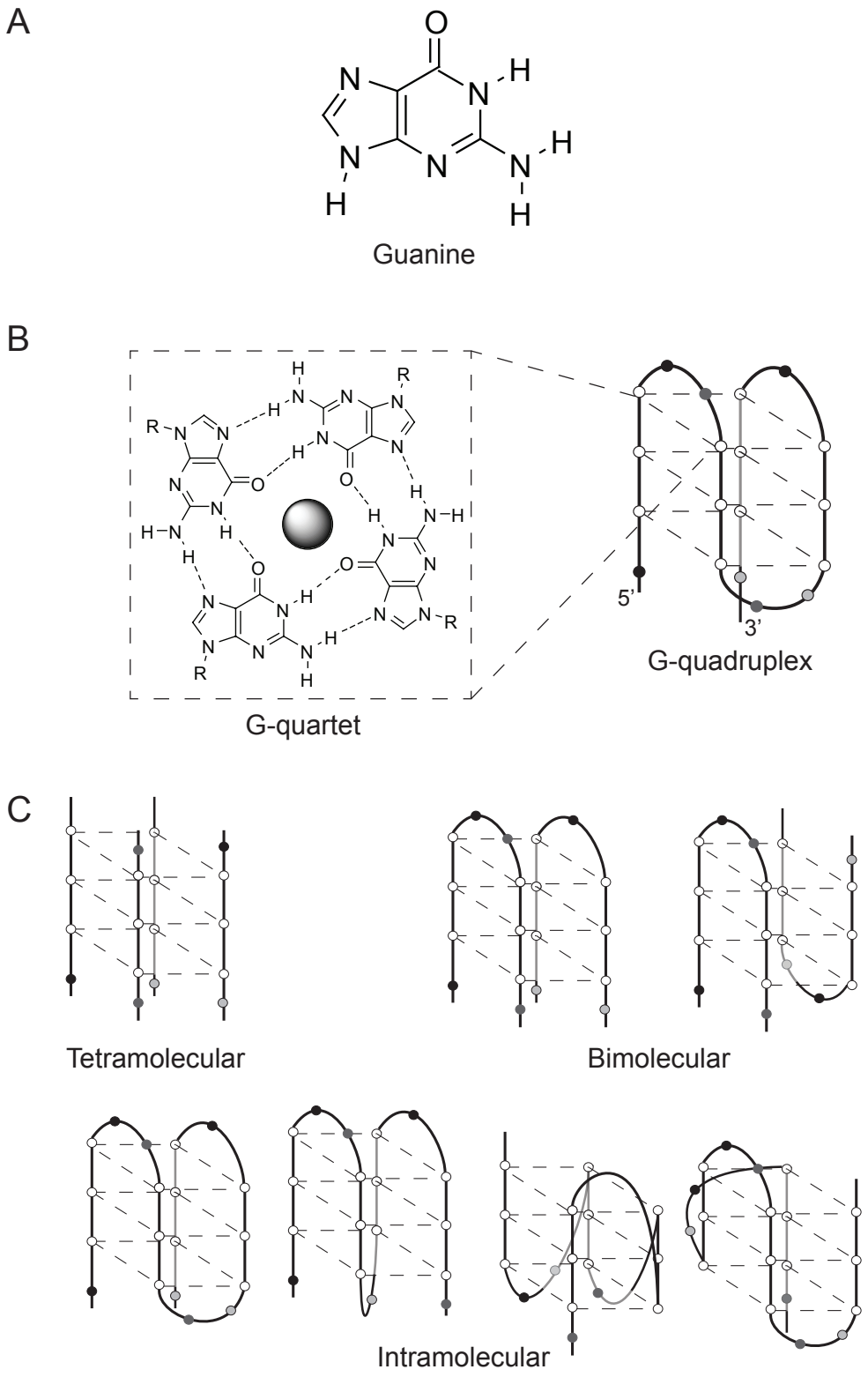

Figure 1.5: G-quadruplex structure and formation
(a) The structure of guanine. **(b)** Hydrogen bonds form between four proximal guanines to form a G-quartet. G-quartets stack to form G-quadruplexes. **(c)** G-quadruplexes can be formed in a variety of ways and structure is dependent on the number of nucleic acid strands involved

and near-physiological conditions are 100 mM KCl and 10 mM Tris-HCl (pH 7.4) (Huppert and Balasubramanian, 2005).

1.2.2 Prevalence, conservation and role of G-quadruplexes

Using the above folding rule, an algorithm (the *quadparser* algorithm) was developed which could identify PQSs in genomic DNA. This algorithm counts both G-rich and C-rich patterns ('G-patterns' and 'C-patterns') since in theory a G-quadruplex could be formed in a complementary strand (Huppert and Balasubramanian, 2005). The algorithm found a large number of sequences within the human genome with G-quadruplex-forming potential, and that as many as 376,000 quadruplexes could potentially exist at the same time (which is unlikely to occur, due to the dynamic equilibrium between quadruplexes and other DNA structures) (Huppert and Balasubramanian, 2005). The PQSs identified are spread throughout the genome. Regions of DNA with G-quadruplex-forming potential have unsurprisingly been identified within telomeres, due to the guanine-rich nature of telomeric regions (Huppert and Balasubramanian, 2005). The quadruplex-forming motif has also been indentified in non-telomeric regions of DNA, most interestingly in promoter regions. Indeed, quadruplex-forming sequences are highly prevalent in human gene promoters, with >40% of annotated genes containing one or more promoter quadruplexes (Huppert and Balasubramanian, 2007). One specific promoter region with quadruplex forming potential has garnered a considerable amount of interest. An extremely stable G-quadruplex structure has been found to form within the promoter region of human c-MYC, an oncogene linked to cell proliferation and inhibition of differentiation, and which is therefore associated with a number of cancers (Ambrus et al., 2005; Siddiqui-Jain et al., 2002). G-quadruplexes can also form within the promoter regions of human VEGF (vascular endothelial growth factor), *KRAS* proto-oncogene and human BCL2 (Cogoi and Xodo, 2006; Dai et al., 2006a; Dai et al., 2006b; Sun et al., 2005).

Since the expression of oncogenes is linked to malignant transformation, the presence of G-quadruplexes in their promoters regions may offer important information on how their expression is regulated (Dexheimer et al., 2006). It has been proposed that since G-quadruplex structures can potentially form within

promoter regions and their presence is transient due to their dynamic behaviour, quadruplexes have a role to play in the regulation of gene expression (Hershman et al., 2008; Huppert and Balasubramanian, 2007; Siddiqui-Jain et al., 2002). G-quadruplexes can also form within RNA, and therefore have an additional link to the regulation of gene expression. RNA G-quadruplexes can inhibit translation *in vivo* – for instance, a highly conserved RNA G-quadruplex in the 5'-UTR of the mRNA of the human zinc-finger protein Zic-1 represses protein synthesis in eukaryotic cells (Arora et al., 2008). Similarly, an RNA G-quadruplex has been found in the 5'-UTR of the human *NRAS* oncogene which has the ability to modulate the translation of the mRNA (Kumari et al., 2007). Sequences with the potential to form G-quadruplexes are well conserved, particularly in promoter regions. An *in silico* study of human, chimpanzee, rat and mouse promoters found G-quadruplex-forming motifs to be highly prevalent near transcription starts sites (Verma et al., 2008). The study also found high levels of conservation between species, with >700 orthologously related promoters in human, mouse and rat containing sequence with quadruplex-forming capabilities (Verma et al., 2008).

1.2.3 G-quadruplexes and telomeres

In humans and other vertebrates, the highest occurrence of regions with the potential to form G-quadruplexes is in the guanine-rich telomeres (Huppert, 2008). G-quadruplexes have been identified in the telomeric regions of a number of organisms including *Stylonychia lemnae*, *Tetrahymena* and *Oxytricha nova*, in spite of differences in telomeric sequence (Schaffitzel et al., 2001; Wang and Patel, 1995; Balagurumoorthy and Brahmachari, 1994; Wang and Patel, 1994; Blackburn, 1991; Henderson et al., 1987). Human telomeric G-quadruplexes have been found to form spontaneously *in vitro* under physiological conditions and are relatively stable (Balagurumoorthy and Brahmachari, 1994). Antibodies against telomeric G-quadruplex DNA have been used to determine whether G-quadruplexes can form *in vivo*, and experiments in *Stylonychia* found strong signals for anti-parallel G-quadruplexes (Schaffitzel et al., 2001). In the study, single-chain antibody fragments (scFvs) antibodies specific for *Stylonychia* telomeric G-quadruplex DNA were selected *in vitro* by ribosome display, then used to probe *Stylonychia* macronuclei and micronuclei (Schaffitzel et al., 2001). Through i*n situ* immunofluorescence

experiments, specific antibody binding to the macronucleus was observed using the scFv antibody Sty49, (Schaffitzel et al., 2001). Other methods of *in vivo* quadruplex detection in a number of organisms include use of highly fluorescent compounds and ligands which bind tightly to G-quadruplexes (Yang et al., 2009; De Cian et al., 2008; Neidle and Parkinson, 2008). G-quadruplexes are not permanent nucleic acid structures and they exist in equilibrium between the G-quadruplex form and single stranded form. The formation and resolution of G-quadruplexes is likely to be tightly regulated. TEBPα and TEBPβ are telomere binding proteins which bind to the 16-nucleotide G-overhang in *Oxytricha*, with TEBPα binding specifically to the overhang and TEBPβ dimerising with TEBPα (Gray et al., 1991; Gottschling and Zakian, 1986). Telomere binding proteins, TEBPs, found in *Stylonychia lemnae*, also cooperate to regulate the formation of G-quadruplexes, and the *in vivo* formation of the structures is regulated by TEBPβ (Paeschke et al., 2005).

Links between telomere-associated proteins and G-quadruplex maintenance have also been noted in other organisms. Rap1, which has a role in telomere maintenance in yeast, binds to and promotes the formation of intermolecular quadruplexes *in vitro* (Giraldo and Rhodes, 1994). The highly conserved telomere binding protein POT1, on the other hand, prevents the formation of G-quadruplexes at telomeres, which in turn promotes the action of telomerase (Zaug et al., 2005; Lei et al., 2003). G-quadruplexes can also be removed through the action of helicases – for example, the yeast helicase Sgs1 and human WRN and BLM helicases (which all bind G-quadruplexes with high affinity via conserved RQC domain) all have potent G-quadruplex unwinding abilities *in vitro* (Huber et al., 2006; Fry and Loeb, 1999; Sun et al., 1999; Sun et al., 1998). The RQC domain of Sgs1 in *S. cerevisiae* can stabilise G-quadruplexes and can compensate for the dysfunction of the essential telomere binding protein Cdc13 (Smith et al., 2011). The temperature sensitivity of *cdc13-1* strains is suppressed when the RQC domain is over-expressed in *SGS1* null mutants. This phenotypic suppression can also be achieved through over-expression of *STM1*, which encodes the G-quadruplex binding protein Stm1 (Smith et al., 2011).

1.2.4 G-quadruplex binding ligands and cancer

Monovalent cation-mediated G-quadruplex formation at telomeres can negatively regulate the action of telomerase *in vivo* (Zahler et al., 1991). Since around 85% of all human cancers are linked to telomerase activity regulation, the stabilising of G-quadruplexes has been under scrutiny for many years as an option for anti-cancer therapeutics (Neidle and Read, 2000; Kim et al., 1994). As described above, the presence of G-quadruplex structures can be transient, existing in equilibrium between a folded- and an unfolded-form. If the G-quadruplex structure were to be stabilised, this could potentially provide a method of permanently preventing telomerase activity. Inhibition of telomerase activity by ligand-mediated G-quadruplex stabilisation was first demonstrated using 2,6-diamidodianthraquinone (Sun et al., 1997). Therefore a number of G-quadruplex binding ligands are under investigation for their efficacy in inhibiting telomerase activity with a view to treating cancer.

Both synthetic and natural agents can act as ligands which bind G-quadruplexes. Many ligands which have so far demonstrated G-quadruplex binding abilities contain a core polyaromatic ring. For instance, compounds such as those belonging to the acridine family, which contain this polyaromatic ring, have a high affinity but low selectivity for duplex DNA, utilising base stacking and intercalation (Read et al., 2001; Harrison et al., 1999; Read et al., 1999). Other families of G-quadruplex stabilising compounds which contain polyaromatic heterocyclic ring systems include porphyrins, perylenes and anthraquinones (Neidle and Balasubramanian, 2007; Kerwin, 2000; Neidle and Read, 2000). The best characterised G-quadruplex binding ligand is the trisubstituted acridine BRACO-19, which has the ability to interact with three G-quadruplex grooves due to the compound's three side arms (Moore et al., 2006; Schultes et al., 2004). Studies *in vivo* demonstrate that BRACO-19 can cause telomere shortening and significant changes in telomerase catalytic activity (Burger et al., 2005).

Many G-quadruplex binding ligands are of interest in the development of anti-cancer drugs, mainly due to the role of G-quadruplexes in the inhibition of telomerase activity. G-quadruplex binding ligands have already demonstrated efficacy against certain cancer cell lines. Amongst the synthetic compounds currently under study is

TMPyP4 (5,10,15,20-tetratkis-(N-methyl-4-pyridyl)-21,23-H-porphyrin). TMPyP4 is a cationic porphyrin, which requires the binding of a metal ion to function. It has a high affinity but low selectivity for quadruplex nucleic acids (Freyer et al., 2007; Ren and Chaires, 1999). It has already been shown to inhibit telomerase *in vitro* and is effective against some cancer cell lines, such as MX-1 mammary tumours and PC-3 human prostate carcinomas (Mikami-Terao et al., 2009; Mikami-Terao et al., 2008; Grand et al., 2002). TMPyP4 also affects the c-MYC oncogene-dependent transcription of several genes including *TERT*, which encodes the human homologue of the *S. cerevisiae* telomerase reverse transcriptase subunit Est2 (Mikami-Terao et al., 2009; Mikami-Terao et al., 2008; Grand et al., 2002). Treatment with TMPyP4 induces the elevated transcription of a number of oxidative stress response genes in human cell lines (Grand et al., 2002). Another G-quadruplex binding ligand under investigation as an effective cancer treatment is the pentacyclic acridine RHPS4 (Cookson et al., 2005). Whereas TMPyP4 has the ability to both intercalate between adjacent G-tetrads and also stack onto the external G-quartet, RHPS4 strongly interacts with the two external G-quartets of the G-quadruplex, a complex which has been solved by NMR (Wei et al., 2006; Phan et al., 2005; Gavathiotis et al., 2003; Gavathiotis et al., 2001; Haq et al., 1999). Studies have shown that RHPS4 inhibits cell proliferation of human melanoma lines in a dose-dependent manner during short term treatment, and acts in a telomere-length independent manner to cause telomere dysfunction (Leonetti et al., 2004). The compound is also effective against uterus carcinoma cells, MCF-7 breast cancer cells and has an anti-metastatic effect on human melanoma xenografts in mice (Leonetti et al., 2008; Phatak et al., 2007; Cookson et al., 2005). RHPS4 triggers a rapid and potent ATR-dependent DNA damage response at telomeres in human cell lines and leads to the displacement of hTERT (the catalytic subunit of telomerase) from the nucleus, as well as chromosome fusions (Phatak et al., 2007; Salvati et al., 2007). Although no G-quadruplex binding ligands are in use currently as anti-cancer drugs, several (for example, Quarfloxin) have entered phase II clinical trials on cancer patients (Balasubramanian et al., 2011; Drygin et al., 2009).

1.3 The Pentose Phosphate Pathway (PPP)

1.3.1 Cancer cell metabolism and the pentose phosphate pathway

Highly proliferating cells, such as those found in tumours, require increased concentrations of nucleotides in order to replicate DNA and rapidly progress through the cell cycle. The most widely acknowledged alteration to cellular metabolism in cancer cells is the production of energy through glycolysis followed by the fermentation of lactic acid in the cytosol (aerobic glycolysis), instead of oxidation of pyruvate in mitochondria. This alteration in metabolism is also known as the Warburg effect and the existence of an oxidative pathway for glucose-6-phosphate metabolism was first demonstrated in the 1930s (Dickens, 1938; Warburg and Christian, 1937; Lipmann, 1936; Warburg et al., 1935). Since aerobic glycolysis is an inefficient method of ATP generation (generating only 2 ATPs per molecule of glucose, compared to oxidative phosphorylation generates up to 36 ATPs per glucose molecule), the advantage that the Warburg effect confers on cancer cells is unclear. It has been suggested that the changes in metabolism favour the production of cellular components required for rapid division and proliferation (Vander Heiden et al., 2009). This includes nucleotides and amino acids, the precursors of which (ribose-5-phosphate and erythrose-4-phosphate) are generated by the pentose phosphate pathway (PPP) (Figure 1.6). The PPP (which is also known as the phosphogluconate pathway or the hexose monophosphate shunt) is also a source of NADPH, which is required for nucleic acid production and fatty acid synthesis.

In cancer cells, around 85% of pentoses incorporated into DNA are provided by the PPP (Raïs et al., 1999). Activity of the glycolytic enzyme pyruvate kinase is modulated in response to growth factor signalling which occurs in cancer cells (Christofk et al., 2008a; Christofk et al., 2008b), which may promote flux into the PPP. Flux into the PPP can also be affected by the expression of a p53-inducible regulator of glycolysis and apoptosis known as *TIGAR*, the expression of which leads to a reduction in ROS levels (Bensaad et al., 2006). *TIGAR* expression results in the inhibition of phosphofructokinase, which redirects glucose towards the PPP (Bensaad et al., 2006). The first step of the oxidative phase of the PPP is catalysed by glucose-6-phopshate dehydrogenase (G6PDH; Zwf1 *in S. cerevisiae*) (Reaction 3

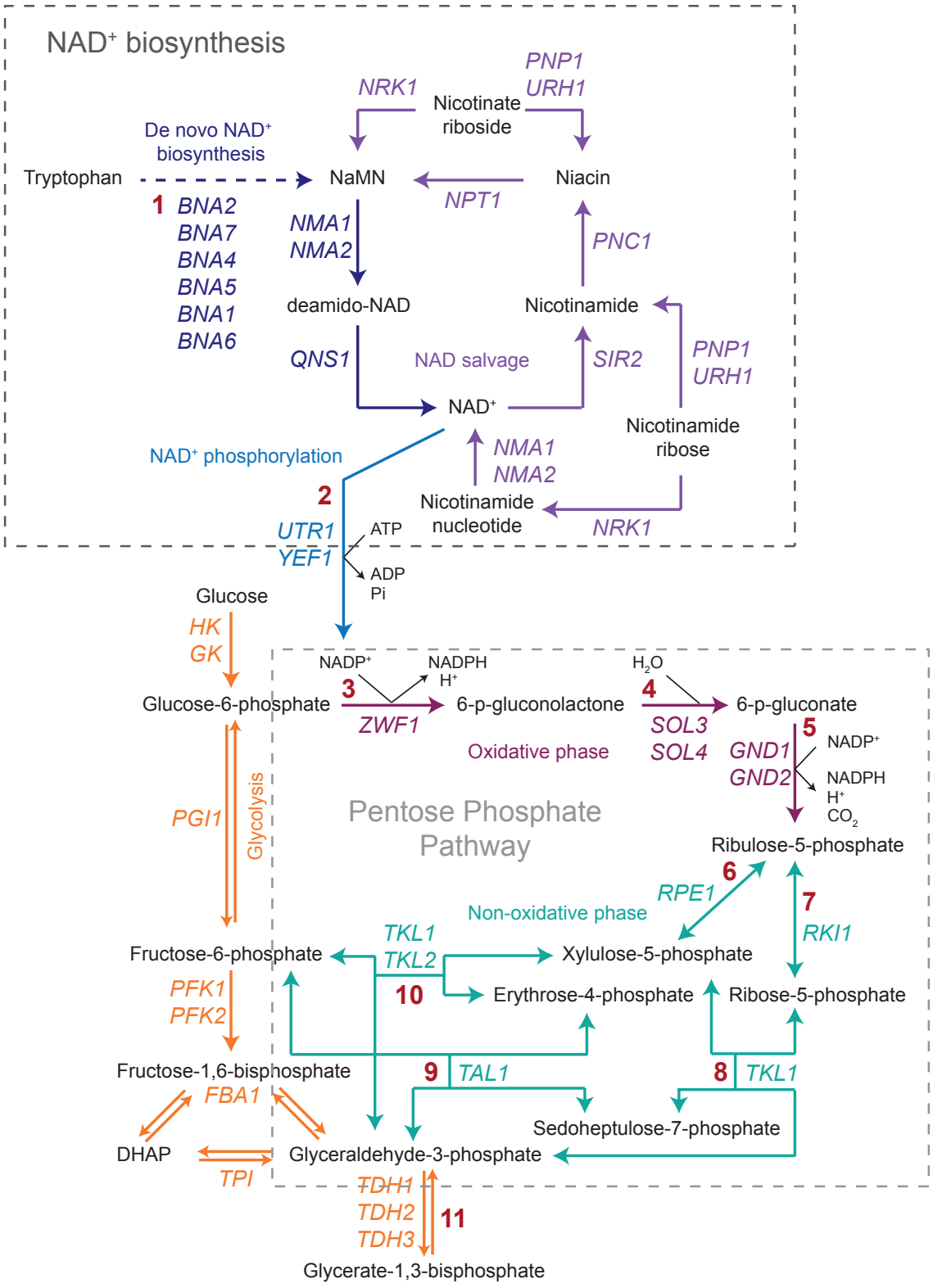

Figure 1.6: NAD⁺ biosynthesis, NAD⁺ phosphorylation and the PPP in yeast
NAD⁺ biosynthesis and the pentose phosphate pathway (PPP) are linked through the action of the NAD⁺ kinases Utr1 and Yef1 (Reaction 2). The different colours represent different stages or process of the pathways: for instance, the oxidative and non-oxidative phases of the PPP. Red numbers indicate reactions which will be referred to throughout this thesis. Taken from the Saccharomyces Genome Database (SGD, 2011) and Krüger et al. (2011).

in Figure 1.6). It has been demonstrated that an increase in G6PDH activity can be observed in tumour cells, correlating with an upregulation of the PPP in response to the increased requirement for NADPH and nucleotides (Jonas et al., 1992). An increase in G6PDH activity favours proliferation and survival, since it results in increased concentrations of both NAPDH (for protection against the strong oxidative environment encountered by tumour cells) and ribose-5-phosphate (for production of nucleotides for increased proliferation). G6PDH activity can be controlled by p53, which binds to the enzyme and prevents it from forming dimers (Jiang et al., 2011). Loss of p53 activity (frequently associated with the development of many cancers) removes this inhibition and can therefore favour tumour growth.

In non-transformed tissues, most of the ribose-5-phosphate necessary for nucleotide biosynthesis is generated through the oxidative phase of the PPP. However, in tumour cells the non-oxidative phase may also be an important source of the nucleotide precursor (Langbein et al., 2006; Boros et al., 2000; Cascante et al., 2000). Accompanying an increase in PPP flux, transaldolase (TA) expression is increased in many tumours (Samland and Sprenger, 2009; Lam et al., 2002). Transaldolase catalyses the conversion of erythrose-4-phosphate and sedoheptulose-7-phosphate to glyceraldehyde-3-phosphate and fructose-6-phosphate (Reaction 9 in Figure 1.6). Interestingly, there are links between the overexpression of certain isoforms of key PPP genes and various cancers. In humans, the transketolase family includes two transketolase-like proteins (TKTL1 and TKTL2) as well as transketolase (TK). Transketolases catalyse several steps of the non-oxidative phase of the PPP (Reactions 8 and 10 in Figure 1.6). The TKTL form of the human transketolase demonstrates very low activity in normal, untransformed cells; however, in cancer tissues, TKTLs are present and active, and work at a higher basal rate than TK (Coy et al., 2005). TKTL1 is over-expressed in a range of cancer cell lines, from invasive colon and urethelial tumours to uterine cervix cancer cells (HeLa) (Chen et al., 2009; Krockenberger et al., 2007; Langbein et al., 2006). Their expression also correlates with tumour progression in addition to proliferation rate (Langbein et al., 2008; Krockenberger et al., 2007; Langbein et al., 2006). Due to their over-expression in malignant tissues and the role of the PPP tumour development, TKTLs can be thought of as proto-oncogenes (Langbein et al., 2008; Krockenberger et al., 2007; Langbein et al., 2006).

1.3.2 The PPP and conservation between species

The pentose phosphate pathway is linked to glycolysis and gluconeogensis via glucose-6-phosphate and the intermediates fructose-6-phosphate and glyceraldehyde-4-phosphate which are produced by the pathway (Figure 1.6). In *S. cerevisiae*, the majority of glucose is fed into glycolysis, with as little as ~15% of glucose diverted through the PPP under normal growth conditions (Frick and Wittmann, 2005). This proportion can change due to various stresses, such as the presence of reactive oxygen species (ROS) and blockage of glycolysis through inactivation of key enzymes such as glyceraldehyde 3-phosphate dehydrogenase (GAPDH) and phosphofructokinase (Ralser et al., 2007; Bensaad et al., 2006; Ralser et al., 2006). In higher organisms the activity of the enzymes which drive the oxidative phase of the PPP can be altered by changes in nutritional and hormonal conditions (Tomlinson et al., 1988; Back et al., 1985; Eggleston and Krebs, 1974). The PPP is well conserved between species; as in yeast, 80-90% of glucose oxidation in humans takes place via glycolysis, with the remaining 10-20% occurring via the PPP (Wamelink et al., 2008). The strong conservation of the pathway suggests that it plays an important and necessary role in cellular metabolism.

The main roles of the PPP stem from its products. As noted above in Chapter 1.3.1, the PPP is a source of NADPH, ribose-5-phosphate and erythrose-4-phosphate. The first step of the oxidative phase of the pathway is the predominant source of cellular NADPH, the alternative sources in yeast being the third step in oxidative phase of the PPP (catalysed by 6-phosphogluconate dehydrogenase, 6PGDH), and the activity of the cytosolic acetaldehyde dehydrogenase Adh1. The latter enzyme contributes to NADPH generation to a lesser extent than the reactions of the PPP; 80% of the total NADPH required under normal conditions in budding yeast is generated by the first step of the PPP, with the remainder being produced by the activity of Adh1 (Celton et al., 2012). NADPH is an essential cellular reducing agent, maintaining the redox balance and protecting against the harmful effects of oxidative damage. NADPH is also important for fatty acid biosynthesis, where it is used in the conversion of acetyl-CoA and malonyl-CoA into palmitate in a reaction catalysed by fatty acid synthetase (FAS) (Wakil et al., 1983). The non-oxidative phase of the PPP produces ribose-5-phosphate and erythrose-4-phosphate. The

former is a precursor for purine ribonucleotide biosynthesis and latter can be used to generate amino acids such as tyrosine, phenylalanine and tryptophan. Deletion of genes key to both phases of the pentose phosphate pathway in yeast is lethal. For instance, a strain which harbours null mutations for both the glucose-6-phosphate dehydrogenase *ZWF1* and the transketolase *TKL1* is not viable (Deutscher et al., 2006). Since NADPH can still be produced in *zwf1*Δ strains (Grabowska and Chelstowska, 2003), the lethality which occurs in the double mutant may be due to the lack of ribose-5-phosphate, which would otherwise be generated by either branch of the PPP (see Figure 1.6).

1.3.3 The oxidative phase of the PPP

The pentose phosphate pathway is composed of two independent phases – the non-reversible oxidative phase, and the fully reversible non-oxidative phase (Figure 1.6). NADPH is generated in the first step of the oxidative phase of the PPP, in which 6-phospho-gluconolactone is produced from glucose-6-phosphate, reducing $NADP^+$ to NADPH in the process. The NADPH-generating first step of the oxidative phase of the PPP is rate-limiting and is catalysed by glucose-6-phosphate dehydrogenase (G6PDH, Zwf1 in *S. cerevisiae*). Human and yeast G6PDH demonstrate 47% homology in terms of amino acid sequence (Kletzien et al., 1994). G6PDH is constitutively expressed and is considered to have an important housekeeping function. In humans the G6PDH gene is X-linked (hence its constitutive expression), but its activity is regulated in specific tissues (Kletzien et al., 1994). For instance, hepatic G6PDH activity can increase in response to the presence of insulin, glucocorticoids and carbohydrates in the diet (Kletzien and Berdanier, 1993). It has also been shown that dietary fat can decrease the induction of G6PDH activity (Katsurada et al., 1989; Tomlinson et al., 1988).

G6PDH activity is predominantly regulated by the $NADP^+$/NADPH ratio. In human erythrocytes, the affinity of G6PDH for $NADP^+$ increases from low to high when the concentration of $NADP^+$ is increased, a result which may be explained by the presence of multiple $NADP^+$ binding sites within the enzyme (Luzzatto, 1967). NADPH inhibits G6PDH by competing with $NADP^+$ for binding sites, but it may also enhance the affinity of the remaining binding site(s) for $NADP^+$ (Luzzatto,

1967). $NADP^+$ is also necessary for stabilising G6PDH in the proper conformation, a property which NADPH lacks; therefore an increase in NADPH concentration results in a destabilising effect (Kotaka et al., 2005; Au et al., 2000). These alterations in affinity and stability caused by the $NADP^+$/NADPH ratio can potentially result in 30-50 fold changes in the NADPH-producing capacity of G6PDH (Holten et al., 1976). Other means of G6PDH regulation are by the binding of $MgCl_2$ and, in *Xenopus laevis* and human cell lines, by the binding of a heat shock protein (Cosentino et al., 2010). G6PDH deficiency in humans results in haemolytic anaemia and is the most widespread enzyme deficiency in the world - a prevalence which correlates with areas inhabited by populations historically exposed to endemic malaria (Nkhoma et al., 2009). This is thought to be due to defective NADPH-regenerating systems in red blood cells of sufferers, which is an unfavourable environment for *Plasmodia* development (Cappellini and Fiorelli, 2008).

In addition to NADPH, the oxidative phase of the PPP also generates H_2O and CO_2. The 6-phospho-gluconolactone generated in the first step of the pathway is hydrolysed in a reaction catalysed by 6-phospho-gluconolactonase (6PGL, Sol3 and Sol4 in yeast) to produce 6-phospho-gluconate (Reaction 4 in Figure 1.6). This reaction is spontaneous, but is accelerated by the action of 6PGL. It is thought that this enzyme prevents the conversion of 6-phospho-gluconolactone into the γ form, which cannot spontaneously hydrolyse, and instead accelerates the hydrolysis of the δ form of the lactone (Miclet et al., 2001). In *Plasmodium falciparum*, G6PDH and 6PGL activities are combined in the same enzyme (Clarke et al., 2001). The 6-phosphogluconate generated by 6-phospho-gluconolactone hydrolysis is in turn decarboxylated by 6-phosphogluconate dehydrogenase (6PGDH, Gnd1 and Gnd2 in yeast) to produce ribulose-5-phosphate and more NADPH, along with carbon dioxide and water (Reaction 5 in Figure 1.6). The resulting ribulose-5-phosphate feeds into the reversible non-oxidative phase of the pathway.

1.3.4 The non-oxidative phase of the PPP

In the non-oxidative phase of the pathway, the pentose carbon backbone from two ribulose-5-phosphate molecules is rearranged to produce sugars which feed back

into glycolysis. This effectively creates a cycle; indeed, the PPP is sometimes referred to as the pentose phosphate cycle, especially in early literature. However, several of the intermediates produced in these rearrangements are also important precursors to biological molecules; ribose-5-phosphate and erythrose-4-phosphate, as described earlier, are the precursors of purine nucleotides and certain amino acids respectively. The ribulose-5-phosphate which feeds into the non-oxidative phase of the PPP from the oxidative phase is converted to xylulose-5-phosphate and ribose-5-phosphate by the action of Rpe1 and Rki1 respectively (Reactions 6 and 7 in Figure 1.6). The human homolog of Rki1, the yeast ribose-5-phosphate ketol-isomerase, is known as RPI. RPI deficiency results in progressive leukoencephalopathy (Huck et al., 2004; Van der Knaap et al., 1999). Xylulose-5-phosphate and ribose-5-phosphate are rearranged and inter-converted to generate fructose-6-phosphate, glyceraldehyde-3-phosphate, sedoheptulose-7-phosphate and erythrose-4-phosphate (Reactions 8, 9 and 10 in Figure 1.6). Reactions of the non-oxidative phase of the pentose phosphate pathway are catalysed by transketolase (Tkl1/2 in yeast) and transaldolase (Tal1). Deficiency of human transaldolase (TALDO) is associated with liver disease (Wamelink et al., 2008).

Because of the reversible nature of the reactions of the non-oxidative phase of the PPP, flux can occur in either direction, from glycolysis or from the oxidative phase of the pathway. This means that ribose-5-phosphate, the precursor for nucleotide biosynthesis, can be manufactured via either route. Indeed, the two differing phases of the PPP can be regulated separately, depending on whether there is a necessity for the reducing power NADPH or the nucleotide precursor ribose-5-phosphate (Clasquin et al., 2011). It has been found recently that one of the intermediates of the non-oxidative phase of the PPP, sedoheptulose-7-phosphate, can be produced through the action of Shb17 in symphony with transketolase activity (Clasquin et al., 2011). This can favour ribose-5-phosphate production since it increases the availability of intermediates for generation of the purine nucleotide precursor.

1.3.5 The PPP and the oxidative stress response

The reductive capacity of NADPH is used to reduce antioxidants so that they can participate in the response to oxidative stress. Oxidative stress occurs when the

levels of reactive oxygen species (ROS) (produced during respiration by the mitochondria, for example) are high (Chance et al., 1979). The oxidative stress response lowers ROS levels and ROS-induced damage. One major element of the oxidative stress response is the action of antioxidants such as glutathione (GSH), which terminate the chain of oxidation reactions caused by the presence of free radicals such as ROS. GSH, for example, is oxidised to form glutathione disulphide (GSSG) upon reducing ROS. GSSG is returned to its reduced form of GSH by the action of glutathione reductase (GSR). GSR itself is reduced by NADPH. As mentioned above, cellular NADPH is predominantly generated by the first step of the oxidative phase of the PPP (Celton et al., 2012). NADPH is also used to reduce the flavoenzyme thiroredoxin reductase, which in turn keeps the redox proteins thiroredoxins in a reduced state. The oxidation of NADPH to $NADP^+$ through these reactions decreases the NADPH/$NADP^+$ ratio. As described above (Chapter 1.3.3), this alteration in the ratio can affect G6PDH activity, since NADPH enforces an inhibitory effect on the enzyme. Therefore a reduction in NADPH levels, for instance, through the oxidative stress response, results in an increase in $NADP^+$ concentration, which increases the affinity of G6PDH for $NADP^+$ and increases G6PDH activity, which in turn generates more NADPH.

Flux through the PPP in response to oxidative stress can also increase via the inactivation of glyceraldehyde-3-phosphate dehydrogenase (GAPDH, Tdh1-3 in yeast) (Ralser et al., 2007; Grant et al., 1999). High levels of ROS inactivate GAPDH, which blocks glycolysis and redirects carbohydrate flux into the PPP (Ralser et al., 2007; Grant et al., 1999). In this way, GAPDH inactivation acts as a metabolic switch to counteract oxidative stress. In addition to this metabolic switching, the transcription of PPP genes also increases in response to oxidative stress, through the action of the transcription factor Stb5 (Larochelle et al., 2006). Studies into other oxidative stress responses have found that the cytosolic superoxide dismutase (Sod1) and the pentose phosphate pathway play overlapping roles in protection against the presence of reactive oxygen species (ROS). The overexpression of the transketolase-encoding gene *TKL1* suppresses *sod1*Δ phenotypes in a Zwf1-dependent manner, proposed to be caused by an increase in flux through the PPP (Slekar et al., 1996). The pentose phosphate pathway and oxidative stress seem intrinsically linked, especially through transcriptional

regulation, and studies have shown that PPP activity alone in response to oxidative stress can actually influence further transcriptional alterations (Krüger et al., 2011).

1.3.6 The PPP and nucleotide production

The ribose-5-phosphate produced in the non-oxidative phase of the pentose phosphate pathway can either continue through this pathway, resulting in the production of glycolytic intermediates such as glyceraldehyde-3-phosphate and fructose-6-phosphate, or go on to produce nucleotides. The latter occurs through the action of phosphoribosylpyrophosphate synthetase and ribose-phosphate pyrophosphokinases, which use ribose-5-phosphate to produce phosphoribosyl pyrophosphate (PRPP), which is then metabolised further to make nucleotides. There are multiple reactions involved in the production of nucleotides (dNTPs); however, the rate-limiting reaction in the production of all dNTPs is catalysed by ribonucleotide reductase (RNR). RNR catalyses the formation of deoxyribonucleotides from ribonucleotides. Reduction of RNR by thioredoxin (itself reduced by NADPH) stimulates RNR enzyme activity (Holmgren, 1989). Since ribonucleotide reductase also indirectly requires reduction by NADPH to function, this means there are two ways in which nucleotide production is linked to the pentose phosphate pathway.

Yeast ribonucleotide reductase is a class 1 RNR and is proposed to be an $\alpha_2\beta_2$ tetramer, composed of a large subunit and a small subunit (Sjöberg, 1997). The larger α_2 subunit (R1) houses the active site and, during normal growth, consists of a homodimer of Rnr1; however, under DNA damage conditions *RNR3* expression is induced strongly, leading to the hypothesis that Rnr3 expression may increase total RNR activity (Domkin et al., 2002). The smaller β subunit (R2) is composed of a Rnr2/Rnr4 heterodimer (Chabes et al., 2000). As described previously in Chapter 1.1.5, the expression of all of the RNR genes can be induced following DNA damage, and this alteration in expression is mediated by Dun1, an effector of the DNA damage response (Huang and Elledge, 1997; Elledge, 1996; Zhou and Elledge, 1993). *RNR3* is most significantly upregulated, with up to a 100-fold increase in expression. Dun1 additionally regulates RNR activity by targeting its inhibitor, Sml1, for degradation (Zhao and Rothstein, 2002). Ribonucleotide reductase activity

can also be regulated allosterically by nucleotide concentration, in which a high level of dATPs inhibits the action of RNR by dATP feedback inhibition (Chabes et al., 2003). Research has found that RNR activity (and therefore the concentration of nucleotides) is under tight regulation – too few dNTPs, and DNA repair is compromised, but too many, and random mutations can occur (Kumar et al., 2011; Kumar et al., 2010; Chabes et al., 2003).

Cells can balance the demands of redox homeostasis and biosynthesis placed on the PPP through the use of riboneogenesis. Clasquin et al. reported that a thermodynamically driven pathway which converts PPP intermediates into ribose-5-phosphate without NADPH production is present in yeast (Clasquin et al., 2011). This pathway, termed riboneogenesis, can increase ribose-5-phosphate production when the relative demand for ribose compared to the demand of NADPH is high (Clasquin et al., 2011). Riboneogenesis requires the action of Shb17, which catalyses the committed reaction of the pathway, along with the activities of Tkl1 and Rki1 (Clasquin et al., 2011). *SHB17*, *TKL1* and *RKI1* expression correlate across the yeast metabolic cycle, suggesting that they act together to produce ribose (Clasquin et al., 2011). *SHB17* and *TKL1* expression also anticorrelates with *ZWF1* expression, which suggests that riboneogenesis and the oxidative phase of the PPP occur during different phase of the yeast metabolic cycle (YMC) (Clasquin et al., 2011).

1.3.7 Other key roles of the PPP

An increase in PPP activity is also observable in ageing cells and in age-related conditions, such as age-linked neurological disorder Alzheimer's disease. Studies into the disease have found that the activities of both G6PDH and 6PGDH, which catalyse the NADPH-producing steps of the PPP (Reactions 3 and 5 in Figure 1.6), increase in the inferior temporal cortex of patients with Alzheimer's (Palmer, 1999). Age-related increases in the activity of G6PDH and 6PGDH have also been observed in the brains of rats (El-Hassan et al., 1981). It is thought that an increase in age correlates with an increase in the prevalence of oxidative stress; therefore modulating the pentose phosphate pathway may provide protection against age-related diseases (Finkel and Holbrook, 2000). However, the relationship between the

pentose phosphate pathway and lifespan is a complicated one and is not yet thoroughly understood (Ralser et al., 2007).

The PPP also plays a role in embryonic development and growth. G6PDH activity controls the levels of ROS the embryo is exposed to; ROS levels which are controlled at a low level trigger the proper differentiation and growth of the placenta and trophoblast during the first trimester (Ufer et al., 2010). G6PDH activity is also linked to the differentiation of specific tissues, such as cardiomyocytes, and the control of ROS levels is also important in fertility in the maturation of spermatozoa (Chung et al., 2010; Perl et al., 2006). G6PDH activity appears to have many physiological roles, and deficiency in the enzyme can lead to problems with cell growth and signalling, the response to viral infections and can increase susceptibility to degenerative diseases, as well as haemolytic anaemia (as discussed in the Chapter 1.3.3) (Ho et al., 2007). The pentose phosphate pathway is also of interest to the wine making industry. *S. cerevisiae* usually poorly assimilates gluconate (which is metabolised by the PPP) when cultured on the substrate. Strains with increased flux through the PPP exhibit metabolic changes, including higher fermentation rates and reduced acetate production, which are advantageous to the wine-making process (Cadière et al., 2011).

1.4 Aims and objectives

The aims and objectives of my project were to investigate the effect of treating yeast with the G-quadruplex binding ligand TMPyP4. Due to its ability to bind G-quadruplexes and interact with telomerase, I expected to find that deletion of key telomere- and telomerase-related genes would alter the sensitivity of *Saccharomyces cerevisiae* to TMPyP4 and that this would provide some indication as to its mechanism at telomeres.

I also aimed to study the gene deletions which caused an increased sensitivity to this molecule more closely, including their interaction with telomeres in the absence of TMPyP4, specifically the relationship with telomere capping, through study of the telomere-capping mutant *cdc13-1*.

2 Materials and Methods

2.1 Robotics and *in silico* methods

2.1.1 Yeast culture conditions

The single gene deletion collection was stored at -80^{o}C in 384-well plates (Greiner BioOne) in 15% glycerol (Tong and Boone, 2005). Yeast strains were cultured in complete synthetic media (CSM) with appropriate amino-acids and G418 (final concentration, 200 µg/ml) added. W303 genetic background strains were cultured in YEPD (ade).

2.1.2 Plate filling

Rectangular, single chamber, SBS footprint plates (omnitrays; Nunc Thermo Fisher Scientific) were filled with 35 ml molten agar media using a Perimatic GP peristaltic pump (Jencons (Scientific) Limited, Leighton Buzzard, UK) fitted with a foot switch. 96-well plates (non bar-coded; Greiner Bio-One Ltd.) were filled with liquid media or distilled H_2O (200 µl per well) using a Wellmate plate-filler with stacker (Matrix Technologies, Thermo Fisher Scientific).

2.1.3 Robotics

Solid agar to solid agar pinning was performed on a Biomatrix BM3-SC robot (S&P Robotics Inc., Toronto, Canada) using either 384-pin (1 mm diameter) or 1536-pin (0.8 mm diameter) pintools. Inoculation from solid agar to liquid media was performed on the Biomatrix BM3-SC robot using a 96-pin (1 mm diameter) pintool. Dilution and spotting of liquid cultures onto solid agar plates was performed on a Biomek FX robot (Beckman Coulter (UK) Limited, High Wycombe, UK) equipped with a pintool magnetic mount and a 96-pin (2 mm diameter) pintool (V&P Scientific, Inc., San Diego, CA, USA).

2.1.4 Growth assays

Liquid-to-solid agar 384-format robotic spot tests were performed as described previously (Addinall et al., 2008). Briefly, colonies were inoculated from the solid agar single gene deletion collection plates into 96-well plates containing 200 µl CSM supplemented with G418 media in each well (see Robotics, above). The cultures were grown to saturation for 3 days, without shaking, at 23°C. Cultures were resuspended, diluted approximately 1/100 in 200 µl H_2O and spotted onto solid CSM and CSM supplemented with 100 µM TMPyP4 (in H_2O), 1.5 mM H_2O_2, 100 mM HU (in H_2O) or 200 µM RHPS4 (in 1% DMSO) plates.

2.1.5 Plate incubation and photography

The plates were incubated at 30^{o}C for 5 days in an S&P robotics automated integrated imager and incubator and photographed at 6 hour intervals. The spImager camera (a Canon EOS Rebel T3i) was used in fully manual mode. Using S&P robotics RoboSoft software, the plate number, batch number and a time stamp (date in year, month, day and time in hour, minute, second) were incorporated as the image name (e.g K000012_030_001_2011-10-17_17-06-15.JPG).

2.1.6 Image analysis

The image analysis tool Colonyzer was used to quantify cell density from captured photographs (Lawless et al., 2010). Colonyzer corrects for lighting gradients, removing spatial bias from density estimates. It is designed to detect cultures with extremely low cell densities, allowing it to capture a wide range of culture densities after dilute spotting on agar. Colonyzer is available under GPL at http://research.ncl.ac.uk/colonyzer. Modelling of fitness was carried out as described in Addinall et al. (2011).

2.1.7 Microarray analysis

The Affymetrix Cell Intensity (CEL) files generated in the Greenall microarray (accession number E-MEXP-1551) were downloaded from ArrayExpress, data was

normalised using RMA (Robust Multiple-array Average) in GeneSpring GX 10.0, and at each time point the average wild type intensity was used as the baseline control (i.e. *cdc13-1*0 – wt0, *cdc13-1*60 – wt60) (Greenall et al., 2008; Parkinson et al., 2007; Grewal and Conway, 2000). Normalised data was subjected to the unpaired T-test (with an asymptotic *p*-value computation) and data was corrected using the Bonferroni family-wise error rate (FWER). Genes with p-value < 0.05 and a $\log_2$ fold change between wild type and *cdc13-1* ≥ 2 were classed as differentially expressed.

CEL files were uploaded to CARMAweb and normalised by RMA (Rainer et al., 2006). The moderated t-statistic (using the Bioconductor *limma* package) was used to calculate *p*-values and the Bonferroni correction was applied. Genes with p-value < 0.05 and a $\log_2$ fold change between wild type and *cdc13-1* ≥ 2 were classed as differentially expressed.

2.1.8 GO analysis

GO Analysis was carried out using the GOstat bioinformatics tool (Beißbarth and Speed, 2004). Data was analysed using a Fisher's Exact Test, Benjamini & Hochberg False Discovery Rate (FDR) and a significance level of 0.01 to give over-represented terms.

2.2 Yeast protocols

2.2.1 Yeast strains

Table 2.1 lists the yeast strains that were used in this study. The majority of the yeast strains used were based on the W303 *S. cerevisiae* background. All contain the following mutations, unless indicated: *ade2-1, trp1-1, can1-100, leu2-3,112 his3-11,15 ura3, GAL$^+$ psi$^+$ ssd1-d2 RAD5*.

* indicates strains generated in this study

Strain (DLY)	**Genotype**	**Source**
640	*MATa*	R. Rothstein
1096	*MATa chk1::HIS3*	D. Lydall
1108	*MATa cdc13-1-int*	D. Lydall
1195	*MATα cdc13-1-int*	D. Lydall
1255	*MATa rad9::HIS3 cdc13-1-int*	D. Lydall
1256	*MATα rad9::HIS3 cdc13-1-int*	D. Lydall
1273	*MATα exo1::LEU2*	D. Lydall
1320	*MATa rad53::HIS3 sml1::KanMX4*	D. Lydall
1569	*MATα rad52::TRP1*	D. Lydall
2641	*MATα chk1::HIS3 cdc13-1-int*	D. Lydall
2787	*MATα yku70::LEU2*	D. Lydall
3001	*MATα*	R. Rothstein
5441	*MATα rad9::HIS3*	D. Lydall
5514	*MATa pho86::KANMX*	D. Lydall
5541	*MATa tkl1::KANMX*	D. Lydall
5543	*MATa tkl1::KANMX cdc13-1-int*	D. Lydall
5544	*MATa tkl1::KANMX cdc13-1-int*	D. Lydall
5547	*MATa tkl1::KANMX rad9::HIS3 cdc13-1-int*	D. Lydall

5548	*MATa tkl1::KANMX rad9::HIS3 cdc13-1-int*	D. Lydall
5549	*MATα rpe1::KANMX*	D. Lydall
5550	*MATα rpe1::KANMX*	D. Lydall
5557	*MATa zwf1::KANMX*	D. Lydall
5558	*MATα zwf1::KANMX*	D. Lydall
5559	*MATα zwf1::KANMX cdc13-1-int*	D. Lydall
5560	*MATa zwf1::KANMX cdc13-1-int*	D. Lydall
5561	*MATa zwf1::KANMX rad9::HIS3 cdc13-1-int*	D. Lydall
5625	*MATa tal1::KANMX rad9::HIS3 cdc13-1-int*	D. Lydall
5708*	*MATα tal1::KANMX cdc13-1-int*	D. Lydall
5709*	*MATα tal1::KANMX cdc13-1-int*	D. Lydall
5710*	*MATa tal1::KANMX cdc13-1-int*	D. Lydall
5711*	*MATα tal1::KANMX*	D. Lydall
5775	*MATa bar1::hisG cdc15-2-int*	D. Lydall
6345*	*MATa yku70::LEU2 tkl1::KANMX*	2787 x 5541
6346*	*MATα yku70::LEU2 tkl1::KANMX*	2787 x 5541
6816	*MATa rad53::HIS3 sml1::URA3 cdc13-1-int*	D. Lydall
6930	*MATa rad24::TRP1*	D. Lydall
7076	*MATα rad53::HIS3 sml1::URA3 cdc13-1-int*	D. Lydall
7105	*MATa bar1::hisG cdc15-2-int*	D. Lydall
7428*	*MATa zwf1::NATMX*	5557 transformed with NatMX
7429*	*MATa zwf1::NATMX*	5557 transformed with NatMX
7440*	*MATa zwf1::NATMX tal11::KANMX*	7428 x 5708
7442*	*MATα zwf1::NATMX tal11::KANMX cdc13-1-int*	7428 x 5708
7443*	*MATa zwf1::NATMX tal11::KANMX cdc13-1-int*	7428 x 5708
7444*	*MATα zwf1::NATMX cdc13-1-int*	7428 x 5708

7445*	*MATa zwf1::NATMX cdc13-1-int*	7428 x 5708
7502*	*MATα tal11::KANMX rad53::HIS3 sml1::URA3 cdc13-1-int*	6816 x 5708
7506*	*MATa tal11::KANMX chk1::HIS3 cdc13-1-int*	5708 x 1096
7507*	*MATα tal11::KANMX chk1::HIS3 cdc13-1-int*	5708 x 1096
7515*	*MATα tkl11::KANMX rad53::HIS3 sml1::URA3 cdc13-1-int*	7076 x 5541
7518*	*MATa tkl1::KANMX chk1::HIS3 cdc13-1-int*	5541 x 2641
7519*	*MATα tkl1::KANMX chk1::HIS3 cdc13-1-int*	5541 x 2641
7554*	*MATa tal11::NATMX*	5711 transformed with NatMX
7565*	*MATα tal11::KANMX rad53::HIS3 sml1::URA3 cdc13-1-int*	6816 x 5708
7570*	*MATα tal11::NATMX tkl1::KANMX yku70::LEU2*	7554 x 6346
7571*	*MATa tal11::NATMX tkl1::KANMX yku70::LEU2*	7554 x 6346
7572*	*MATα tal11::NATMX tkl1::KANMX*	7554 x 5543
7574*	*MATα tal11::NATMX tkl1::KANMX cdc13-1-int*	7554 x 5543
7575*	*MATa tal11::NATMX tkl1::KANMX cdc13-1-int*	7554 x 5543
7576*	*MATa tal11::NATMX yku70::LEU2*	7554 x 6346
7577*	*MATα tal11::NATMX yku70::LEU2*	7554 x 6346
7578*	*MATa tal11::NATMX cdc13-1-int*	7554 x 5543
7579*	*MATα tal11::NATMX cdc13-1-int*	7554 x 5543
7580*	*MATa tkl11::KANMX rad53::HIS3 sml1::URA3 cdc13-1-int*	7076 x 5541
7684*	*MATa tkl11::NATMX*	5544 transformed with NatMX
7711*	*MATα tal1::NATMX rpe1::KANMX*	7578 x 5549
7717*	*MATa tkl1::NATMX rpe1::KANMX*	7684 x 5549
7721*	*MATα tkl1::NATMX*	7684 x 5549
DDY179	*MATa/MATα cdc13-1/CDC13 rad9::HIS3/RAD9*	D. Lydall

Table 2.1: Yeast strains used in this study

2.2.2 Plasmids

Plasmids used in this study are listed in Table 2.2. Plasmids were stored at -20^{o}C in 1 x TE.

Plasmid	Details	Source
pDL1155	Plasmid used to switch from kanMX cassette to natMX cassette	p4339 (provided by C. Boone)
pDL1042	Plasmid for amplification of kanMX6 cassette by PCR	pFA6a-kanMX6 (Longtine et al., 1998)

Table 2.2: Plasmids used in this study

2.2.3 Oligonucleotides

Oligonucleotides used in this study were purchased from Sigma-Aldrich, stored at -20^{o}C in 1 x TE and are listed in the table below:

Oligo	Sequence	Target
1606	TCAGCATCCATGTTGGAATT	KanMX
1802	GGTCCACCGGCACCT	NatMX
1877	GGCGCGTCTTAATTTTCTTC	*PIF1*
1878	TCGTTCCAGGATAAAGGACTG	*PIF1*
1937	TGGCGAATTCTTCAATGTACG	*ZWF1*
1939	TCCGTTCGCAATCTCTCGA	*TKL1*
1951	TTGTCAACTCGTCAAGTCAC	*TAL1*

Table 2.3: Oligos used in this study

2.2.4 Enzymes

Enzymes used in this study are all listed below. The buffers supplied with the enzymes were used in conjunction.

Enzyme	Buffer	Source
EcoRI	EcoRI buffer	New England Biolabs

Table 2.4: Enzymes used in this study

2.2.5 Kits

Kits used in this study are all listed below

Kit	Source
XL1-blue sub-cloning grade competent cells	Stratagene
QIAprep Spin Miniprep Kit	Qiagen
QIAquick Gel Extraction Kit	Qiagen

Table 2.5: Experimental kits used in this study

2.2.6 Recipes for yeast media

YEP

Yeast Extract/Peptone (YEP) media used in experiments consisted of 1% Yeast Extract (w/v), 2% Bacto Peptone (w/v) and 50 mg/ml adenine in water, along with either 2% dextrose, galactose or raffinose as a carbon source. For 1 L of media of YEPD (yeast extract/peptone/dextrose), 10 g Yeast Extract and 20 g Bacto Peptone was added to 985 ml of water, then autoclaved and cooled to 60^{o}C, before the addition of 50 ml sterile dextrose solution, (40% w/v) and 15 ml sterile adenine solution (0.5% w/v).

Dropout media

Nutritional selective media was composed as follows: 0.13% dropout amino acid powder, 0.17% yeast nitrogen base, 0.5% ammonium sulphate and 2% bacto agar, 2% dextrose as the carbon source. In order to confer selective pressure, different quantities of amino acids were added to the media. Table 2.6 below indicates the amino acid combinations needed to generate the appropriate selection.

Amino acid	Amount (g)
Adenine	2.5
L-arginine (HCl)	1.2
L-aspartic acid	6.0
L-glutamic acid (monosodium salt)	6.0
L-histidine	1.2
L-leucine	3.6
L-lysine (mono-HCl)	1.8
L-methionine	1.2
L-phenylalanine	3.0
L-serine	22.5
L-threonine	12.0
L-tryptophan	2.4
L-tyrosine	1.8
L-valine	9.0
Uracil	1.2

Table 2.6: Amino acid combinations for dropout media (1L)

LB media

For 1 L of Luria-Bertani Broth (LB Broth), 5 g Yeast Extract and 10 g Bacto Peptone, and 10 g NaCl was added to 985 ml of water, then autoclaved and cooled to 60^{o}C, before the addition of ampicillin, giving the final concentration of 50 mg/ml.

SOC media

For 1 L of SOC media, 5 g Yeast Extract and 20 g Bacto Peptone, 0.5 g NaCl, 2.5 ml KCl (1 M) was added to 982.5 ml of water, then autoclaved and cooled to 60^{o}C.

Agar plates

The above recipes were also used to generate agar plates of the media. In addition, 20 g of Bacto Agar was added to the liquid media prior to autoclaving, giving a final concentration of 20 g/L. To generate plates containing a selective marker, filter sterilised antibiotics (Geneticin (G418) and Nourseothricin-dihydrogen sulphate (CloNAT)) were added, to give a final concentration of 200 µg/ml.

2.2.7 Isolating genomic DNA from yeast

The appropriate yeast strains were grown to saturation overnight in YEPD media, then spun at 13,000 rpm for 1 minute. The resulting pellet was resuspended in 250 µl of 0.1 M EDTA (pH 7.5), 1:1000 β-mercaptoethanol and 2.5 mg/ml zymolyase 20T, before incubation at 37^{o}C for 1 hour until spheroplasted. 55 µl of miniprep mix (0.25 M EDTA (pH 8.5), 0.5 M Tris base, 2.5% SDS) was added, and then samples were mixed by vortexing before incubation at 65^{o}C for 30 minutes. 63 µl of 5 M KAc was added, then samples were mixed by vortexing before incubation on ice for 30 minutes. Samples were spun at 13,000 rpm for 20 minutes, supernatants transferred to a new tube containing 720 µl of 100% ethanol and spun at 13,000 rpm for 10 minutes. After being drained thoroughly, 130 µl 1xTE containing 1 mg/ml RNAase A was added to the pellet and samples were incubated at 37^{o}C for 35 minutes. 150 µl isopropanol was added and samples were spun at 13,000 rpm for 20 minutes. After draining, samples were washed with 70% ethanol (100 µl, 5 minute spin), aspirated and air dried for 30 minutes, before being resuspended in 40 µl 1 x

TE, with incubation overnight at 37°C. This yielded approximately 10 μg of genomic DNA.

2.2.8 Transformation of E. coli

Bacterial transformations were carried out using XL1-blue Sub-cloning grade competent cells. Plasmid extractions from transformed bacterial cultures were carried out using a QIAprep Spin Miniprep Kit. The transformations were carried out as per the provided protocol.

2.2.9 Restriction digests

Digestion mixtures used in restriction digests were as follows:

Component	Concentration	Volume (μl)
DNA	-	5
Enzyme	-	1
Buffer	10x	2
BSA	100x	0.5
H_2O	-	12

Table 2.7: Composition of the restriction digest reaction mixture

Digestions were carried out at 37°C for an hour to overnight.

2.2.10 Disruption of ORFs with KanMX or NatMX

The appropriate deletion strain was taken from the Boone Synthetic Deletion Library (single gene deletion, with KanMX in place of the ORF, in the S288C background) and grown at 23°C on a YEPD agar plate containing the antibiotic G418 (Tong and Boone, 2005). The KanMX marker was amplified using primers designed to anneal 500 bp upstream and 500bp downstream of the deleted gene (where applicable). In absence of the appropriate deletion strain in the Boone Synthetic Deletion library, the KanMX cassette was amplified from the pFA6a-KanMX6 plasmid. The amplification was confirmed using gel electrophoresis, and the PCR product used to transform a W303 diploid strain, DDY179.

To replace the KanMX cassette with the NatMX cassette, marker switching was used. The TA::MX4-natR switcher cassette was excised from the p4339 plasmid by digestion with EcoRI, isolated using gel electrophoresis and gel extraction using the QIAquick Gel Extraction Kit (Qiagen). The cassette was then transformed into strains carrying the KanMX cassette as below (Chapter 2.2.12).

2.2.11 PCR and gel electrophoresis

For PCR, the ExTaq, ExTaq 10x Buffer and dNTPs were supplied by Takara. Oligonucleotides used were designed using Invitrogen Primer Design software and supplied by Sigma Aldrich. The PCR reaction mixture used in this study was as follows:

Component	Final Concentration	Volume (µl)
Template	-	1
Forward Primer	0.3 µM	0.5
Reverse Primer	0.3 µM	0.5
dNTPs	0.25 mM	4.8
ExTaq (5 units/µl)	0.05 units/µl	0.5
ExTaq Buffer	1x	5
H_2O	-	37.7

Table 2.8: Composition of the PCR reaction mixture

The PCR conditions used in this study are as follows:

Temperature (^oC)	Time (mins)	Cycles
95	5	1
94	1	
55	1	35
72	5	
72	20	1
4	Hold	-

Table 2.9: PCR Conditions

Gel electrophoresis was carried out using 0.8% agarose gel (0.48 g Electran Agaraose (VWR International), 60 ml 1x TAE buffer, 10 µl of SYBR SAFE). The gel tank contained 1xTAE buffer. 6X blue loading buffer (0.25% bromophenol blue, 0.25% xylene cyanol, 15% ficoll, 120 mM EDTA pH 8.0 in dH_20) was added to DNA samples to a final concentration of 1X. 5 µl 1 kb DNA Ladder (250 µg)

(Invitrogen) was run alongside samples to indicate band size. Electrophoresis was conducted at 80V for 45 minutes to 1 hour depending on the size of band being detected. Visualisation of gels was carried out using the Fuji LAS 4000 imager. Any gel extraction under taken was carried out by excising the correct band from the gel and isolating the DNA using a QiaQuick Gel Extraction kit, following the supplied protocol.

2.2.12 Lithium acetate transformation of yeast cells

Transformations of yeast strains by PCR products or plasmids were carried out using a LiAC transformation protocol. PCR products were initially purified by the following protocol to generate transforming DNA:

40 µl	PCR product
0.8 µl	0.5 M EDTA
4 µl	3 M NaAc pH 5.2
120 µl	Isopropanol

The mixture was precipitated at -20^{o}C for 10 minutes, before being spun in a centrifuge for 10 minutes at 13,000 rpm. The pellet was washed with 500 µl 70% ethanol, spun again for 10 minutes at 13,000 rpm, the supernatant removed and the ethanol evaporated off, before resuspension in 10 µl dH_2O.

25 ml of fresh YEPD was inoculated with cells from a saturated overnight culture of the recipient yeast strain, and incubated at 23^{o}C until the cell count doubled twice, confirmed by cell count using a haemocytometer, and the equation:

$$\frac{25}{\text{No. of grids}} \times \text{No. of cells counted} \times 10^4$$

The yeast culture was spun in a centrifuge to yield a pellet of yeast cells, then washed with 50 ml dH_2O, followed by a wash with 5 ml LiAc/TE (10 mM Tris-Cl, 0.1 mM EDTA, 0.1 M LiAc, pH 7.5), before being resuspended in 1 ml of LiAc/TE. Transforming DNA was added to 100 µl of yeast suspension, along with 10 µl of

Salmon sperm DNA (10 µg/µl). 700 µl of 40% PEG in LiAc/TE (8 ml 50% PEG, 1 ml 10 x LiAc, 1 ml 10 x TE) was added and then vortexed to mix, before incubating at 30°C for 30 minutes. Following incubation, 70 µl DMSO was added and then heat shocked at 42°C for 15 minutes. The reaction was then chilled on ice for 1-2 minutes, before being spun at 6000 rpm for 3 minutes, resuspended in 1 x TE and plated onto appropriate selective medium. Plates were incubated at 23°C for 2-3 days (or until colonies appeared) before colony purification to select for transformed yeast.

When transforming yeast strains with plasmids, the same protocol was followed, apart from the purification step of the transforming DNA. Instead, 5 µl of plasmid was added directly to the yeast suspension, along with Salmon sperm DNA.

2.2.13 Strain verification

The genotype of generated strains was verified using PCR. Reverse primers which bound downstream of the start codon of the marker cassette (~ 500 bp into the KanMX cassette, ~ 200 bp into the NatMx cassette) were used in conjunction with forward primers which bound within the region upstream of the deleted gene. The presence of a band of around 800 bp indicated correct transformation and location of the cassette. Wild type strains and, where possible, original S288C versions of the gene deletion strains, were tested as negative and positive controls respectively.

2.2.14 Mating of haploids, sporulation and tetrad scoring

Diploid strains were generated through mating of two strains of opposite mating type (MATa x MATα). Mating occurred through streaking of the strains together on a YEPD plate and incubation at 23°C overnight. Successful diploid strains were identified using selection on plates containing the appropriate marker or lacking the appropriate amino acid which diploid strains were able to grow but haploid parent strains were not. Selection plates were incubated at 23°C overnight and the process repeated to select against a second marker and identify diploid strains.

Diploid yeast strains were grown to saturation overnight in 2 ml of YEPD at 23°C then spun at 13,000 rpm for 1 minute. The pellet was washed in dH_2O twice then resuspended in 2 ml 1% KOAc and incubated for 2-3 days at 23°C. Sporulated yeast culture were spun down and washed with dH_2O twice, then resuspended in 1 ml dH_2O, and stored at 4°C. 1.2 µl glusulase (DuPont NEN Research Products) was added to a 50 µl aliquot of the sporulated yeast suspension and incubated at 30°C for 12 minutes. The digested spores were placed on ice and 1 ml dH_2O added. 50 µl of the digested spores were spread on a YEPD plate and dissected using a Microtec tetrad microscope. The plates were incubated at 23°C for 2-3 days, before the tetrads were streaked out onto fresh a YEPD plate and grown for a further day at 23°C.

Plates were replicated using velvets onto appropriate selective media for identification of genotype and mating type, assessed by mating with MATa and MATα strains. Growth was scored after 2-3 days incubation at 23°C (or 36°C, when identifying temperature-sensitive *cdc13-1* strains) to determine genotype. Haploids with the desired phenotype were stored in 15% glycerol at -80°C as part of the yeast strain library.

2.2.15 Spot test growth assays

Yeast strains were grown to saturation in 2 ml YEPD media at 23°C overnight. Saturated cultures were serially diluted 5-fold in fresh YEPD in a 96-well plate. Yeast cultures were then transferred onto solid agar YEPD plates (or appropriate media plates) using a sterilised 48-pin replica plating tool (Sigma), and left to dry. The plates were then placed at a range of temperatures for several days, determined by the genotype of the yeast strains being tested.

2.3 G6PDH assay

2.3.1 Culture inoculation and time course

150 µl saturated cultures were inoculated in 120 ml fresh YEPD and incubated overnight at 23°C at 180 rpm. Total cell number was counted using a haemocytometer and cells were diluted in fresh YEPD to a 120 ml culture at 8 x 10^6 cells/ml. Flasks were returned to 23°C for 2-2.5hrs or until cell density reached 1.5 x 10^7 cells/ml. Total bud numbers were counted, 1 x 3 ml and 1 x 1 ml samples of cultures were taken (T = 0) and cultures divided into two flasks and diluted in fresh YEPD to 100 ml cultures at 8 x 10^6 cells/ml. In temperature-dependent experiments, one flask was returned to 23°C and one flask was placed at 36°C. In α-factor dependent experiments, α-factor (Sigma; 1:25,000 dilution of 5 x 10^{-4} M; 0.842 mg/ml in H_2O stock) was added to a concentration of 20 nM. 1 x 3 ml and 1 x 1 ml samples of cultures were taken 15, 60, 120, 180 and 240 minutes after dilution and the start of incubation. Total bud numbers were counted after 90 and 180 minutes and cultures diluted in fresh YEPD to 100 ml cultures at 8 x 10^6 cells/ml. Where applicable, the α-factor concentration was maintained at 20 nM.

2.3.2 Protein extraction

Cells were harvested from 3 ml samples by low-speed centrifugation at 3,000 rpm for 3 minutes. The cell pellet was washed with cold 5 ml 10 mM potassium phosphate buffer (pH 7.5) containing 2 mM EDTA, then resuspended in 1 ml of the same buffer and transferred to a 1.5 ml eppendorf tube. Cells were harvested by low-speed centrifugation, the supernatant aspirated then stored at -80°C immediately. To extract the cell lysates, the pellet was thawed on ice then resuspended in 100 µl cold 100 mM potassium phosphate buffer (pH 7.5) containing 2 mM $MgCl_2$ and 1 mM DTT and transferred to a 2 ml screw cap tube. 200 µl 0.5 mm glass beads were added to the screw cap tube, then cells were lysed using a ribolyser (5.5 for 30 seconds). Samples were stored on ice for ~2 minutes then lysis repeated. Cell breakage was checked under a microscope. Using scissors, the lids were removed from 1.5 ml eppendorf tubes. The 2 ml screw cap tubes were punctured using a needle and placed inside the lidless-eppendorfs, then centrifuged

at 2,000 rpm for 2 minutes. The screw cap tubes were removed and eppendorf lids were replaced. Cell debris was separated out by high-speed centrifugation (13,200 rpm for 10 minutes) and the supernatant transferred to a fresh 1.5 ml eppendorf. Protein concentration of supernatant was determined using Bradford assay (Bradford, 1976) and samples diluted to 200 µg/ml using 100 mM potassium phosphate buffer (pH 7.5) containing 2 mM $MgCl_2$ and 1 mM DTT. Cell extract samples were stored at -20^{o}C.

2.3.3 Enzymatic assays

Enzyme assays were carried out in triplicate to determine average reading. Assay buffer was prepared as below:

Reagent	Stock concentration	Volume (µl)	Final concentration
Cell extract	200 µg/ml	15	30 µg/ml
dH_2O	-	68.5	-
Tris HCl (0.5 M)	500 mM	10	50 mM
$MgCl_2$ (1 M)	1 M	0.5	5 mM
$NADP^+$ (0.04 M)	40 mM	1	0.4 mM
G-6-P (0.1 M)	100 mM	5	5 mM
Total Volume	-	100	-

Table 2.10: G6PDH reaction mixture

15 µl cell extract (or 15 µl H_2O) and 80 µl assay buffer were added per well to 96-well plate. Absorbance at 340 nm was measured in a FLUOstar plate reader (BMG Labtech) at 37^{o}C. 5 µl glucose-6-phosphate was added to each well using a multichannel pipette and the plate was tapped to mix. Absorbance was measured at 340 nm after 1, 5 and 10 minutes. Average absorbance was calculated and specific activity calculated using the following equation:

$$\mu\text{mol of NADP reduced/min/mg protein} = \frac{\left(\frac{\mu\text{mol of NADP reduced}}{\text{min}}\right)}{\text{mg protein}}$$

2.3.4 Determination of cell cycle position

1 ml samples of cultures were spun at top speed (13,200 rpm) for 1 minute. Cell pellets were then washed with 1 ml H_2O then resuspended in 200 µl 70% ethanol and incubated at room temperature for 1 hour. Samples were washed twice with 1 ml H_2O and resuspended in 200 µl DAPI (4',6-diamidino-2-phenylindole, Sigma) in H_2O. Samples were sonicated for 6 seconds at an amplitude of 5 microns and 8 µl aliquot was examined under a fluorescence microscope (Nicon eclips 50i, 40x objective). A multicounter was used to counter the proportion of 100 cells in each cell cycle stage, following the below classification system, taken from (Zubko et al., 2006).

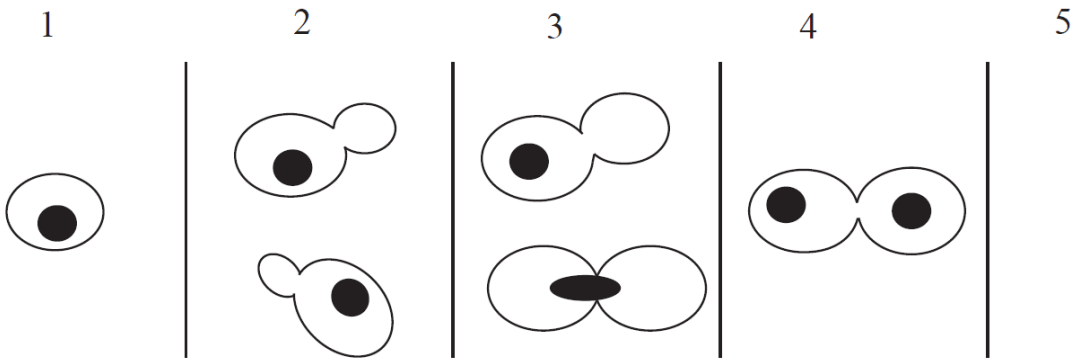

Cell cycle analysis. Classifications are 1: no bud, single cell, single nucleus. 2: Bud < 50% diameter of mother cell. Single nucleus. 3: Bud > 50% diameter of mother cell. Single nucleus. 4: Two buds, two nuclei. 5: none of the other types

3 The pentose phosphate pathway protects against sensitivity to the G-quadruplex-binding ligand TMPyP4

3.1 Introduction

G-quadruplexes are nucleic acid structures which can form within guanine-rich regions of DNA and RNA. As described in Chapter 1.2, G-quadruplexes have been predicted to form in key regions of the chromosome such as the centromeres, promoter regions and the G-rich telomeres. Stabilising G-quadruplexes through the binding of ligands has consequences for transcription and can prevent the action of telomerase (Mikami-Terao et al., 2009; Mikami-Terao et al., 2008; Grand et al., 2002). For this reason, G-quadruplex-stabilising ligands are under investigation for their potential use as anti-cancer drugs.

One such G-quadruplex binding ligand is the cationic porphyrin TMPyP4 (5,10,15,20-tetratkis-(N-methyl-4-pyridyl)-21,23-H-porphyrin). It is thought that TMPyP4 binds to the outside of the G-quadruplex and stabilises the folded nucleic acid structure as shown in Figure 3.1a (Wei et al., 2006; Phan et al., 2005; Haq et al., 1999). TMPyP4 has been shown to act against certain cancer cell lines, such as retinoblastoma cells, MX-1 mammary tumours and PC-2 human prostate carcinomas (Mikami-Terao et al., 2009; Mikami-Terao et al., 2008; Grand et al., 2002). It has also been demonstrated that TMPyP4 has the ability to inhibit telomerase *in vitro*. The presence of TMPyP4 also affects the c-MYC oncogene-dependent transcription of several genes including TERT, the human homologue of the *S. cerevisiae* telomerase subunit Est2 (Grand et al., 2002).

In order to study the mechanisms of TMPyP4 action and the effect of TMPyP4 treatment at the cellular level, I studied the responses of a genome-wide single deletion library of budding yeast strains to the presence of the G-quadruplex binding ligand. I hoped that studying the differential sensitivity to TMPyP4 of deletion strains would provide some insight into TMPyP4 action. Given that TMPyP4 has a

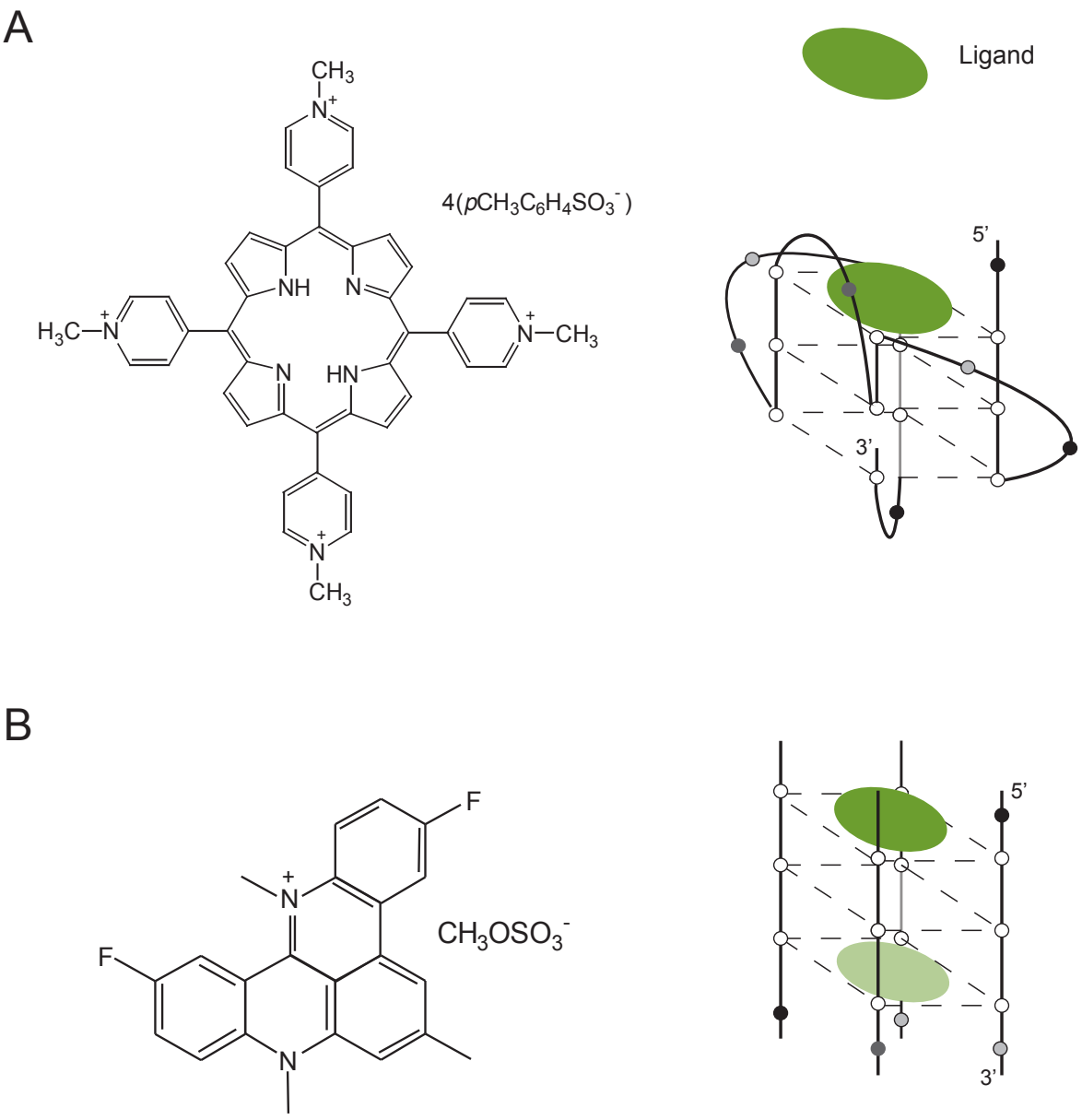

Figure 3.1: Structure and binding locations of two G-quadruplex binding ligands
The chemical structure of **(a)** TMPyP4 and **(b)** RHPS4 and the predicted binding sites of the ligands to compatible G-quadruplex conformations.

proven ability to bind G-quadruplexes and inhibit telomerase activity, I expected to find a trend towards telomere-, telomerase- or DNA damage response-related deletions displaying differential sensitivity towards the G-quadruplex binding ligand.

In addition to screening the gene deletion collection for TMPyP4-sensitivity, I also screened for sensitivity to RHPS4 (3,11-difluoro-6,8,13-trimethyl-8H-quino[4,3,2-kl]acridinium methosulfate), another G-quadruplex binding ligand (Cookson et al., 2005). RHPS4 is a pentacyclic acridine and binds to G-quadruplexes in a different manner and location compared with TMPyP4 (Figure 3.1b) (Gavathiotis et al., 2003; Gavathiotis et al., 2001). RHPS4 has also demonstrated efficacy against cancer cell lines, such as MCF-7 breast cancer cells and uterus carcinoma cells (Phatak et al., 2007; Cookson et al., 2005). Therefore, I wanted to discern whether there was any correlation or similarities between gene deletion strains which were sensitive to the two G-quadruplex binding ligands, in order to try and elucidate a common mechanism by which G-quadruplex binding ligands function.

3.2 Results

3.2.1 G-quadruplexes location and TMPyP4-sensitivity in S. cerevisiae

The sequence necessary for potential G-quadruplex formation was determined by Huppert and Balasubramanian (2005). Their *Folding Rule* states: "A sequence of the form $d(G_{3+}N_{1-7}G_{3+}N_{1-7}G_{3+}N_{1-7}G_3)$ will fold into a quadruplex under near-physiological conditions." The *quadparser* computer algorithm was developed to rapidly analyse genomic data and identify regions in which G-quadruplexes could emerge (potential quadruplex sequences, PQSs) (Huppert and Balasubramanian, 2005). Data on the location of PQSs within the *S. cerevisiae* genome was downloaded from the quadruplex.org database, including the genomic coordinates, strand and sequence for each PQS (Wong et al., 2010a; Wong et al., 2010b), and using this data, the relative positions of regions with G-quadruplex forming potential within the yeast genome were plotted (Figure 3.2). The algorithm identified 11 PQSs proximal to the telomeric regions of 7 yeast chromosomes, and 27 PQSs spread throughout the rest of the genome (Wong et al., 2010a). Unlike studies of the human genome, in which G-quadruplex forming sequences were found in the promoter of c-MYC, few to none of these non-telomeric PQSs seem to be located in the promoter regions of key genes (Huppert and Balasubramanian, 2005; Seenisamy et al., 2004; Grand et al., 2002). The identification of PQSs within the *S. cerevisiae* genome indicate that it is appropriate to test a ligand targeted to these sequences in yeast.

I aimed to study the differential sensitivity of single gene deletion strains to the G-quadruplex binding ligand TMPyP4, in order to determine mechanism of the ligand's action, targets and the cellular response to TMPyP4. A small scale test with several gene deletion strains in the W303 background indicated that exposure to 100 μM TMPyP4 resulted in a growth defect (Figure 3.3). Therefore I tested the differential sensitivity of the gene deletion collection to 100 μM TMPyP4 at 30^{o}C.

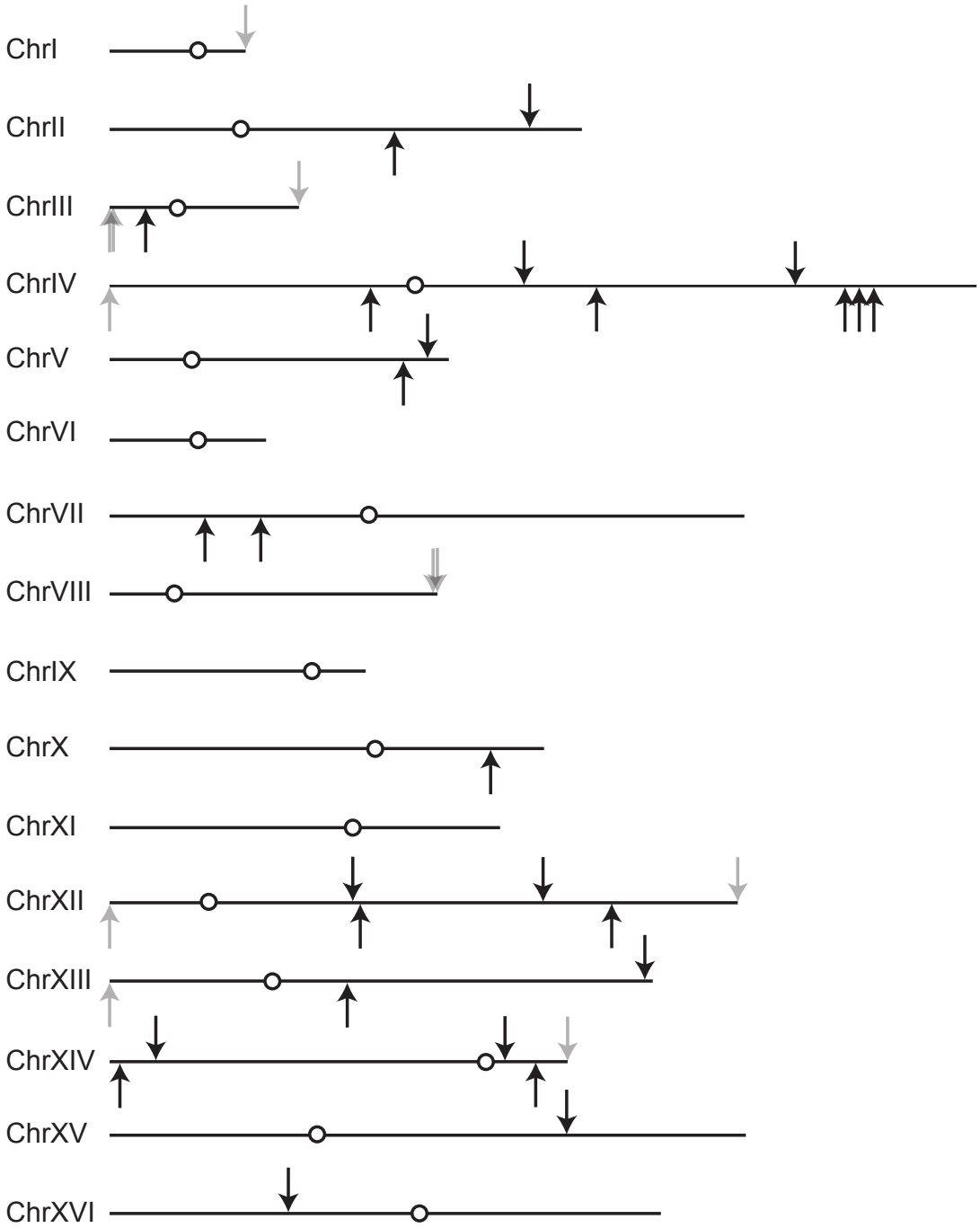

Figure 3.2: Relative positions of predicted sites of G-quadruplex formation
Location of putative quadruplex sequences (PQSs) within the S. cerevisiae genome. Arrows indicate PQSs, where down arrows = Watson, up arrows = Crick, pale arrows represent predicted telomeric PQSs and circles denote centromeres. Data taken from the quadruplex.org database (Wong et al., 2010a)

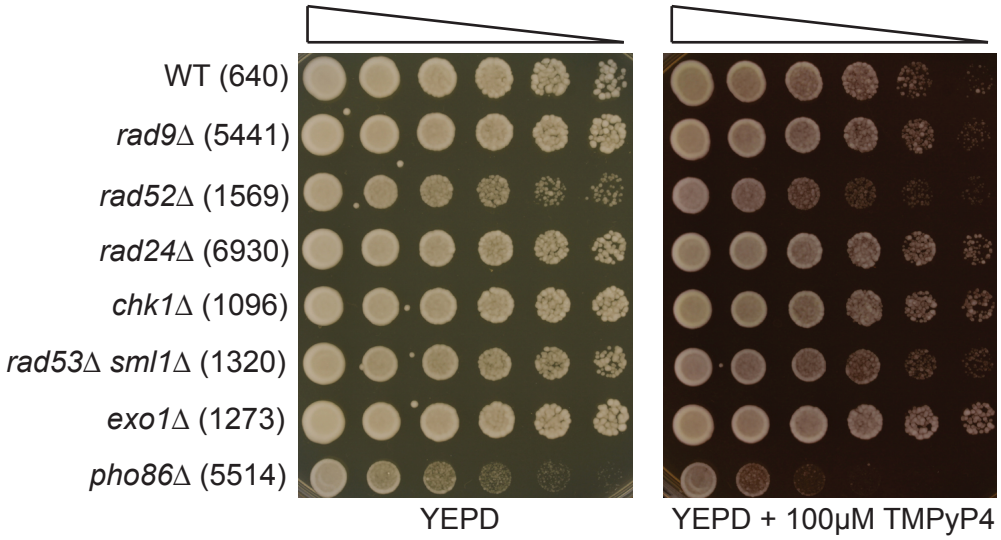

Figure 3.3: Treatment with TMPyP4 causes a reduction in growth
Strains were grown to saturation in YEPD before a 5-fold serial dilution and pinning onto plates containing and lacking 100 μM TMPyP4. Both plates were incubated at 30°C for 3 days.

3.2.2 A genome-wide screen found TMPyP4-sensitive yfg∆ strains

Using a genome-wide collection of around 4,300 *S. cerevisiae* gene deletion strains (*yfg*∆, **y**our **f**avourite **g**ene deletion, which indicates any of the viable systematic gene deletions), I screened for differential sensitivity to TMPyP4. Figure 3.4a demonstrates how variable the TMPyP4-sensitivity was from strain to strain. Plate 10 (of 15) contained the second most sensitive deletion strain, *ccs1*∆ (highlighted in pink) which as demonstrated in the figure grew on control media but failed to grow on media containing TMPyP4. However other strains, such as *asc1*∆ (highlighted in blue) grew on both media. The screen was replicated four times and quantitative fitness analysis (QFA) was performed by Conor Lawless as described by Addinall et al. (2011). Briefly, the fitness of each individual culture in the screen was deduced through time course photography of the agar plates and image processing and data analysis, followed by calculation of maximum doubling rate (MDR) and maximum doubling potential (MDP) of the single deletion mutant strains by fitting logistic growth model parameters to growth curves (Figure 3.4b). Strain fitness was defined as the product of MDP and MDR (Fitness, F, population doublings^2/day).

When comparing the fitness of each deletion strain on media supplemented with TMPyP4 with fitness on media lacking the compound (Figure 3.4c), it can be observed that the presence of TMPyP4 causes a reduction in growth across the population. Each point on the graph represents a single deletion mutant. The dashed grey line indicates equal growth on both control media and media containing TMPyP4, and the solid grey line indicates expected fitness based on the population model (linear regression). There is a clear difference between the two lines, which indicates around 40% reduction in growth across the population when exposed to TMPyP4 in comparison to growth on media lacking the ligand. However, it is worth noting that a proportion of this 40% reduction observed is a result of the difference in agar colour between control and TMPyP4 plates, due to the colour of the compound.

The vertical distance of the points on the graph from the expected fitness linear regression model can be used to estimate the fitness differential (FD) for each *yfg*∆. Studying the data in closer detail, I used an arbitrary cut-off of FD $\geq$ 0.5 to define gene deletions which suppress the TMPyP4-induced fitness defect and defined those

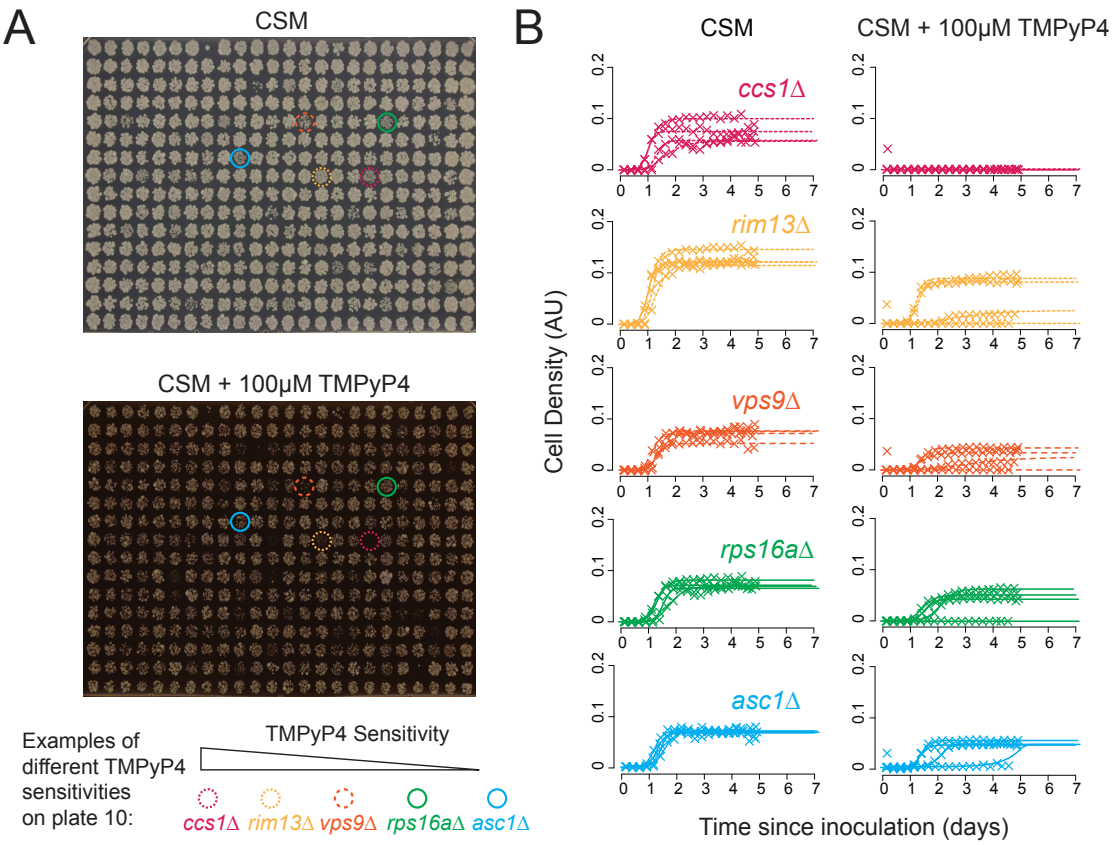
A
CSM
CSM + 100μM TMPyP4
Examples of different TMPyP4 sensitivities on plate 10:
TMPyP4 Sensitivity
ccs1Δ rim13Δ vps9Δ rps16aΔ asc1Δ
B
CSM
CSM + 100μM TMPyP4
ccs1Δ
rim13Δ
vps9Δ
rps16aΔ
asc1Δ
Cell Density (AU)
Time since inoculation (days)

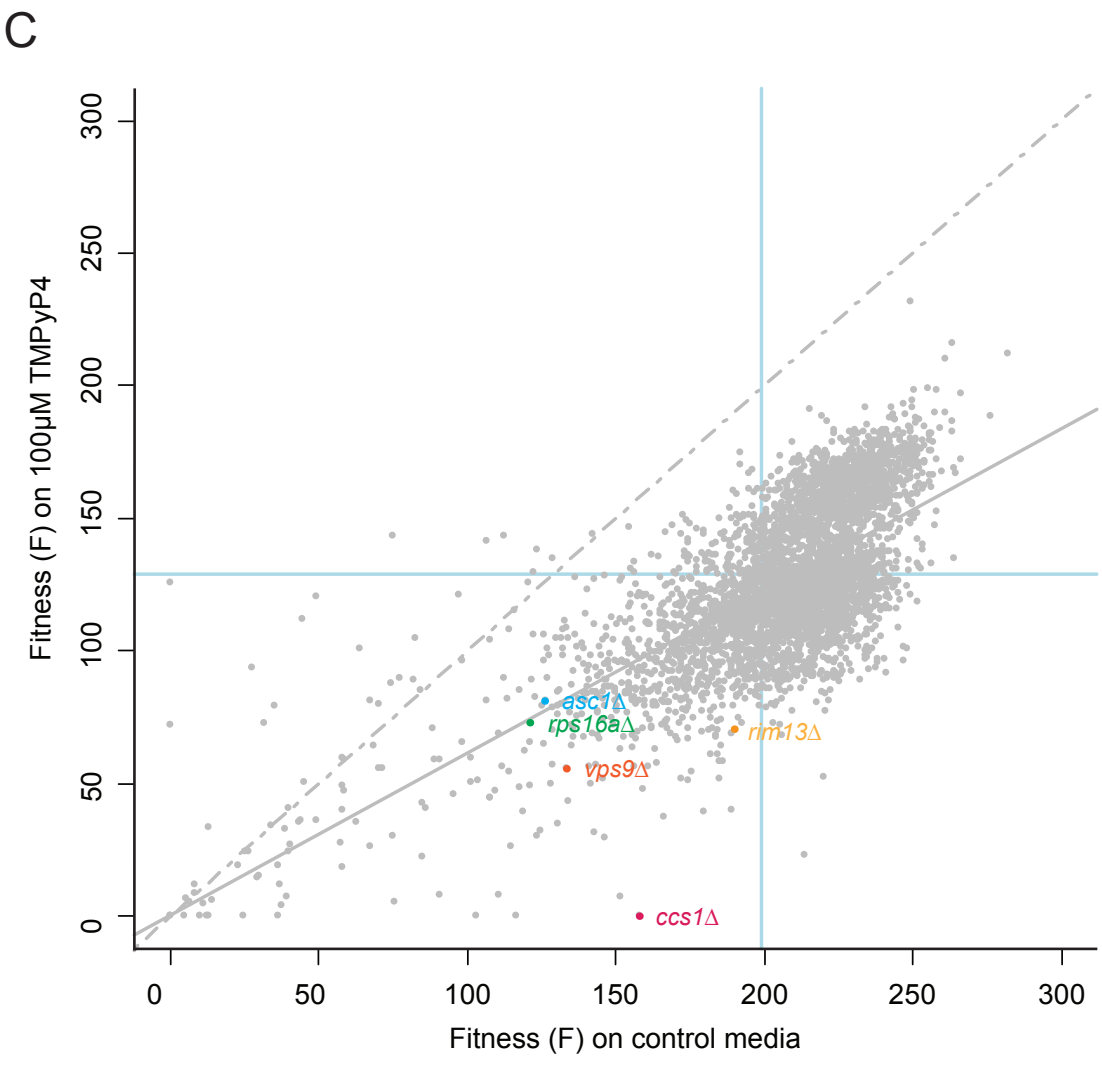
C
Fitness (F) on 100μM TMPyP4
Fitness (F) on control media
asc1Δ
rps16aΔ
rim13Δ
vps9Δ
ccs1Δ

Figure 3.4: Image analysis and statistical modelling of the genome-wide screen
Image analysis and calculation of the growth fitnesses of single deletion strains on control media (CSM) and CSM containing 100 μM TMPyP4. Five different gene deletion strains are highlighted throughout the figure to demonstrate the methodology. **(a)** Plate 10 of 15 of the genome-wide screen grown on CSM and CSM containing 100 μM TMPyP4. Images were taken after 3 days incubation at 30^{o}C. Circles highlight the position of the five gene deletion strains on CSM and TMPyP4 plates. **(b)** Image analysis of individual replicate cultures determined cell density of the four genes highlighted in **(a)** and the logistic growth model was fitted to each culture density time-series. Average maximum Doubling Rate (MDR) and Maximum Doubling Potential (MDP) were determined from the fitted curves. **(c)** The growth fitness (Fitness, F, population doublings2/day) of ~4,300 single gene deletion mutants on control media compared with the growth fitness on media containing 100 μM TMPyP4. Fitness = product of maximum doubling rate (MDR) and maximum doubling potential (MDP) of the single deletion mutant strains. Each point on the graph represents a single deletion mutant. Dashed grey line denotes equal growth on CSM and CSM containing 100 μM TMPyP4. Solid grey line denotes expected fitness based on the population model (linear regression). Blue lines indicate the average position of *his3*Δ strains (a proxy for 'wild type' growth).

with a FD ≤ -0.5 as enhancing the TMPyP4-induced fitness defect. Using these parameters, 76 gene deletions were classified as TMPyP4-resistant and 107 gene deletions were defined at TMPyP4-sensitive by the genome-wide screen.

3.2.3 19 null mutations cause TMPyP4-sensitivity

In order to confirm the results of the genome-wide study, the high-throughput screen was repeated by Stephanie Merchan using the same single deletion library and growth conditions; however, a simpler method of fitness analysis was used (carried out by Darren Wilkinson), based on single time-point data. This end-point assay provided another 4 replicates of the screen and therefore a large amount of data for each gene deletion strain. The fitness definition used in the second screen differed from the one carried out in the analysis of data from the first screen, since the fitness for each *yfg*Δ in the second screen was calculated from cell density estimate from the final time point. Therefore, I defined TMPyP4 tolerance in the second screen as final fitness differential (FFD). Arbitrary cut-offs were again used to define TMPyP4-resistant and –sensitive strains (FFD ≥ 0.25 and FFD ≤ -0.2 respectively).

The results from the two screens were compared (Figure 3.5), and there were a number of genes which, when deleted, resulted in increased sensitivity or resistance to the porphyrin in both screens (Table 3.1). 19 null mutations resulted in increased sensitivity to TMPyP4 and two null mutations resulted in reduced sensitivity to the G-quadruplex binder in both screens. Therefore repetition of the screen provided a list of gene deletions which I could be confident caused sensitivity to TMPyP4.

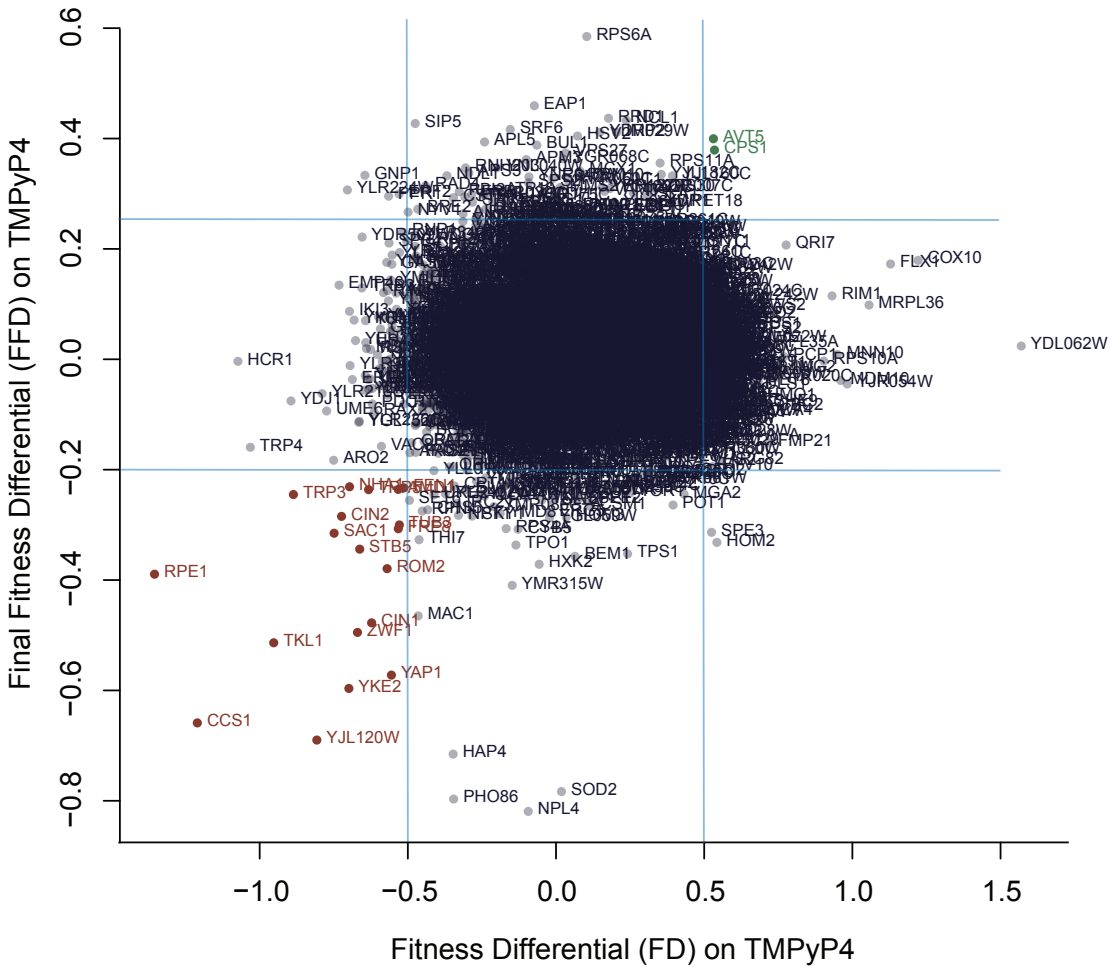

Figure 3.5: Comparison of screen data reveals TMPyP4-sensitive strains
Correlation plot of fitness differential values from two genome-wide screens for TMPyP4-sensitivity (correlation = 0.066). Genes in red (bottom left-hand corner) were found to increase TMPyP4-sensitivity when deleted according to both experiments (FD ≤ -0.5 in the initial screen and FFD ≤ -0.2 in the follow-up screen). Genes in green (top right-hand corner) were found to decrease TMPyP4-sensitivity when deleted according to both experiments (FD ≥ 0.5 in the initial screen and FFD ≥ 0.25 in the follow-up screen). Blue lines denote FD thresholds.

ORF	Gene	SGD Description
Sensitive		
YMR038C	*CCS1*	Copper chaperone for superoxide dismutase Sod1p, involved in oxidative stress protection
YJL120W	*YJL120W*	Dubious open reading frame unlikely to encode a protein; partially overlaps the verified gene YJL121C/RPE1
YPR074C	*TKL1*	Transketolase, similar to Tkl2p; catalyzes reactions in the pentose phosphate pathway
YJL121C	*RPE1*	D-ribulose-5-phosphate 3-epimerase, catalyzes a reaction in the non-oxidative part of the pentose-phosphate pathway
YLR200W	*YKE2*	Subunit of the heterohexameric Gim/prefoldin protein complex involved in the folding of alpha-tubulin, beta-tubulin, and actin
YNL241C	*ZWF1*	Glucose-6-phosphate dehydrogenase (G6PD), catalyzes the first step of the pentose phosphate pathway
YKL212W	*SAC1*	Phosphatidylinositol phosphate (PtdInsP) phosphatase involved in hydrolysis of PtdIns[4]P
YPL241C	*CIN2*	GTPase-activating protein (GAP) for Cin4p; tubulin folding factor C involved in beta-tubulin (Tub2p) folding
YHR178W	*STB5*	Transcription factor, involved in regulating multidrug resistance and oxidative stress response
YOR349W	*CIN1*	Tubulin folding factor D involved in beta-tubulin (Tub2p) folding
YKL211C	*TRP3*	Bifunctional enzyme exhibiting both indole-3-glycerol-phosphate synthase and anthranilate synthase activities
YLR371W	*ROM2*	GDP/GTP exchange factor (GEF) for Rho1p and Rho2p
YML007W	*YAP1*	Basic leucine zipper (bZIP) transcription factor required for oxidative stress tolerance
YLR138W	*NHA1*	Na+/H+ antiporter involved in sodium and potassium efflux through the plasma membrane
YGL026C	*TRP5*	Tryptophan synthase, catalyzes the last step of tryptophan biosynthesis
YLR047C	*FRE8*	Protein with sequence similarity to iron/copper reductases, involved in iron homeostasis
YML124C	*TUB3*	Alpha-tubulin; associates with beta-tubulin (Tub2p) to form tubulin dimer, which polymerizes to form microtubules
YML035C	*AMD1*	AMP deaminase, tetrameric enzyme that catalyzes the deamination of AMP to form IMP and ammonia
YCR034W	*FEN1*	Fatty acid elongase, involved in sphingolipid biosynthesis
Resistant		
YBL089W	*AVT5*	Putative transporter, member of a family of seven S. cerevisiae genes (AVT1-7) related to vesicular GABA-glycine transporters
YJL172W	*CPS1*	Vacuolar carboxypeptidase yscS; expression is induced under low-nitrogen conditions

Table 3.1: TMPyP4-sensitive and -resistant gene deletion strains

3.2.4 TMPyP4-sensitive gene deletion strains include PPP-related genes

Gene Ontology (GO) analysis of the 19 null mutations which resulted in higher sensitivity to TMPyP4 than the rest of the population revealed that over-represented terms include the pentose phosphate shunt, nucleotide metabolic process and tryptophan biosynthetic process (Table 3.2).

Gene Ontology Term	**Genes annotated to the term**	***p*-value**
Pentose phosphate shunt	*RPE1, ZWF1, TKL1*	3.60E-04
Heterocycle metabolic process	*TRP5, RPE1, TRP3, ROM2, AMD1, ZWF1, TKL1*	5.20E-04
Nucleotide metabolic process	*RPE1, ROM2, AMD1, ZWF1, TKL1*	4.07E-03
Tryptophan biosynthetic process	*TRP5, TRP3*	9.21E-03

Table 3.2: GO analysis of TMPyP4-sensitive gene deletion strains

Over 25% of the genes which, when deleted, cause TMPyP4-sensitivity encode proteins with links to the pentose phosphate pathway (PPP): *ZWF1, RPE1, TKL1, YJL120W* and *STB5*. Zwf1, the yeast glucose-6-phosphate dehydrogenase (G6PDH), catalyses the initial rate-limiting step of the oxidative phase of the PPP (Reaction 3 in Figure 1.6) and plays an important role in the response to oxidative stress through NADPH production in the reaction it catalyses. *RPE1* encodes Rpe1, a D-ribulose-5-phosphate 3-epimerase, and the reaction it catalyses forms one of the steps linking the oxidative and non-oxidative phases of the PPP together (Reaction 6 in Figure 1.6). *YJL120W* is a dubious open reading frame which partially overlaps with the *RPE1* gene and therefore may confer its sensitivity upon deletion due to disruption of Rpe1 expression. *TKL1* encodes the transketolase Tkl1, which plays a major role in the non-oxidative phase of the PPP (Reactions 8 and 10 in Figure 1.6). Upregulation of a mutant form of the human transketolase, TKTL1, is linked with various cancers (Chen et al., 2009; Krockenberger et al., 2007; Langbein et al., 2006).

The transcription of many PPP genes is regulated by Stb5, a transcription factor encoded for by *STB5* which is involved in multidrug resistance and the oxidative stress response (Cadière et al., 2010; Larochelle et al., 2006). The precursor for nucleotide synthesis, ribose-5-phosphate, is produced by the PPP (by reactions 7 and 8 in Figure 1.6). Amd1 catalyses the deamination of AMP to form IMP and ammonia, and therefore may be involved in regulation of intracellular adenine

nucleotide pools. This provides a further link between the PPP and sensitivity to TMPyP4, and therefore this sensitivity could either be due to the nucleotide production process, the oxidative stress response or an as yet unknown process.

The pentose phosphate pathway is not the only functionally related group of deletion strains that were found through the screen to be TMPyP4-sensitive. The deletion of *YKE2*, *TUB3*, *CIN1* and *CIN2*, all of which are involved in tubulin folding and microtubule formation, also caused TMPyP4-sensitivity. *YKE2* encodes a subunit of the heterohexameric Gim/prefolding protein complex which is involved in the folding of alpha-tubulin, beta-tubulin and actin (Siegers et al., 1999; Geissler et al., 1998). *TUB3* is one of two alpha-tubulin encoding genes (the other being *TUB1*). Alpha- and beta-tubulin form tubulin heterodimers, which polymerise to form microtubules. Cin1 (the homolog of mammalian cofactor D) and Cin2 (the tubulin cofactor C homolog) are involved in folding of the beta-tubulin Tub2 (Feierbach et al., 1999; Hoyt et al., 1997; Stearns et al., 1990). Cin2 also acts as a GTPase-activating protein (GAP) for Cin4 (Veltel et al., 2008). The mechanisms by which tubulin processing responds to G-quadruplex binding are unclear. Tubulin polymerisation or stabilisation of microtubules can arrest cells in mitosis, and therefore some anti-cancer agents target tubulin (Li and Sham, 2002). TMPyP4, along with other G-quadruplex binding ligands, induces elongated chromosomes incapable of separating in anaphase (Izbicka et al., 1999). Deletion of key microtubule formation genes may therefore exacerbate difficulties in chromosome segregation, resulting in increased TMPyP4-sensitivity.

The deletion of *CCS1* and *YAP1*, genes which both encode proteins with roles in the oxidative stress response (a copper chaperone for the superoxide dismutase Sod1 and a transcription factor which regulates anti-oxidant gene expression, respectively) also causes sensitivity to TMPyP4 (Moye-Rowley, 2002; Gasch et al., 2000; Culotta et al., 1997). Additionally, deletion of genes involved in tryptophan biosynthesis (*TRP3* and *TRP5*) also induces a fitness differential on media supplemented with TMPyP4. The remaining sensitive genes in Table 3.1 encode proteins involved in phosphatidylinositol (PtdInsP) biosynthesis (*SAC1*), GDP/GTP exchange for Rho1 and Rho2 (*ROM2*), Na+/H+ transport (*NHA1*), iron homeostasis (*FRE8*) and fatty acid elongation (*FEN1*). Interestingly, I did not observe any

telomere- or DNA damage response-related genes amongst those which displayed differential sensitivity to TMPyP4 in both screens; instead, the results from the screen prominently feature the pentose phosphate pathway.

3.2.5 ppp∆ strains are sensitive to TMPyP4 in the W303 background

The data from the genome-wide screen suggest that there is a link between pentose phosphate pathway (PPP) dysfunction and sensitivity to TMPyP4. The major roles of the PPP in eukaryotes are in the production of NADPH and in ribose-5-phosphate generation. Therefore, I wanted to explore the PPP and its link with TMPyP4 further. In order to confirm the results from the genome-wide screen, I carried out a serial dilution spot test of *ppp*∆ strains in the W303 background (Figure 3.6a), which differs from the background used in the screen (S288C). As observed in the high-throughput screen, deletion of *RPE1*, *ZWF1* and *TKL1* resulted in sensitivity to TMPyP4. I also tested the sensitivity of a *tal1*∆ strain, which, according to the screen data, is not TMPyP4-sensitive. *TAL1* encodes the transaldolase Tal1 which catalyses a reaction in the non-oxidative phase of the PPP (Reaction 9 of Figure 1.6). My spot test confirmed that *TAL1* deletion does not cause TMPyP4-sensitivity. This may be due to the role of Tal1 in the PPP, which may not be essential for the resistance to the G-quadruplex binding ligand, or deletion of the gene does not result in the metabolic changes necessary to cause TMPyP4-sensitivity. Additionally, not all *ppp*∆ strains are sensitive to the same oxidants (Krüger et al., 2011) Alternatively, the functional transaldolase homologue Nqm1 may compensate for the lack of transaldolase activity due to *TAL1* deletion (Huang et al., 2008).

I hypothesised that the sensitivity to TMPyP4 exposure caused by deletion of PPP-related genes is due to disruption of the metabolic pathway. I therefore hypothesised that combining several *ppp*∆ mutations in the same strain should not alter the sensitivity to TMPyP4. If the TMPyP4-sensitivity caused by deleting *RPE1*, *ZWF1* and *TKL1* were due to differing methods, rather than PPP dysfunction, one would expect to see an increase in sensitivity upon combining PPP gene deletions. Figure 3.6a demonstrates that deleting several PPP genes together in the same strain and growing them in the presence of TMPyP4 results in similar fitnesses to the equivalent single deletion strains. In addition, deletion of *TAL1* in several of these strains does not suppress sensitivity to the G-quadruplex binding ligand. For instance, *tal1*∆ *rpe1*∆ demonstrates the same TMPyP4-sensitivity as *rpe1*∆ alone, which implies that *TAL1* deletion does not provide resistance to TMPyP4 treatment. This suggests that the sensitivity to TMPyP4 is caused by disruption of the same pathway – the PPP – rather than alternative reasons, and the lack of alteration in

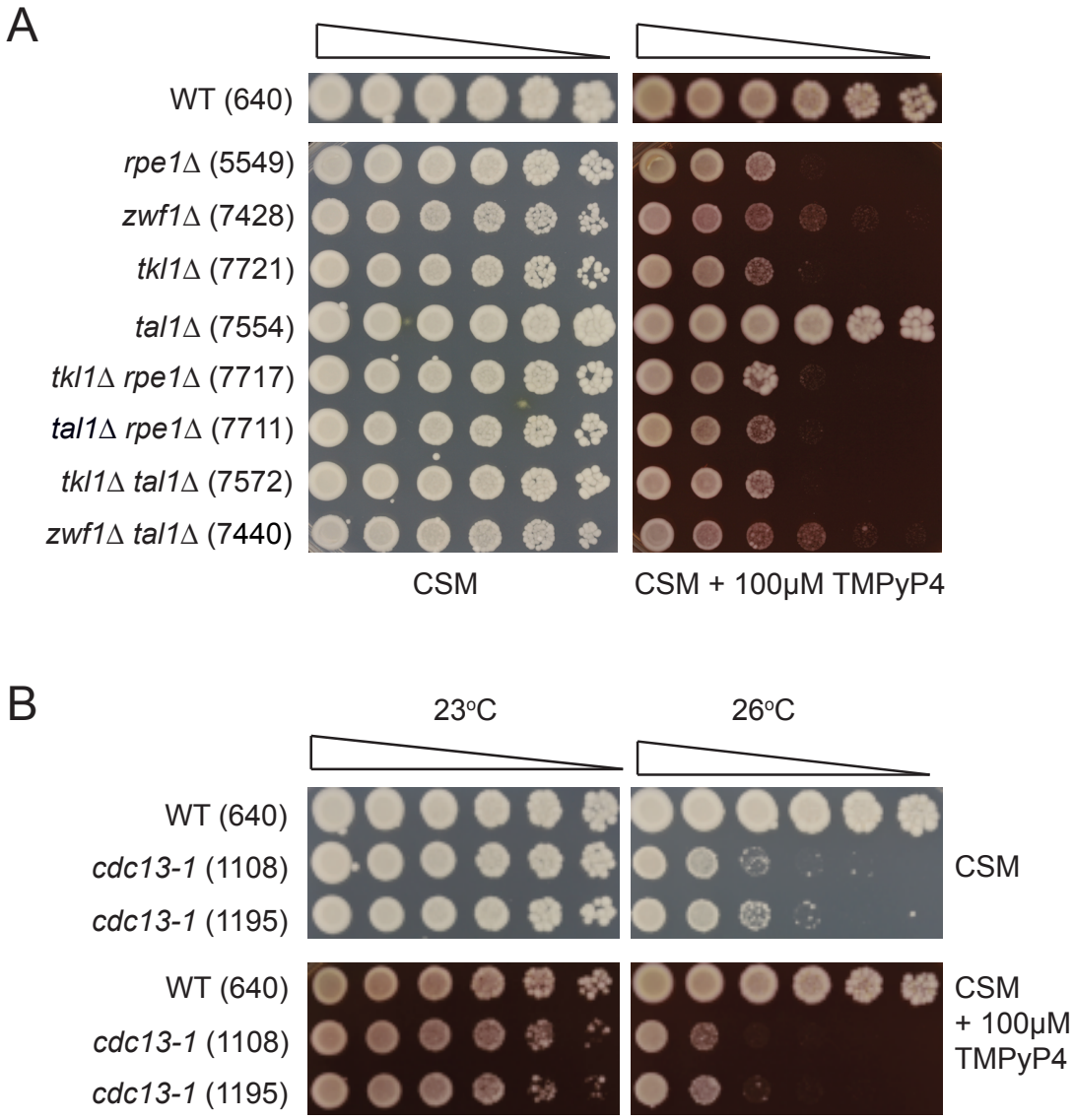

Figure 3.6: TMPyP4-sensitivity of *ppp*Δ strains and telomere capping mutants
(a) Spot test for TMPyP4-sensitivity of *ppp*Δ strains in the W303 background. Strains were grown to saturation in YEPD before a 5-fold serial dilution and pinning onto plates containing and lacking 100 μM TMPyP4. Plates were incubated at 30°C for 3 days. **(b)** Spot test for *cdc13-1* sensitivity to TMPyP4. Strains were cultured, pinned and incubated as in **(a)**.

TMPyP4 sensitivity in multiple PPP gene deletion strains suggests that any major disruption to the operation of the pentose phosphate pathway is sufficient to cause sensitivity to the G-quadruplex binding ligand.

Treatment with TMPyP4 can affect telomere biology due to preventing the action of telomerase (Mikami-Terao et al., 2009; Mikami-Terao et al., 2008). The hypothesis is that this is due to the stabilising effect TMPyP4 has upon binding to G-quadruplexes, which can in theory occur at telomeres. Research has suggested that stabilised G-quadruplexes can alter telomere biology and the response to telomere uncapping (Smith et al., 2011). As described in Chapter 1, Cdc13 is a protein which binds to the single stranded DNA (ssDNA) found at the end of telomeres in *S. cerevisiae*, capping them and preventing their recognition as double strand breaks (DSBs). When the capping ability of Cdc13 is disrupted, such as through the temperature sensitivity of the *cdc13-1* mutant strain, a DNA damage response occurs, resulting in cell cycle arrest. *cdc13-1* is deficient in telomere capping at restrictive temperatures (above 26^{o}C). In a 2011 paper, Smith et al. describe how stabilising G-quadruplexes can rescue the temperature sensitivity of the telomere capping mutant *cdc13-1* at semi-permissive temperatures (Smith et al., 2011). G-quadruplexes were stabilised by over-expressing *STM1*, by treating yeast with a G-quadruplex binding molecule or by overexpressing the HF1 single-chain antibody (scFv). This reportedly had the effect of improving the growth of temperature-sensitive *cdc13-1* strains at up to 30^{o}C.

I therefore decided to test whether exposure of *cdc13-1* to TMPyP4 at permissive and semi-permissive temperatures would alter the growth phenotype of the mutant strain. The data reported by Smith et al. (2011) suggest that an improvement in *cdc13-1* growth at semi-permissive temperatures should be observed if TMPyP4 were stabilising G-quadruplexes at telomeres. Figure 3.6b demonstrates that there is no improvement in the growth of *cdc13-1* at 26^{o}C when treated with TMPyP4. The mutant strains do display a slight reduction in growth on media containing TMPyP4 at 26^{o}C – however, the fact that a reduction in growth is also observed upon exposure to the porphyrin at a permissive temperature of 23^{o}C suggests that this apparent increase in sensitivity is due to a slight sensitivity of the mutant strain to the presence of TMPyP4. A reduction in fitness was observed across the population

in the genome-wide screen upon TMPyP4-treatment (see Figure 3.3) therefore this is not entirely surprising. The results of this experiment therefore suggest that either the G-quadruplex stabilising effect of TMPyP4 at telomeres is not sufficient for temperature sensitivity suppression, or that the presence of TMPyP4 has additional effects at telomeres, such as oxidative stress induction (von Zglinicki, 2002).

3.2.6 A genome-wide screen found TMPyP4- and H_2O_2-sensitive yfg∆ strains

The pentose phosphate pathway is important for protection against oxidative stress (Juhnke et al., 1996; Slekar et al., 1996). This is because the first step of the oxidative phase of the pathway is the main source of the reducing equivalent NADPH (Reaction 3 in Figure 1.6). NADPH plays a key role in the antioxidant system, since it is used to reduce glutathione reductase, thioredoxin and other antioxidants. Therefore strains which lose the ability to produce NADPH through the PPP are sensitive to the presence of reactive oxygen species (ROS) (Juhnke et al., 1996). In my screen I found that deletion of several key members of the PPP results in an increase in sensitivity to TMPyP4. In addition, two of the TMPyP4-sensitive gene deletions uncovered by the screen were *ccs1*∆ and *yap1*∆ both of which have important roles in the oxidative stress response, as a copper chaperone to the superoxide dismutase Sod1 and a transcription factor required for oxidative stress tolerance respectively (Moye-Rowley, 2002; Gasch et al., 2000; Culotta et al., 1997). If the sensitivity to TMPyP4 exhibited by *ccs1*∆ were due to its role as a chaperone to Sod1, I would expect a *sod1*∆ strain to display similar sensitivity to TMPyP4. However, since the library used in the genome-wide experiment does not include a *sod1*∆ strain, this could not be confirmed through the high-throughput screen.

In order to determine whether the deletion strains which are sensitive to TMPyP4 are also sensitive to the presence of reactive oxygen species, I carried out a genome-wide screen of the single deletion library for mutant strains which were sensitive to 1.5 mM hydrogen peroxide (H_2O_2). When comparing the results from the TMPyP4 screen with those of the H_2O_2 screen, I found that 15 gene deletion strains were sensitive to both treatments (Figure 3.7a and Table 3.3). The same five PPP-related genes which were sensitive to TMPyP4 were also sensitive to H_2O_2. This is also true for *YAP1*, *SAC1*, *AMD1* and *FEN1* deletions. In order to confirm these results in the W303 background, I carried out a serial dilution spot test of *ppp*∆ strains on media with or without 1.5 mM H_2O_2 or 100 µM TMPyP4 (Figure 3.7b). As observed in the screen, the PPP gene deletion mutants were sensitive to the presence of hydrogen peroxide. The data from the TMPyP4 and H_2O_2 screens suggest that the sensitivity shown by *ppp*∆ strains to TMPyP4 is due to an oxidative stress response taking place upon treatment with the G-quadruplex binder. This is potentially due to the

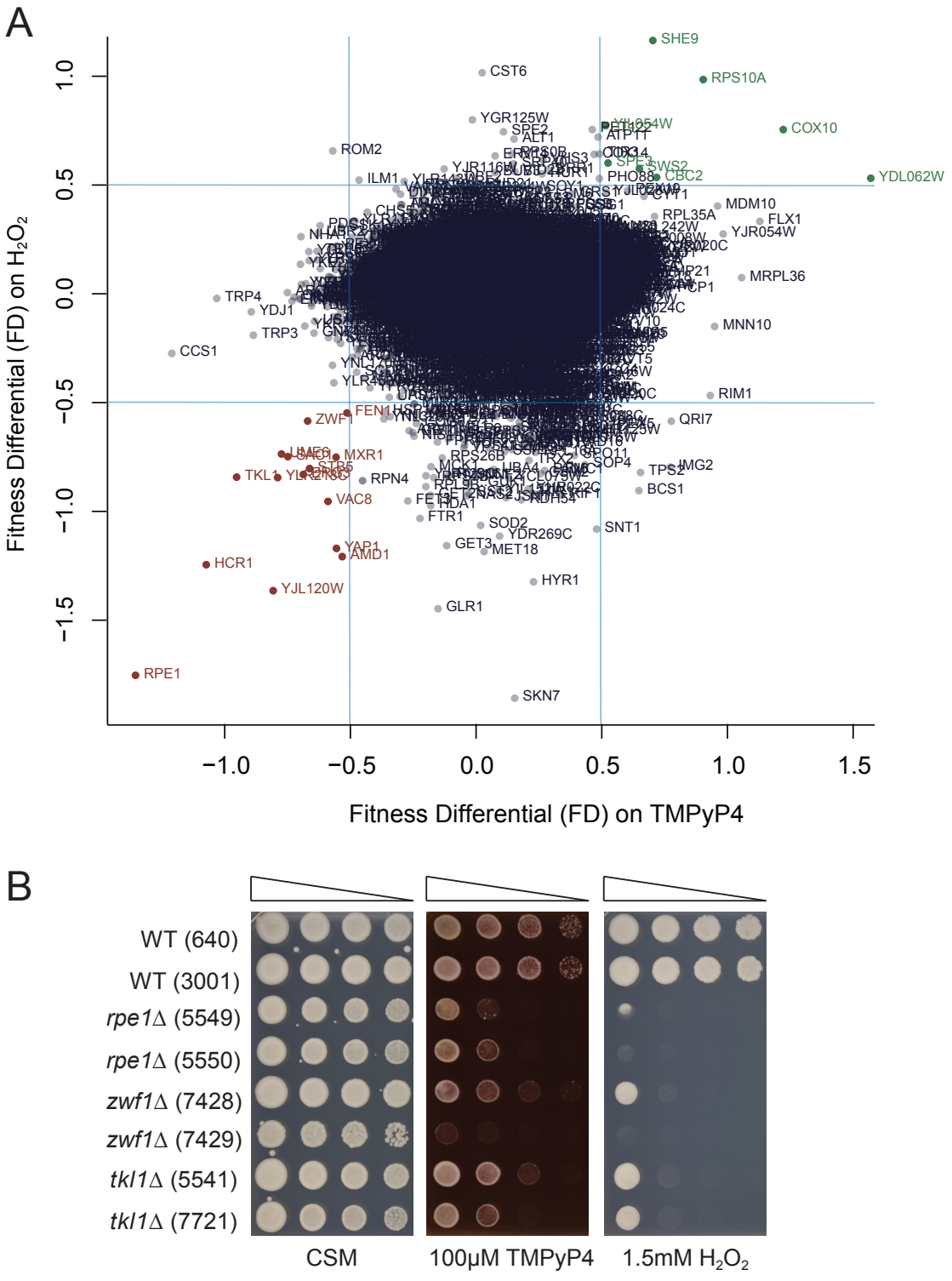

Figure 3.7: *ppp*Δ strains are TMPyP4- and H_2O_2-sensitive
(a) Correlation plot of fitness differential values from genome-wide screens for TMPyP4- and H_2O_2-sensitivity (correlation = 0.033). Genes in red (bottom left-hand corner) were found to increase sensitivity to both TMPyP4 and H_2O_2 when deleted (FD ≤ -0.5). Genes in green (top right-hand corner) were found to decrease sensitivity to both TMPyP4 and H_2O_2 when deleted (FD ≥ 0.5). Blue lines denote FD thresholds. **(b)** Spot test for TMPyP4- and H_2O_2-sensitivity of *ppp*Δ strains in the W303 background. Strains were grown to saturation in YEPD before a 5-fold serial dilution and pinning onto indicated media. Plates were incubated at 30°C for 3 days.

ORF	Gene	SGD Description
Sensitive		
YJL121C	*RPE1*	D-ribulose-5-phosphate 3-epimerase, catalyzes a reaction in the non-oxidative part of the pentose-phosphate pathway
YLR192C	*HCR1*	Involved in translation initiation as a substoichiometric component (eIF3j) of translation initiation factor 3 (eIF3)
YJL120W	*YJL120W*	Dubious open reading frame unlikely to encode a protein; partially overlaps the verified gene YJL121C/RPE1
YPR074C	*TKL1*	Transketolase, similar to Tkl2p; catalyzes reactions in the pentose phosphate pathway
YLR218C	*YLR218C*	Twin Cx(9)C protein involved in cytochrome c oxidase assembly or stability
YLR056W	*ERG3*	C-5 sterol desaturase, catalyzes the introduction of a C-5(6) double bond into episterol
YDR207C	*UME6*	Key transcriptional regulator of early meiotic genes, binds URS1 upstream regulatory sequence
YKL212W	*SAC1*	Phosphatidylinositol phosphate (PtdInsP) phosphatase involved in hydrolysis of PtdIns[4]P
YEL013W	*VAC8*	Phosphorylated and palmitoylated vacuolar membrane protein that interacts with Atg13p
YHR178W	*STB5*	Transcription factor, involved in regulating multidrug resistance and oxidative stress response
YML007W	*YAP1*	Basic leucine zipper (bZIP) transcription factor required for oxidative stress tolerance
YML035C	*AMD1*	AMP deaminase, tetrameric enzyme that catalyzes the deamination of AMP to form IMP and ammonia
YER042W	*MXR1*	Methionine-S-sulfoxide reductase, involved in the response to oxidative stress
YNL241C	*ZWF1*	Glucose-6-phosphate dehydrogenase (G6PD), catalyzes the first step of the pentose phosphate pathway
YCR034W	*FEN1*	Fatty acid elongase, involved in sphingolipid biosynthesis
Resistant		
YDL062W	*YDL062W*	Dubious open reading frame unlikely to encode a protein; partially overlaps uncharacterized ORF YDL063C
YPL172C	*COX10*	Catalyzes the first step in the conversion of protoheme to the heme A prosthetic group required for cytochrome c oxidase activity
YOR293W	*RPS10A*	Protein component of the small (40S) ribosomal subunit
YPL178W	*CDC2*	Catalytic subunit of DNA polymerase delta
YDR393W	*SHE9*	Mitochondrial inner membrane protein required for normal mitochondrial morphology
YNL081C	*SWS2*	Putative mitochondrial ribosomal protein of the small subunit, has similarity to E. coli S13 ribosomal protein
YPR069C	*SPE3*	Spermidine synthase, involved in biosynthesis of spermidine and also in biosynthesis of pantothenic acid
YIL054W	*YIL054W*	Protein of unknown function; expressed at both mRNA and protein levels

Table 3.3: TMPyP4- and H_20_2-sensitive and -resistant gene deletion strains

porphyrin structure of TMPyP4, since porphyrins have the ability to produce reactive oxygen species upon exposure to certain wavelengths of light (Granville et al., 2001).

3.2.7 Exposure to light increases toxicity of TMPyP4

Given that porphyrins can produce ROS upon exposure to light, and that it is this property which is potentially causing the sensitivity to TMPyP4, I wanted to test whether increasing exposure to light would accelerate or heighten sensitivity to the porphyrin. Therefore, I carried out a serial dilution spot test of pentose phosphate pathway deletion strains, alongside wild type strains, on media lacking and containing 100 μM TMPyP4 and either exposed the plate to light or kept it in the dark for 3 days at 30^{o}C. As the results in Figure 3.8 demonstrate, exposure to light does indeed increase sensitivity of all strains to TMPyP4 treatment, including the wild type. The *ppp*Δ strains exhibited significantly increased sensitivity to TMPyP4 when incubated in the light in comparison to growth in the dark.

Incubating plates in the dark at the same temperature resulted in an increase in growth of all strains when compared to Figure 3.6 and Figure 3.7b, where measures were not taken to protect plates from light nor expose them to it. However, several of the *ppp*Δ strains demonstrated TMPyP4-sensitivity even in the dark, especially *tkl1*Δ, *tkl1*Δ *rpe1*Δ and *tal1*Δ *rpe1*Δ. The results of this experiment suggest that the toxic effects of TMPyP4 can be enhanced upon exposure to light and that deletion of key PPP genes can still increase sensitivity to the ligand, even when strains were grown in the dark.

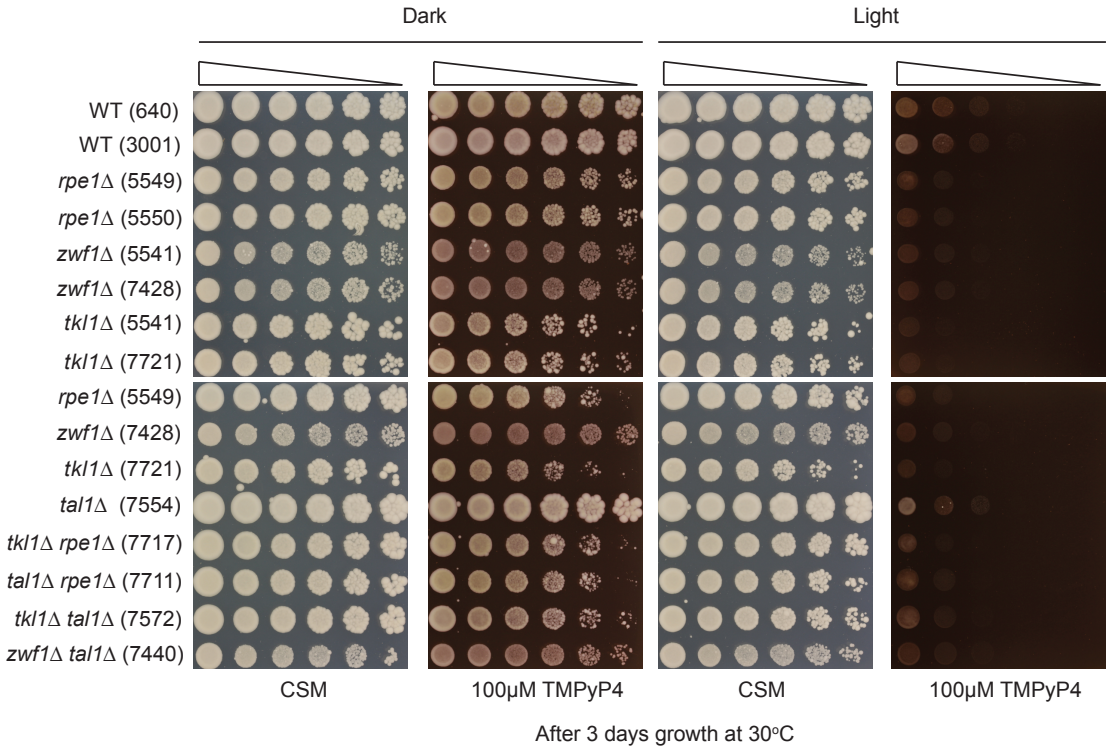

Figure 3.8: Exposure to light increases the sensitivity of yeast strains to TMPyP4
Spot test for light-activated TMPyP4-sensitivity of *ppp*Δ strains. Strains were grown to saturation in YEPD before a 5-fold serial dilution and pinning onto plates containing and lacking 100 μM TMPyP4. All plates were incubated at 30°C for 3 days in an incubator fitted with a light. Plates labelled 'Dark' were wrapped in reflective foil to shield them from the light.

3.2.8 Few yfg∆ strains are sensitive to both TMPyP4 and RHPS4

As mentioned in the introduction of this chapter, I also screened for differential sensitivity to another G-quadruplex binding ligand, RHPS4 (Cookson et al., 2005). This ligand is a pentacyclic acridine and binds to G-quadruplexes in a different manner and with different specificity and affinity to TMPyP4 (Wei et al., 2006; Phan et al., 2005; Gavathiotis et al., 2003; Gavathiotis et al., 2001; Haq et al., 1999). If the two compounds were operating by similar mechanisms, and exerting the same effect, I expected to see a large overlap between the data sets and similarities between the screen results in terms of strains defined as having differential sensitivity. However, upon comparison of the genome-wide data following the TMPyP4 and RHPS4 screens, I found little similarity between the G quadruplex binding ligand sensitive strains. Studying the RHPS4 and TMPyP4 data more closely, there are only 2 gene deletion strains which are classed as sensitive to both G-quadruplex binding ligands, based on the arbitrary cut off of – *fre8*∆ and *amd1*∆ - whereas there are 16 deletion strains which are RHPS4- and TMPyP4-resistant (Figure 3.9 and Table 3.4).

In addition to the TMPyP4, H_2O_2 and RHPS4 screens, I also screened for differential sensitivity to hydroxyurea (HU). In clustering all of the fitness (F) data from the 6 screens (CSM and 1% DMSO controls, plus 4 treatment conditions) together in a heatmap, I found that the fitness profile in response to TMPyP4 treatment most resembled the profile in response to hydrogen peroxide treatment (Figure 3.10). This suggests that TMPyP4 is exerting similar effects and eliciting similar phenotypic responses to the presence of hydrogen peroxide, and has little similarity with RHPS4.

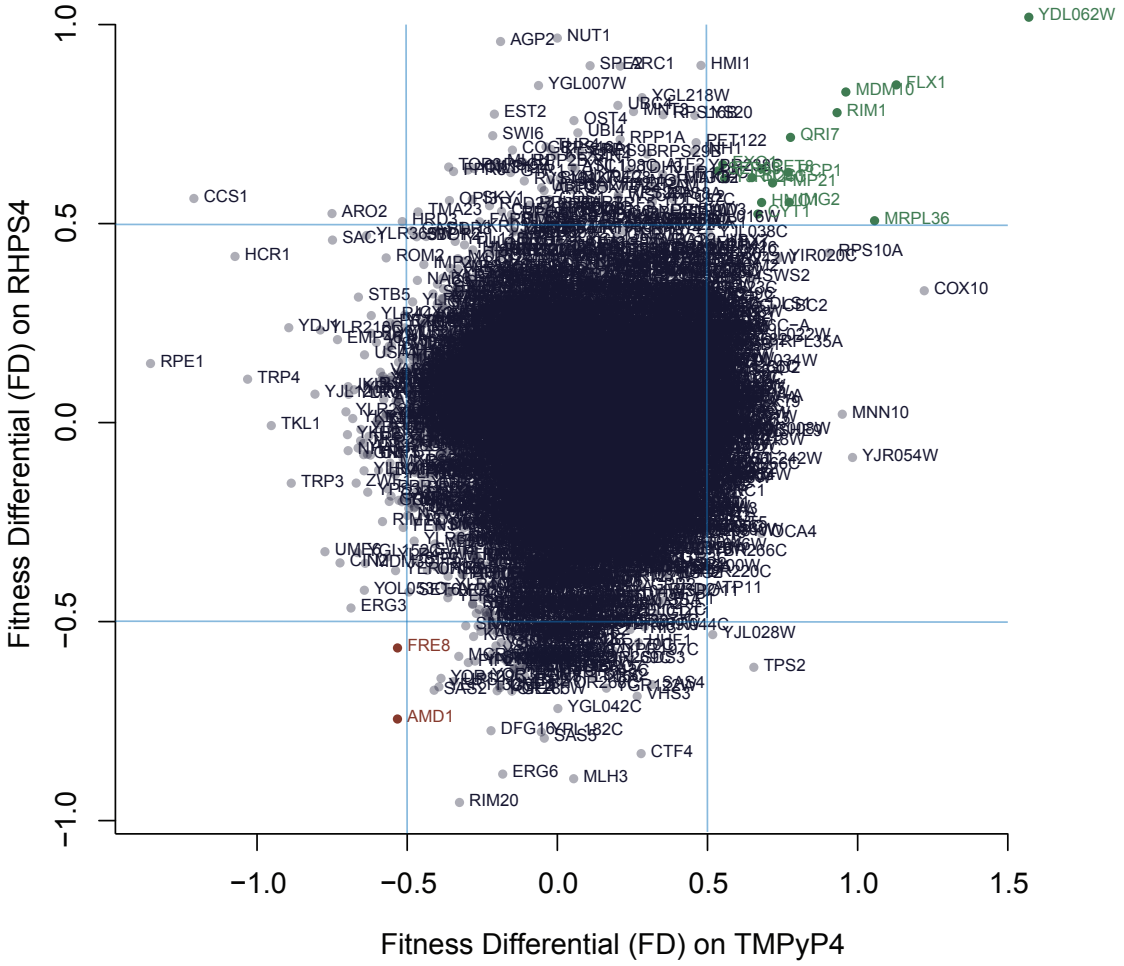

Figure 3.9: Only two deletion strains are sensitive to both TMPyP4 and RHPS4
Correlation plot of fitness differential values from genome-wide screens for TMPyP4- and RHPS4-sensitivity (correlation = 0.096). Genes in red (bottom left-hand corner) were found to increase sensitivity to both TMPyP4 and RHPS4 when deleted (FD ≤ -0.5). Genes in green (top right-hand corner) were found to decrease sensitivity to both TMPyP4 and RHPS4 when deleted (FD ≥ 0.5). Blue lines denote FD thresholds.

ORF	Gene	SGD Description
Sensitive		
YML035C	*AMD1*	AMP deaminase, tetrameric enzyme that catalyzes the deamination of AMP to form IMP and ammonia
YLR047C	*FRE8*	Protein with sequence similarity to iron/copper reductases, involved in iron homeostasis
Resistant		
YDL062W	*YDL062W*	Dubious open reading frame unlikely to encode a protein; partially overlaps uncharacterized ORF YDL063C
YIL134W	*FLX1*	Protein required for transport of flavin adenine dinucleotide (FAD), a synthesis product of riboflavin, across the mitochondrial membrane
YAL010C	*MDM10*	Subunit of both the ERMES complex and of the mitochondrial sorting and assembly machinery (SAM complex)
YCR028C-A	*RIM1*	Single-stranded DNA-binding protein essential for mitochondrial genome maintenance
YDL104C	*QRI7*	Highly conserved mitochondrial protein, essential for t6A modification of mitochondrial tRNAs that decode ANN codons
YOR033C	*EXO1*	5'-3' exonuclease and flap-endonuclease involved in recombination, double-strand break repair and DNA mismatch repair
YNL003C	*PET8*	S-adenosylmethionine transporter of the mitochondrial inner membrane, member of the mitochondrial carrier family
YIL074C	*SER33*	3-phosphoglycerate dehydrogenase, catalyzes the first step in serine and glycine biosynthesis
YGR101W	*PCP1*	Mitochondrial serine protease required for the processing of mitochondrial proteins and maintenance of mitochondrial DNA and morphology
YDR375C	*BCS1*	Mitochondrial protein of the AAA ATPase family; has ATP-dependent chaperone activity
YJR024C	*YJR024C*	5'-methylthioribulose-1-phosphate dehydratase; acts in the methionine salvage pathway
YBR269C	*FMP21*	Putative protein of unknown function; the authentic, non-tagged protein is detected in highly purified mitochondria in high-throughput studies
YCR071C	*IMG2*	Mitochondrial ribosomal protein of the large subunit
YDR174W	*HMO1*	Chromatin associated high mobility group (HMG) family member involved in genome maintenance
YOR065W	*CYT1*	Cytochrome c1, component of the mitochondrial respiratory chain
YBR122C	*MRPL36*	Mitochondrial ribosomal protein of the large subunit

Table 3.4: TMPyP4- and RHPS4-sensitive and -resistant gene deletion strains

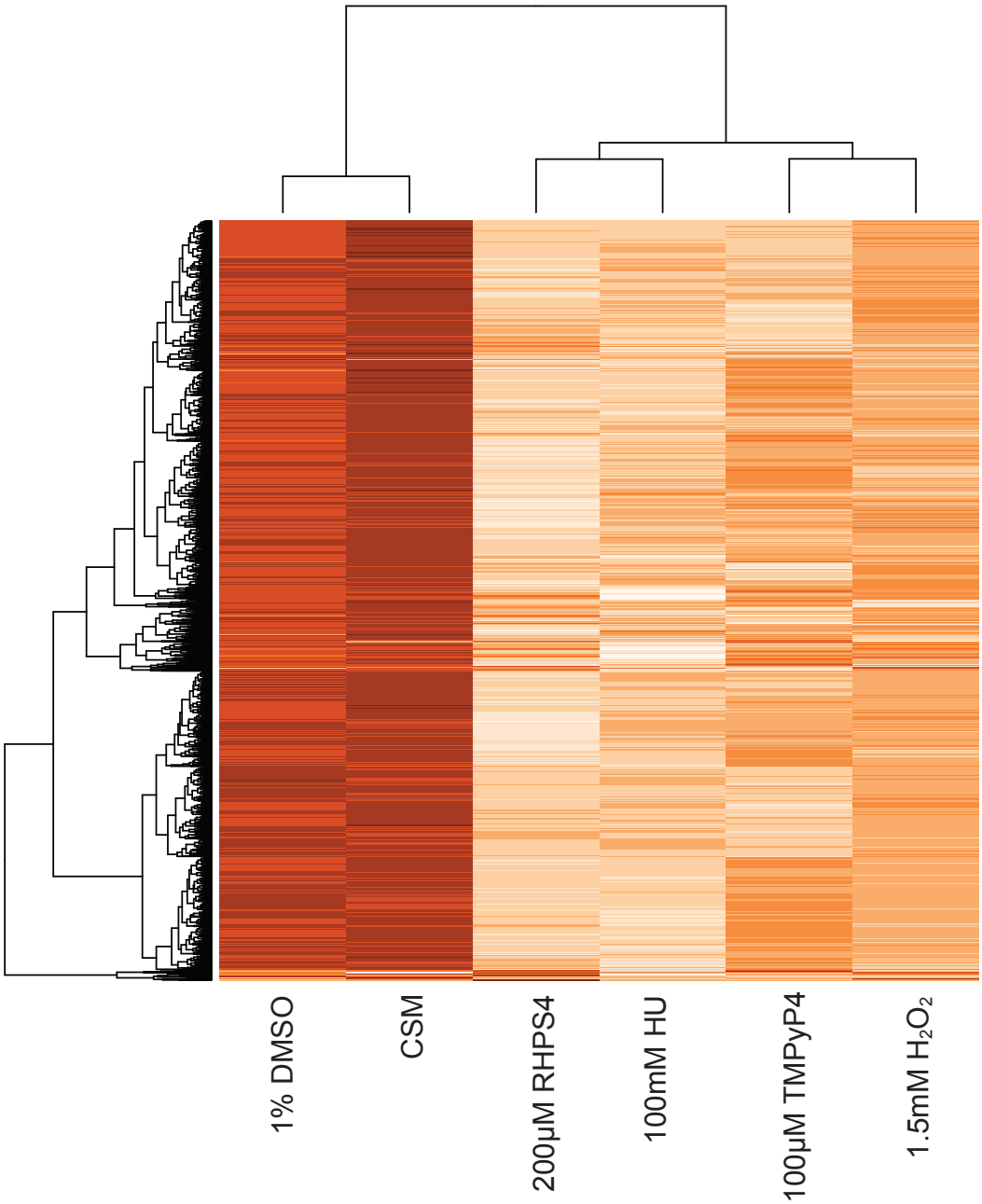

Figure 3.10: Fitnesses of each deletion strain on control and supplemented media
Fitness data for every deletion strain from six genome-wide screens on CSM or CSM supplemented with 1% DMSO, 200 µM RHPS4, 100 mM hydroxyurea (HU), 100 µM TMPyP4 or 1.5 mM H_2O_2. Each coloured line represents mean fitness (F) of *yfg*Δ on the indicated medium, coloured according to relative fitness (low F = pale, high F = dark). Fitness on each medium was compared for each deletion strain and strains were clustered vertically depending on similar fitness changes in response to each treatment. Treatments were clustered horizontally depending on similarity between genome fitness profiles.

3.3 Discussion

In this chapter I studied the response of null mutant strains to exposure to a ligand which stabilises G-quadruplexes. I carried out a genome-wide screen of yeast single deletion strains to examine differential sensitivity to the G-quadruplex binding ligand TMPyP4. Previous work demonstrates that TMPyP4 presence can affect telomerase activity (Mikami-Terao et al., 2009; Mikami-Terao et al., 2008), so therefore I expected to find that deletion of telomerase-, telomere- or DNA damage response-associated genes would result in a change in sensitivity to TMPyP4 in comparison to wild type strains. However, the conclusions of my genome-wide screen revealed little to no evidence for an over-representation of telomere associated genes amongst those which were most sensitive to the G-quadruplex binding ligand. I did observe, however, that genes associated with the pentose phosphate pathway (PPP), the oxidative stress response and tubulin folding demonstrated TMPyP4-sensitivity upon deletion.

TMPyP4 is potentially effective against retinoblastoma cell lines, human prostate carcinoma and mammary tumours (Mikami-Terao et al., 2008; Grand et al., 2002). Interestingly, the PPP also has links with cancer through changes in metabolism within tumour cell lines. The main link is named the Warburg effect, in which cancer cells rely on aerobic glycolysis to generate energy instead of using mitochondrial oxidative phosphorylation (Vander Heiden et al., 2009). Therefore the involvement of the PPP in response to TMPyP4 treatment is of particular interest. Deletion of *ZWF1*, *RPE1* and *TKL1*, which encode key enzymes of the PPP, causes large increases in sensitivity to TMPyP4. The sensitivity to TMPyP4 displayed by *ppp*Δ strains is most likely the result of a reduction in NADPH production, key for antioxidant function and a link to the oxidative stress response. Interestingly, a recent paper by Krüger et al. (2011) suggests that the non-oxidative phase of the PPP harbours a NADPH-independent role in the oxidative stress response, which is proposed to exert its effects through transcriptional alterations.

One could conclude that deletion of PPP genes *ZWF1*, *TKL1* or *RPE1* caused TMPyP4-sensitivity by affecting flux through the pathway. However, when multiple PPP genes were deleted in the same strain, the sensitivity to TMPyP4 remains at

similar levels. For instance, *tkl1*Δ *rpe1*Δ exhibits the same growth phenotype as the single deletion strains of *rpe1*Δ and *tkl1*Δ. This lack of change following additional gene deletions suggests that a change in flux through the PPP is unlikely to be the source of the TMPyP4-sensitivity of *ppp*Δ strains.

In my genome-wide screen for TMPyP4-sensitivity I also found that the oxidative stress-linked gene deletion strains *ccs1*Δ and *yap1*Δ demonstrated sensitivity to the G-quadruplex binding ligand. Therefore I hypothesised that the sensitivity of these deletion strains to TMPyP4 is linked to a deficiency in the oxidative stress response. I screened the genome-wide response to the presence of hydrogen peroxide (H_2O_2), as well as RHPS4, an alternative G-quadruplex binding molecule (Cookson et al., 2005). Through these screens I found greater similarity between the responses to TMPyP4 and H_2O_2 than between the two G-quadruplex binding ligands, consistent with my hypothesis.

TMPyP4 is a porphyrin, a class of compounds historically used in photodynamic therapy, wherein reactive oxygen species (ROS) are produced upon stimulation by light (Granville et al., 2001). This property therefore provides a potential explanation for our observation that defects in the oxidative stress response results in sensitivity to TMPyP4. Grand et al. (2002) noted through transcriptional studies that oxidative stress-linked genes were upregulated in response to TMPyP4 treatment in human cell lines. The results from the transcriptional study by Grand et al. (2002) are consistent with our findings in the genome-wide screen, insofar as deletion of genes involved in the oxidative stress response results in increased sensitivity to TMPyP4. Indeed, upon exposure to light, both wild type and *ppp*Δ strains exhibited significantly increased sensitivity to TMPyP4. Interestingly, the *ppp*Δ strains still demonstrate TMPyP4-sensitivity in spite of incubation in the dark, suggesting that low levels of oxidative stress are still occurring in spite of efforts to protect the plates against light activation.

cdc13-1 is a mutant form of the telomere binding protein Cdc13 which is deficient in telomere capping at restrictive temperatures. Smith et al. (2011) recently demonstrated that stabilisation of G-quadruplexes by three different methods has the ability to suppress that temperature sensitivity of *cdc13-1* at semi-permissive

temperatures. This suggests that stable G-quadruplexes can participate in a rudimentary telomere cap when natural capping is disrupted. TMPyP4 is predicted to bind and stabilise G-quadruplexes, so I tested the effect of the ligand on the temperature sensitivity of *cdc13-1*. I found that TMPyP4 treatment had little effect on the growth phenotype of *cdc13-1* at semi-permissive temperatures, which suggests that the G-quadruplex stabilising effect of TMPyP4 at telomeres is insufficient for the suppression of temperature sensitivity, or that the presence of TMPyP4 exerts additional effects which affect telomeres, such as oxidative stress (von Zglinicki, 2002).

An additional interesting result of the screen is the identification of tubulin-related genes as causing TMPyP4-sensitivity upon deletion. Unlike *ppp*Δ strains, which demonstrated sensitivity to both TMPyP4 and H_2O_2, deletion of tubulin-related genes only caused sensitivity to TMPyP4. Certain anti-cancer drugs target microtubules, which either act by inhibiting tubulin polymerisation or cause the stabilisation of microtubules (Li and Sham, 2002). Since TMPyP4 is not targeted at microtubules, the response of tubulin processing mechanisms to G-quadruplex stabilisation may be an important area of study with regards to the anti-cancer potential of the molecule.

3.4 Future Work

My studies have identified an important role for the pentose phosphate pathway (PPP) in the response to TMPyP4-treatment. The PPP provides a means of protection against the effects resulting from treatment with the porphyrin, most likely due to the production of NADPH which occurs in the oxidative phase of the PPP.

I hypothesise therefore that treatment with TMPyP4 results in ROS generation in yeast. In order to test this hypothesis, the production of ROS in TMPyP4-treated cells could be monitored using dihydroethidium (DHE), the reduced form of the DNA dye ethidium bromide. DHE is commonly used to detect oxidative cellular activities, exhibiting blue fluorescence in the cytosol and red fluorescence upon oxidation and DNA intercalation. DHE can be used with intact cells and the dye would provide an indication as to whether TMPyP4-treatment results in oxidative stress.

The role of the PPP in TMPyP4 resistance could also be explored through the overexpression of PPP genes. Overexpression of *TKL1* can suppress sensitivity of *sod1*Δ to HU and other *sod1*Δ phenotypes, predicted to be through increasing NADPH production (Carter et al., 2005; Slekar et al., 1996). Therefore if *ppp*Δ strains were sensitive to TMPyP4 due to reduced NADPH production and defects in the oxidative stress response, increasing expression of key PPP genes may inhibit this TMPyP4-sensitivity.

The six genome-wide screens carried out in this chapter generated a lot of data which has not been explored here. In particular, the screen for differential sensitivity to RHPS4 could be investigated further; for instance, 16 gene deletion strains exhibited resistance to both RHPS4 and TMPyP4. These strains could be studied in detail to discern whether this response is specific to G-quadruplex binding ligands and whether it relates to the G-quadruplex binding ability of RHPS4 and TMPyP4.

4 The genetic interactions between the response to telomere uncapping and the pentose phosphate pathway

4.1 Introduction

In the previous chapter I demonstrated that deficiencies in the pentose phosphate pathway (PPP) led to sensitivity to the G-quadruplex binding ligand TMPyP4 in *Saccharomyces cerevisiae*. I found that the deletion of key PPP genes leads to an increase in TMPyP4-sensitivity, which could be attributed to the role of the PPP in NADPH production. TMPyP4 is a member of the porphyrin family, a group of compounds which have been used historically in photodynamic therapy, in which light is used to stimulate the production of reactive oxygen species (ROS) and cause apoptosis (Granville et al., 2001). NADPH is key for anti-oxidant function and the removal of ROS, and is therefore of high importance for the cellular response to oxidative stress. The PPP is required for NADPH production, and therefore this could provide some explanation as to why deletion of PPP genes causes TMPyP4-sensitivity.

Interestingly, deletion of key PPP genes also affects the temperature sensitivity of the telomere capping mutant *cdc13-1*. A genome-wide screen using the same single deletion library used in the TMPyP4 screen was carried out in order to study the genetic interactions between single deletion mutants and *cdc13-1* (Addinall et al., 2011; Addinall et al., 2008). This screen identified the deletion of key PPP genes, *TKL1* and *TAL1*, as being capable of suppressing the temperature sensitivity of *cdc13-1* to a significant degree (Figure 4.1).

A number of studies have linked telomere biology and oxidative stress, predominantly in mammalian systems (Richter and Zglinicki, 2007; Kawanishi and Oikawa, 2004; von Zglinicki, 2002). In yeast, a transcriptional study of the response to telomere uncapping in *cdc13-1* strains demonstrated that genes associated with the oxidative stress response, such as *MSN4*, are upregulated following a shift to restrictive temperatures (Greenall et al., 2008). The study also found that the PPP

genes *SOL4* and *GND2* (Reactions 4 and 5 in Figure 1.6) are upregulated in response to telomere uncapping (Greenall et al., 2008).

Due to the conclusions of Chapter 3, in which a link between the PPP and TMPyP4-sensitivity was uncovered, I decided to investigate the interaction between the PPP and telomere uncapping further. I hypothesised that, due to the results of the transcriptional studies (in which oxidative stress response genes are upregulated), any link would most likely be due to the generation of NADPH by the PPP.

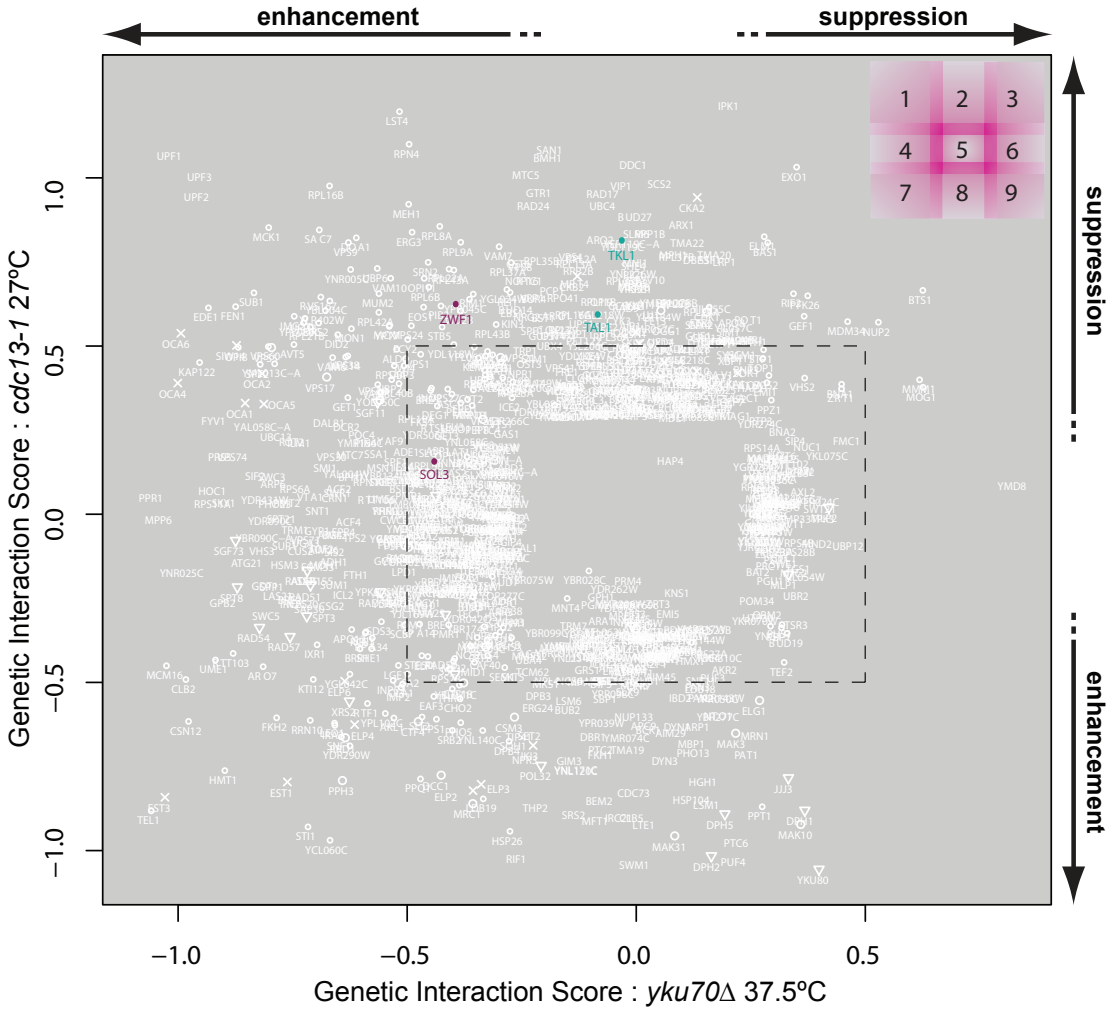

Figure 4.1: Genetic interaction strength comparison between *cdc13-1* and *yku70*Δ
Genes which when deleted cause significant suppression of temperature sensitivity of both *cdc13-1* and *yku70*Δ appear in the top right-hand corner of the plot. Genes which when deleted cause signifcant enhancement of *cdc13-1* and *yku70*Δ temperature sensitivity appear in the bottom left-hand corner of the plot. Genes in the centre of the plot did not interact with *cdc13-1* or *yku70*Δ and so were removed. Symbols indicate genes which are components of selected protein complexes. Genes that interact with both *cdc13-1* and *yku70*Δ are open white circles; those that interact with just one mutation are crossed boxes. PPP genes are highlighted on the plot using the same colours used in Figure 1.6. The dashed black rectangle indicates an arbitrary GIS cutoff of +/- 0.5. Figure adapted from (Addinall et al., 2011).

4.2 Results

4.2.1 Deletion of TKL1 and TAL1 suppresses cdc13-1 temperature sensitivity

Genome-wide screens of the single deletion library (SDL) crossed with a *cdc13-1* strain suggest that temperature sensitivity of the mutant strain can be suppressed through deletion of either *TKL1* or *TAL1* (Figure 4.1; (Addinall et al., 2011; Addinall et al., 2008). *TKL1* encodes Tkl1, the major transketolase utilised in the non-oxidative phase of the pentose phosphate pathway (PPP) (Reactions 8 and 10 in Figure 1.6). Tal1 also has a role in this phase of the pathway, in catalysing the conversion of erythrose-4-phosphate and sedoheptulose-7-phosphate to glyceraldehyde-4-phosphate and fructose-6-phosphate (Reaction 9 in Figure 1.6). The genome-wide screen was carried out in the S288C background of *Saccharomyces cerevisiae*. In order to confirm the suppression of *cdc13-1* temperature sensitivity which occurs when either *TKL1* or *TAL1* are deleted in the mutant strain, I carried out a spot test of the equivalent strains in the W303 background. Deletion of *TKL1* in the *cdc13-1* background suppresses sensitivity of the capping mutant at temperatures up to 27^{o}C (Figure 4.2a). *TAL1* deletion also has a similar effect, but does not improve the growth of *cdc13-1* to the same extent as *TKL1* deletion (Figure 4.2b).

Interestingly, deletion of *TKL1* and *TAL1* improves the growth of *cdc13-1 rad9*Δ strains. *RAD9* encodes an important checkpoint protein which stimulates the DNA damage response and cell cycle arrest. When *RAD9* is deleted in the *cdc13-1* background, temperature sensitivity is suppressed at temperatures up to 28^{o}C, since the uncapped mutant strains continue through the cell cycle (Garvik et al., 1995). Eventually the accumulated damage caused by the presence of uncapped telomeres results in cell death, which is why the temperature sensitivity of *cdc13-1* cannot by totally suppressed by *RAD9* deletion, which also results in the generation of large amounts of ssDNA, at restrictive temperatures (Garvik et al., 1995). As visible in Figure 4.2, *cdc13-1 tkl1*Δ *rad9*Δ and *cdc13-1 tal1*Δ *rad9*Δ strains grow better at 28^{o}C than *cdc13-1 rad9*Δ. This suggests that the phenotypic suppression exerted by *TKL1* and *TAL1* deletion on *cdc13-1* strains is independent of Rad9 activity, since the suppression of temperature sensitivity observed in *cdc13-1 rad9*Δ strains is improved by deletion of either gene.

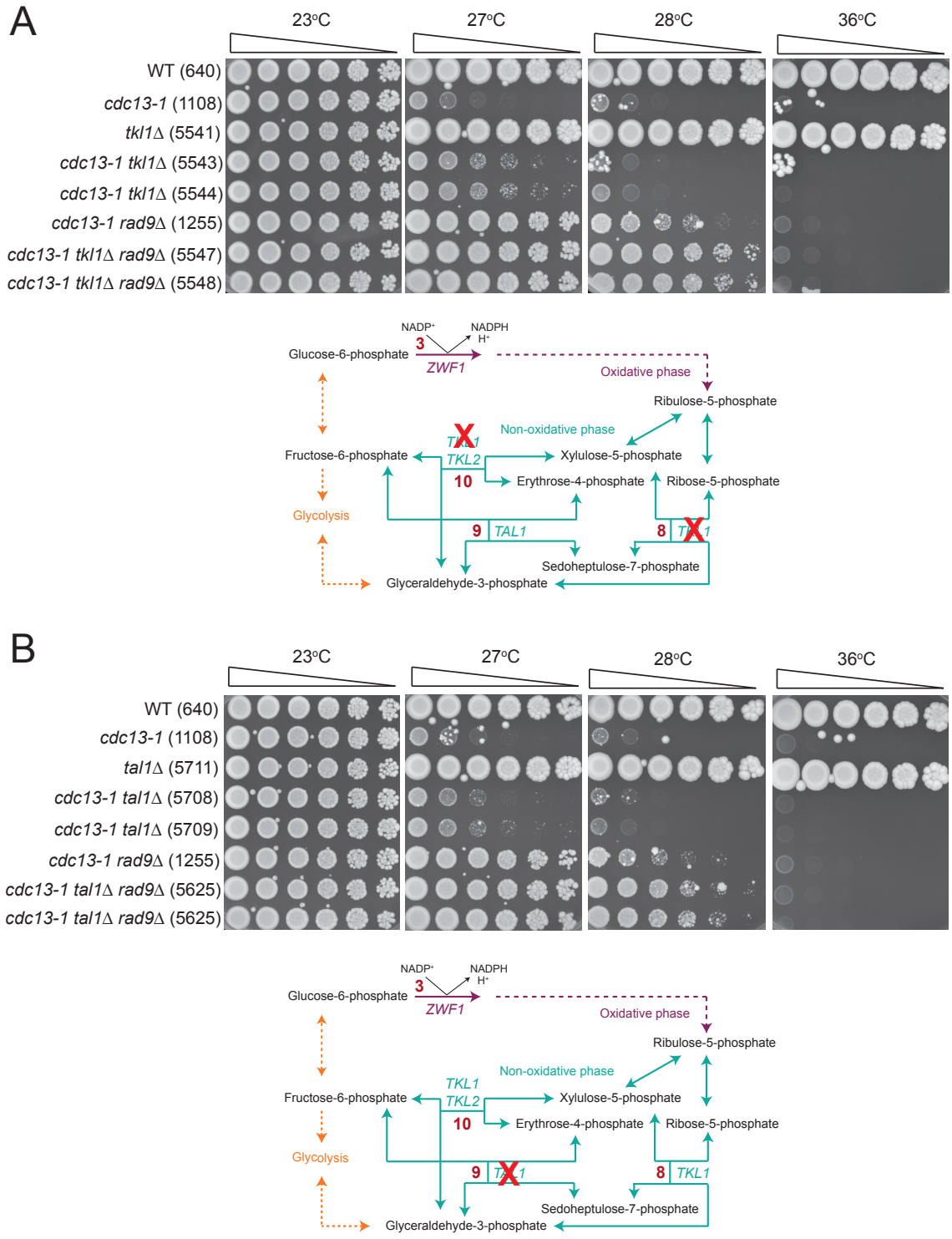

Figure 4.2: Deletion of *TKL1* and *TAL1* suppresses *cdc13-1* temperature sensitivity **(a)** Spot test for temperature sensitivity of *cdc13-1*, *cdc13-1 tkl1*Δ and *cdc13-1 tkl1*Δ *rad9*Δ, and a simplified subsection of Figure 1.6, indicating the disrupted step of the PPP (red X). Strains were grown to saturation in YEPD before a 5-fold serial dilution and pinning onto solid agar plates. Plates were incubated at the indicated temperatures for 3 days. Numbers in the pathway correspond to those in Figure 1.6 **(b)** Spot test for temperature sensitivity of *cdc13-1* and *cdc13-1 tal1*Δ and *cdc13-1 tal1*Δ *rad9*Δ. Strains were cultured, pinned and incubated as in **(a)**. Pathway diagram as in **(a)**.

4.2.2 chk1Δ increases suppression of the cdc13-1 phenotype by tkl1Δ and tal1Δ

The DNA damage response which occurs following telomere uncapping in *cdc13-1* strains is mediated by checkpoint proteins such as Rad9. Rad9 is hyperphosphorylated by Mec1 and Tel1 kinases and transmits the DNA damage checkpoint signal downstream by activating Rad53 and Chk1 (Ma et al., 2006; Sweeney et al., 2005; Blankley and Lydall, 2004; Emili, 1998; Vialard et al., 1998). As demonstrated in Chapter 4.2.1, *RAD9* deletion can suppress the temperature sensitivity of *cdc13-1* at semi-permissive temperatures. Deletion of *CHK1*, which acts downstream of Rad9, in the *cdc13-1* background can also suppress the temperature sensitivity of the mutant strain; *chk1*Δ mutants are partially defective at the metaphase/anaphase checkpoint (Jia et al., 2004; Maringele and Lydall, 2002; Sanchez et al., 1999). This is confirmed in Figure 4.3, in which a *cdc13-1 chk1*Δ strain exhibits improved growth at 26.5^{o}C and 27^{o}C when compared to a *cdc13-1* strain at the same temperatures.

Deletion of either *TKL1* or *TAL1* in the *cdc13-1 chk1*Δ background improves growth further, with increases in temperature tolerance visible for both strains. Since there are two different DNA damage checkpoint pathways which are responsible for metaphase/anaphase arrest of *cdc13-1* mutants (one Rad9/Mec1/Chk1-dependent and the other Mec1/Rad53/Dun1-dependent) additive effects to the phenotypic suppression of *cdc13-1* temperature sensitivity by *CHK1* deletion most likely do not occur due to effects downstream of this checkpoint. Instead the suppression of temperature sensitivity observed in *cdc13-1* strains by *TKL1* or *TAL1* deletion may occur due to downstream effects of the Mec1/Rad53/Dun1-dependent checkpoint pathway. This is especially interesting considering the Mec1/Rad53/Dun1-dependent checkpoint pathway affects the expression and activity of ribonucleotide reductase (Zhao and Rothstein, 2002; Huang and Elledge, 1997; Elledge, 1996; Zhou and Elledge, 1993).

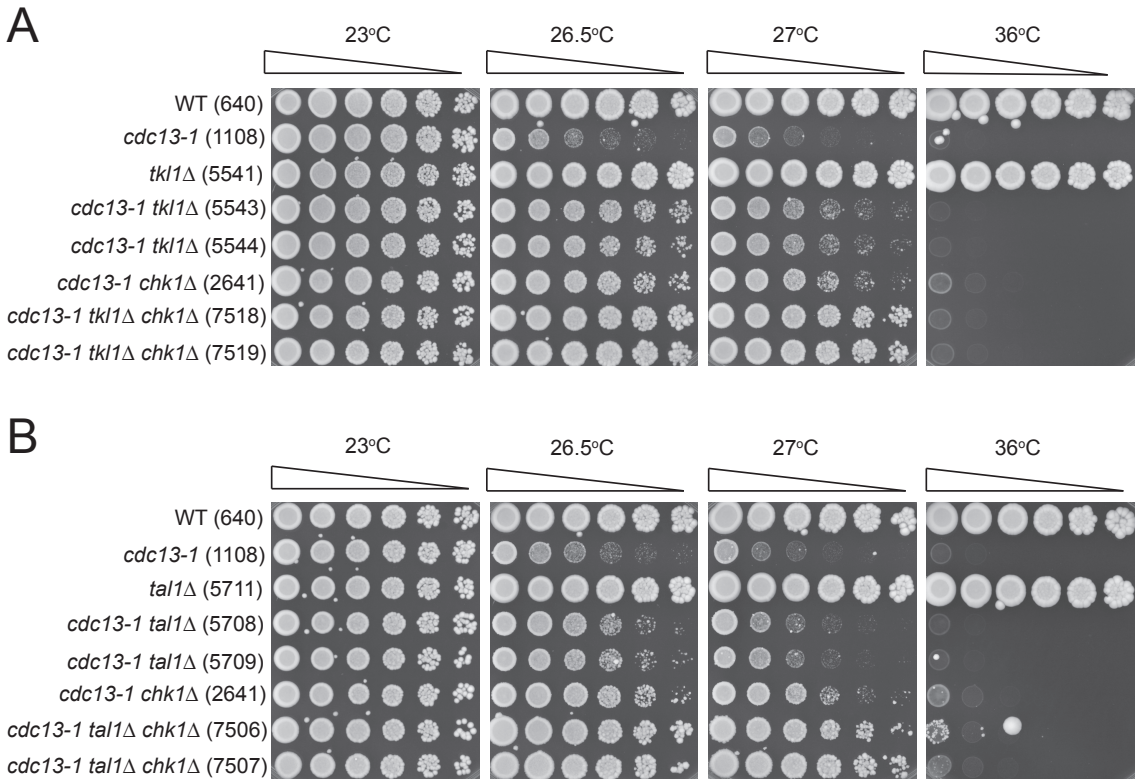

Figure 4.3: Suppression by *TKL1* and *TAL1* deletion is Chk1-independent
(a) Spot test for temperature sensitivity of *cdc13-1*, *cdc13-1 tkl1*Δ and *cdc13-1 tkl1*Δ *chk1*Δ. Strains were grown to saturation in YEPD before pining onto solid agar plates. Plates were incubated at the indicated temperatures for 3 days. **(b)** Spot test for temperature sensitivity of *cdc13-1* and *cdc13-1 tal1*Δ and *cdc13-1 tal1*Δ *chk1*Δ. Strains were cultured, pinned and incubated as in **(a)**.

4.2.3 Suppression of the cdc13-1 phenotype by tkl1Δ and tal1Δ is rad53Δ sml1Δ-dependent

Deletion of *TKL1* and *TAL1* both resulted in the suppression of temperature sensitivity of *cdc13-1 chk1*Δ strains at semi-permissive temperatures. This led me to hypothesise that suppression of *cdc13-1* temperature sensitivity in *cdc13-1 tkl1*Δ and *cdc13-1 tal1*Δ strains is independent of Chk1 activity and is not related to the activities of the Rad9/Mec1/Chk1-dependent checkpoint pathway. This suggests that the suppression of temperature sensitivity observed in *cdc13-1* strains by *TKL1* or *TAL1* deletion may instead occur due to downstream effects of the Mec1/Rad53/Dun1-dependent checkpoint pathway. In order to test this hypothesis, I created strains in which *TKL1* and *TAL1* were absent, as well as *RAD53*. Deletion of *RAD53* is lethal; however, viable spores can obtained through simultaneous deletion of the ribonucleotide reductase (RNR) inhibitor *SML1* (Zhao et al., 1998). Therefore I examined the temperature sensitivity of *cdc13-1 tkl1*Δ *rad53*Δ *sml1*Δ and *cdc13-1 tal1*Δ *rad53*Δ *sml1*Δ strains in comparison to *cdc13-1* and *cdc13-1 rad53*Δ *sml1*Δ strains.

As demonstrated in Figure 4.4, *cdc13-1 rad53*Δ *sml1*Δ strains are less temperature sensitive than *cdc13-1* strains. This can be attributed to the defect in the checkpoint pathway caused by Rad53 deletion, which leads to partial arrest; Rad53 and its downstream target Dun1 are responsible for 50% of the arrest observed in *cdc13-1* mutants (Gardner et al., 1999). Additional deletion of either *TKL1* or *TAL1* in *cdc13-1 rad53*Δ *sml1*Δ strains does not increase suppression of temperature sensitivity at semi-permissive temperatures (Figure 4.4). Therefore this suggests that Tkl1 and Tal1 act downstream of the Mec1/Rad53/Dun1-dependent checkpoint pathway in response to telomere uncapping in *cdc13-1* strains.

However, it is worth noting that the *rad9*Δ, *chk1*Δ and *rad53*Δ *sml1*Δ strains used in these experiments (Figures 4.2 to 4.4) contain a HIS3 auxotrophic maker. Introducing this marker into strains with disruptions to carbohydrate metabolism through mutation of the pentose phosphate pathway may additionally influence metabolism and therefore may affect growth independently of the *cdc13-1* mutation.

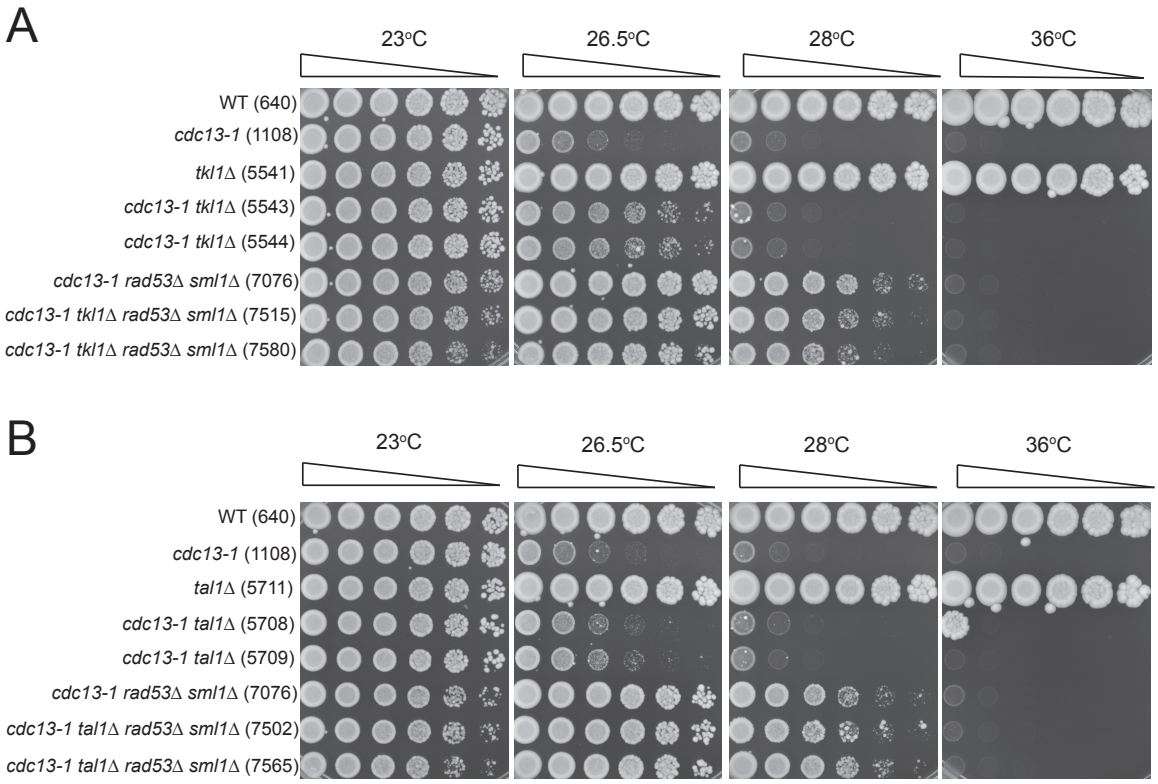

Figure 4.4: Suppression by *TKL1* and *TAL1* deletion is Rad53-dependent
(a) Spot test for temperature sensitivity of *cdc13-1*, *cdc13-1 tkl1*Δ and *cdc13-1 tkl1*Δ *rad53*Δ *sml1*Δ. Strains were grown to saturation in YEPD before pining onto solid agar plates. Plates were incubated at the indicated temperatures for 3 days. **(b)** Spot test for temperature sensitivity of *cdc13-1* and *cdc13-1 tal1*Δ and *cdc13-1 tal1*Δ *rad53*Δ *sml1*Δ. Strains were cultured, pinned and incubated as in **(a)**.

4.2.4 cdc13-1 tkl1Δ tal1Δ does not grow better than single deletion strains

The deletion of *TKL1* and *TAL1* both result in the suppression of temperature sensitivity of *cdc13-1*, *cdc13-1 rad9Δ* and *cdc13-1 chk1Δ* strains at similar temperatures, and neither deletion increases the suppression of temperature sensitivity of *cdc13-1 rad53Δ sml1Δ* strains. Tkl1 and Tal1 both catalyse reactions in the non-oxidative phase of the pentose phosphate pathway (PPP). Since both enzymes operate in the same pathway, I hypothesised that the suppression of *cdc13-1* temperature sensitivity observed following deletion of *TKL1* or *TAL1* is due to deficiencies in the non-oxidative part of the PPP (see Figure 1.6). In order to test this hypothesis, I generated a strain in which both *TKL1* and *TAL1* were absent, alongside the *cdc13-1* mutation (Figure 4.5). Growth of this strain is marginally improved at 27^{o}C compared to *cdc13-1 tkl1Δ* (which demonstrated stronger growth than *cdc13-1 tal1Δ*), but not to a significant extent. Indeed, at 28^{o}C no growth is observed, similar to the single deletion strain alone.

These results suggest that the suppression of *cdc13-1* temperature sensitivity observed in *cdc13-1 tkl1Δ* and *cdc13-1 tal1Δ* strains is due to deficiencies in the non-oxidative phase of the PPP, since the majority of the pathway is blocked in *cdc13-1 tkl1Δ tal1Δ* strains (Figure 4.5). However, the activity of Tkl2, the minor isoform of transketolase, may allow flux to continue through the non-oxidative phase of the PPP, although tests indicate that transketolase activity is undetectable in *tkl1Δ* strains (Schaaff-Gerstenschläger et al., 1993).

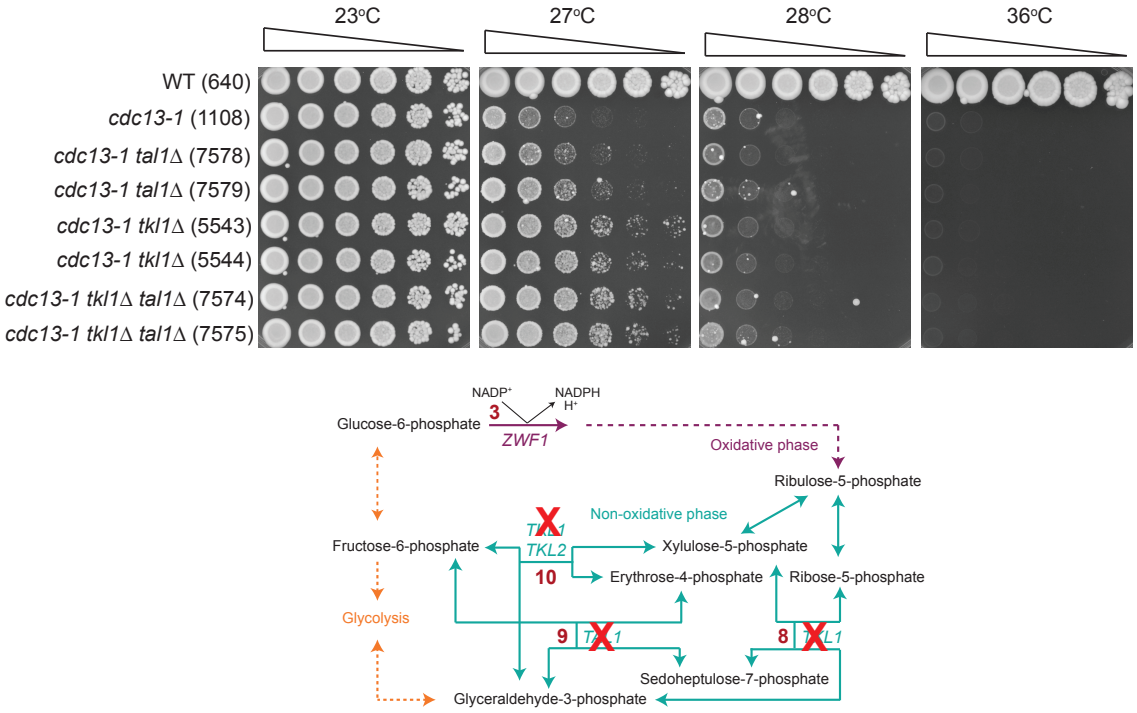

Figure 4.5: Temperature sensitivity of *cdc13-1 tkl1*Δ is not affected by *TAL1* deletion
Spot test for temperature sensitivity of *cdc13-1*, *cdc13-1 tkl1*Δ, *cdc13-1 tal1*Δ and *cdc13-1 tkl1*Δ *tal1*Δ, and a simplified subsection of Figure 1.6, indicating the disrupted steps of the PPP (red X). Strains were grown to saturation in YEPD before a 5-fold serial dilution and pinning onto solid agar plates. Plates were incubated at the indicated temperatures for 3 days. Numbers in the pathway correspond to those in Figure 1.6

4.2.5 The cdc13-1 tal1Δ growth phenotype is dependent on G6PDH activity

Flux through the pentose phosphate pathway can occur by two different routes, depending on the requirements of the cell. The oxidative phase of the PPP produces a large amount of the NADPH used in reactions in the cell, whereas the non-oxidative phase can be used to produce ribose-5-phosphate, the precursor to nucleotides and amino acids. The oxidative phase is non-reversible and results in the production of ribulose-5-phosphate, which feeds into the fully reversible non-oxidative phase. Therefore, if there is a requirement for NADPH, flux is predominantly directed into the oxidative phase via glucose-6-phosphate and the reaction catalysed by Zwf1 (Clasquin et al., 2011; Ralser et al., 2007; Frick and Wittmann, 2005). This can also result in ribose-5-phosphate production, but evidence suggests that ribose-5-phosphate production can be increased by driving flux into the non-oxidative phase via thermodynamic modulation of non-oxidative phase enzymes such as Tkl1 (Clasquin et al., 2011).

Zwf1 is a major enzyme which catalyses the first, rate-limiting step of the oxidative phase of the PPP. It is constitutively expressed and therefore acts much like a housekeeping enzyme (Kletzien et al., 1994). Deletion of *ZWF1* in the *cdc13-1* background does not have a large effect on temperature sensitivity in the W303 background (Figure 4.6). Interestingly, the Addinall et al. (2011) screen found *zwf1*Δ to suppress *cdc13-1* temperature sensitivity to a similar extent to *TKL1* and *TAL1*. This may be due to a difference in yeast background used, since the screen was carried out in S288C.

If the effect that *TKL1* and *TAL1* deletions exert on the growth of *cdc13-1* is entirely due to the roles that they play in the non-oxidative phase of the PPP, then I expected to observe that deletion of *ZWF1* alongside *TKL1* and *TAL1* deletion in the *cdc13-1* background changes the growth phenotype, either improving or reducing growth in comparison to *cdc13-1 tkl1*Δ and *cdc13-1 tal1*Δ strains. Unfortunately, I could not test *cdc13-1 tkl1*Δ *zwf1*Δ strains, since the double deletion of *ZWF1* and *TKL1* is lethal (Deutscher et al., 2006). In order to test my hypothesis, I therefore crossed a *zwf1*Δ strain with a *cdc13-1 tal1*Δ strain, which did not result in lethality. As demonstrated in Figure 4.6, deletion of *ZWF1* actually removes the phenotypic suppression caused by *TAL1* deletion in the *cdc13-1* background at 26.5^{o}C. The

temperature sensitivity of *cdc13-1 tal1*Δ *zwf1*Δ strains resembled that of *cdc13-1 zwf1*Δ strains (and, to some extent, *cdc13-1*) rather than *cdc13-1 tal1*Δ strains, which grew adequately at 26.5^{o}C. This result suggests that the phenotypic suppression observed when *TAL1* is deleted in the *cdc13-1* background is dependent on Zwf1 activity. This could either be due to the reduction in NADPH production, since the major source of NADPH is the first step of the PPP; alternatively, it may be related to the production of ribose-5-phosphate, which can only be produced via the non-oxidative phase of the PPP in the absence of Zwf1.

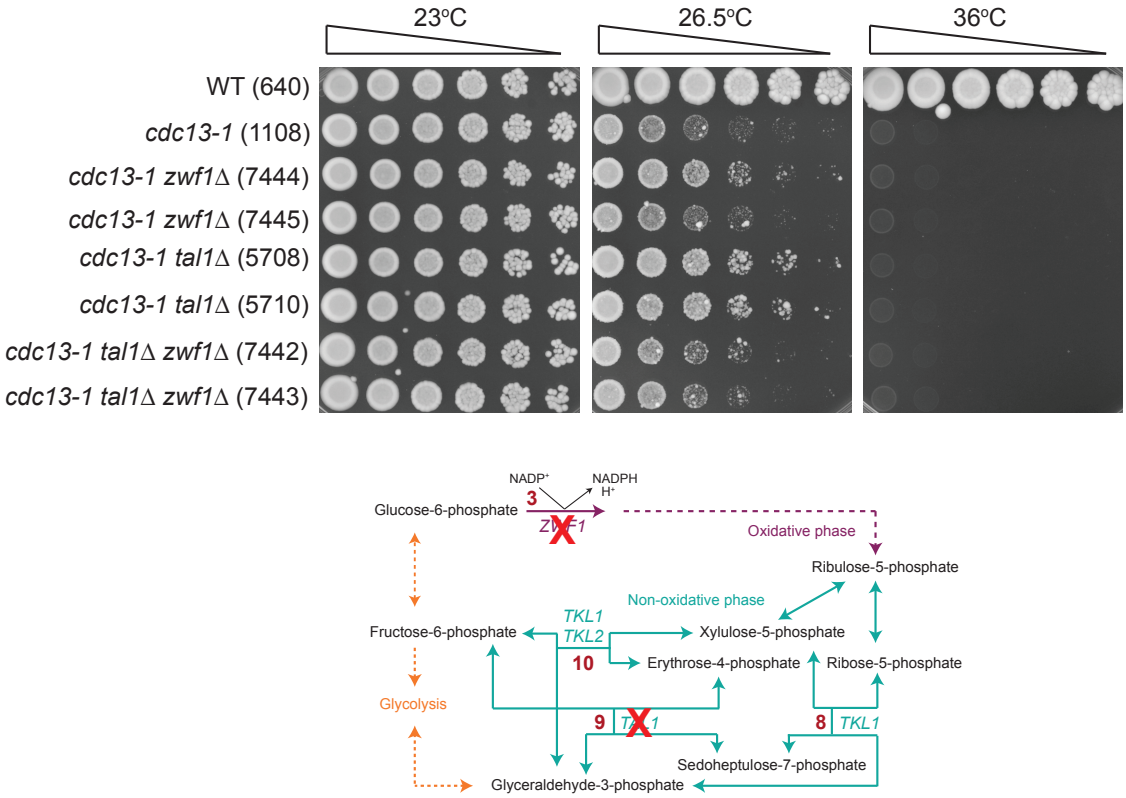

Figure 4.6: Phenotypic suppression by *TAL1* deletion is Zwf1-dependent
Spot test for temperature sensitivity of *cdc13-1*, *cdc13-1 zwf1*Δ, *cdc13-1 tal1*Δ and *cdc13-1 tal1*Δ *zwf1*Δ, and a simplified subsection of Figure 1.6, indicating the disrupted steps of the PPP (red X). Strains were grown to saturation in YEPD before a 5-fold serial dilution and pinning onto solid agar plates. Plates were incubated at the indicated temperatures for 3 days. Numbers in the pathway correspond to those in Figure 1.6

4.2.6 G6PDH activity is not affected by TAL1 or TKL1 deletion

The deletion of *TAL1* could potentially affect Zwf1 activity, which could explain the difference observed between suppression of *cdc13-1* temperature sensitivity by *TAL1* deletion and suppression of temperature sensitivity in *cdc13-1 tal1*Δ *zwf1*Δ strains. For instance, *TAL1* deletion may result in an increase in Zwf1 activity through directing flux through the oxidative phase of the PPP, which may result in a decrease in the temperature sensitivity of *cdc13-1*. This effect is then absent upon deletion of *ZWF1*. In order to investigate whether deletion of *TAL1* had any effect on Zwf1 activity, I carried out an enzyme assay (as described in Chapter 2.3). Zwf1 activity in *tal1*Δ strains was monitored, as well as in wild type, *zwf1*Δ and *tkl1*Δ strains.

The activity of Zwf1 does not change upon deletion of *tal1*Δ or *tkl1*Δ (Figure 4.7 and Table 4.1). However, in the *zwf1*Δ strain, any activity of the enzyme is negligible to undetectable, as would be expected. The results suggest that neither *TAL1* nor *TKL1* deletion has a marked effect on Zwf1 activity. I conclude that the suppression of *cdc13-1* temperature sensitivity by *TAL1* deletion is dependent on flux through the oxidative phase but is not due to an increase in NADPH production.

	Wild Type	***zwf1*Δ**	***tal1*Δ**	***tkl1*Δ**
Specific Activity (µmol/min/mg)	357 ± 34	0 ± 13	317 ± 56	344 ± 34

Table 4.1: Specific activity of Zwf1 in *ppp*Δ strains

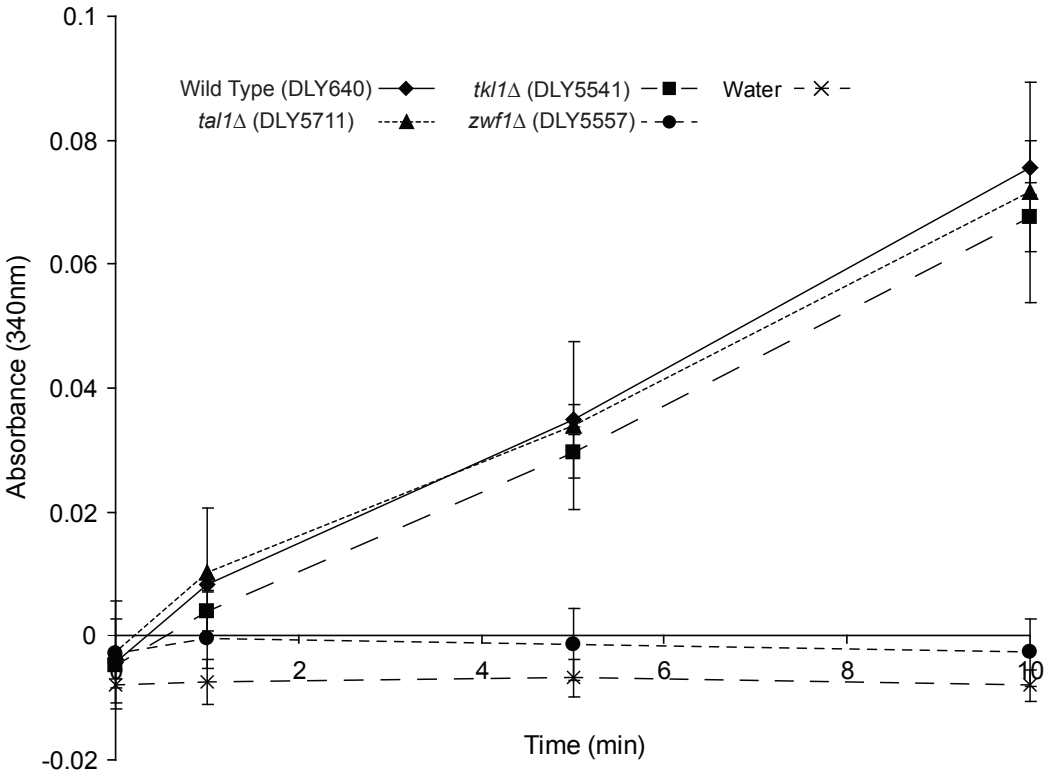

Figure 4.7: Deletion of *TKL1* or *TAL1* does not affect Zwf1 activity
Measurement of Zwf1 (G6PDH) activity in wild type and *ppp*Δ strains by measuring NADPH generation. NADPH generation was determined by measuring absorbance at 340 nm before and 1, 5 and 10 minutes after the addition of glucose-6-phosphate to the reaction mixture. In the water control, water was added to the reaction mixture in place of cell lysate.

4.2.7 TKL1 deletion suppresses yku70Δ temperature sensitivity

I decided to investigate the effect of *TKL1* and *TAL1* deletion on the temperature sensitivity of *yku70*Δ strains in order to establish whether suppression of the telomere uncapping phenotype is *cdc13-1* specific. The Ku complex is a highly conserved complex which binds to the double stranded region of telomeres and plays an important role in homologous recombination as well as telomere uncapping. In *S. cerevisiae*, the Ku complex is composed of Yku70 and Yku80, which bind together in a heterodimeric ring structure distal from the end of the telomere. Telomere uncapping caused by the *cdc13-1* mutation and *YKU70* deletion elicit similar responses but with a number of differences. Whereas uncapping in *cdc13-1* strains results in extensive degradation of the 5' strand and the activation of the Mec1/Rad53/Dun1-depenent and Rad9/Mec1/Chk1- and Pds1-dependent checkpoint pathways, uncapping in *yku70*Δ strains leads to a shorter 3' overhang in comparison and the activation of only the latter checkpoint pathway (Zubko et al., 2004; Maringele and Lydall, 2002).

*yku70*Δ can grow to higher temperatures than *cdc13-1* - the temperature-sensitive effects can only be observed at temperatures over 36^{o}C. In order to test the effect of *TKL1* and *TAL1* deletion in the *yku70*Δ background, I crossed *tkl1*Δ and *tal1*Δ strains with *yku70*Δ and carried out a serial dilution spot test. The results in Figure 4.8 demonstrate that the deletion of *TKL1* and *TAL1* have different effects on the temperature sensitivity of *yku70*Δ. *TAL1* deletion has minimal effects on *yku70*Δ growth and growth at 37^{o}C may even by slightly inhibited. In contrast, *TKL1* deletion causes a significant improvement in *yku70*Δ growth at temperatures up to 37^{o}C. Curiously, this phenotypic suppression disappears upon an increase in temperature of just 0.5^{o}C to 37.5^{o}C. This likely to be due to an independent temperature sensitivity caused by *TKL1* deletion. Indeed, a large-scale study of heat sensitivity of null mutants found that *tkl1*Δ strains demonstrate increased sensitivity to temperatures over 37^{o}C (Sinha et al., 2008).

I also tested the growth of *yku70*Δ *tkl1*Δ *tal1*Δ strains. Growth of these strains resembled that of *yku70*Δ *tkl1*Δ strains, including the sharp reduction in growth at 37.5^{o}C when compared to growth at 37^{o}C. The genome-wide screen data from the Addinall et al. (2011) study suggests that neither *TKL1* deletion nor *TAL1* deletion

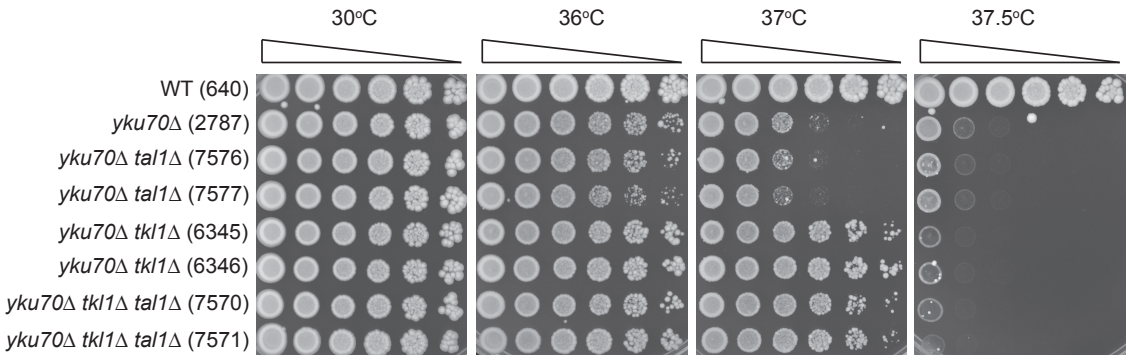

Figure 4.8: *TKL1* deletion suppresses *yku70*Δ temperature sensitivity
Spot test for temperature sensitivity of *yku70*Δ, *yku70*Δ *tkl1*Δ, *yku70*Δ *tal1*Δ and *yku70*Δ *tkl1*Δ *tal1*Δ. Strains were grown to saturation in YEPD before a 5-fold serial dilution and pinning onto solid agar plates. Plates were incubated at the indicated temperatures for 3 days.

has an effect on the temperature sensitivity of *yku70*Δ (Figure 4.1). My data suggests that in the W303 background, the *TAL1* result is comparable. However, *TKL1* deletion in the *yku70*Δ background has a different effect to the one predicted by the screen, which was carried out in the S288C background. This could be an effect specific to W303.

4.3 Discussion

In this chapter I have demonstrated that deletion of pentose phosphate pathway genes *TKL1* and *TAL1* suppresses the temperature sensitivity of the telomere capping mutant strain *cdc13-1*. The suppression observed upon deletion of either *TKL1* or *TAL1* is due to disruption of the same pathway, namely the non-oxidative phase of the PPP. This was confirmed by deletion of both genes in the *cdc13-1* background, which did not result in an increase in phenotypic suppression; rather, growth of *cdc13-1 tkl1*Δ *tal1*Δ strains resembled that of *cdc13-1 tkl1*Δ. In addition, suppression of *cdc13-1* temperature sensitivity by *TKL1* and *TAL1* deletion is independent of the activities of the DNA damage-dependent checkpoint protein Rad9 and the DNA damage checkpoint effector Chk1. The *rad9*Δ and *chk1*Δ null mutations alone cause an increase in growth of *cdc13-1* strains at semi-permissive temperatures due to prevention of the initiation of downstream DNA damage response pathways and cell cycle arrest (Jia et al., 2004; Maringele and Lydall, 2002; Sanchez et al., 1999; Garvik et al., 1995). I found that deletion of either *TKL1* or *TAL1* in the *cdc13-1 rad9*Δ and *cdc13-1 chk1*Δ backgrounds increased the growth of these strains at semi-permissive temperatures further, suggesting that the suppression of temperature sensitivity in *cdc13-1 tkl1*Δ and *cdc13-1 tal1*Δ strains was not part of the Chk1 response pathway. Indeed, deletion of either *TKL1* or *TAL1* in the *cdc13-1 rad53*Δ *sml1*Δ background did not cause further suppression of the temperature sensitivity of the strain, which further reinforces the hypothesis that suppression of *cdc13-1* temperature sensitivity by *TKL1* or *TAL1* is related to the Mec1/Rad53/Dun1-dependent checkpoint pathway.

*ppp*Δ strains are sensitive to oxidative stress. For instance, treating *ppp*Δ strains with various agents that cause oxidative stress such as hydrogen peroxide (H_2O_2), diamide and cumene-hydroperoxide (CHP) leads to a reduction in growth when compared to untreated strains (Krüger et al., 2011). This is thought to be due to a drop in the production of NADPH which is essential for antioxidant function; indeed, in the absence of the antioxidant Sod1, overexpression of *TKL1* can suppress the *sod1*Δ phenotypes in a manner dependent on the activity of Zwf1 (the yeast G6PDH), which suggests that *TKL1* overexpression results in an increase in NADPH production (Carter et al., 2005; Slekar et al., 1996). However, the oxidative stress sensitivities

observed in *ppp*Δ strains may also be attributable to changes in gene expression regulation during the response to oxidative stress (Krüger et al., 2011).

The suppression of the temperature sensitivity of *cdc13-1* strains exhibited by *TAL1* deletion is also dependent on the activity of G6PDH, since deletion of *ZWF1* in the *cdc13-1 tal1*Δ background removed the observed increase in growth of *cdc13-1* at semi-permissive temperatures. This suggested that deletion of *TAL1* affected Zwf1 activity and NADPH production. In order to determine whether Zwf1 activity changes in response to disruption of the non-oxidative phase of the PPP, I measured NADPH production in *tkl1*Δ and *tal1*Δ strains. I found that the activity of Zwf1 did not change following *TKL1* and *TAL1* deletion, which agrees with previous measurements of the NADPH to $NADP^+$ ratio in these strains (Krüger et al., 2011).

Therefore I concluded that the suppression of *cdc13-1* temperature sensitivity by *TKL1* or *TAL1* deletion is independent of NADPH production, and therefore that telomere uncapping in *cdc13-1* strains does not lead to oxidative stress. Previous studies have demonstrated that *tkl1*Δ and *tal1*Δ strains are sensitive to the presence of ROS, which suggests that *cdc13-1 tkl1*Δ and *cdc13-1 tal1*Δ strains should display enhanced growth defects if oxidative stress were occurring (Krüger et al., 2011; Tucker and Fields, 2004; Juhnke et al., 1996). Here, I have shown that it is in fact the opposite and *cdc13-1 tkl1*Δ and *cdc13-1 tal1*Δ strains display improved growth compared to *cdc13-1* strains.

As described in Chapter 1.3.6, the pentose phosphate pathway is important for the production of the nucleotide precursor ribose-5-phosphate. Therefore, one explanation for the suppression of the temperature-sensitive phenotype of *cdc13-1* by deletion of either *TKL1* or *TAL1*, and suppression of *yku70*Δ temperature sensitivity by *TKL1* deletion may be that these null mutations affect the concentration of ribose-5-phosphate available for nucleotide biosynthesis. I hypothesised that deletion of *TKL1*, *TAL1* and the two genes together increased ribose-5-phosphate available for nucleotide biosynthesis due to minimal flux through the non-oxidative phase of the PPP, thereby reducing the recycling of intermediates into glycolysis.

Studies in bacteria have reported increases in ribose-5-phosphate accumulation in transketolase null strains, and the intermediate also accumulates in *tkl1*Δ and *tal1*Δ *S. cerevisiae* strains following exposure to hydrogen peroxide (Krüger et al., 2011; Park et al., 2006). I suspect that the differences between suppression of *cdc13-1* temperature sensitivity seen in *cdc13-1 tkl1*Δ and *cdc13-1 tal1*Δ strains are due to the different increases in ribose-5-phosphate levels, where deletion of *TKL1* results in higher ribose-5-phosphate levels than *TAL1* deletion. This difference is also observable in the *yku70*Δ background, in that *yku70*Δ *tkl1*Δ strains also grow better than *yku70*Δ *tal1*Δ strains at semi-permissive temperatures. Since telomere uncapping in *cdc13-1* strains results in a longer single-stranded 3' overhang than in *yku70*Δ strains, I suggest that the requirement for nucleotides for repair is greater in *cdc13-1* strains and that Tkl1 activity has a larger impact on nucleotide production (Zubko et al., 2004; Maringele and Lydall, 2002).

4.4 Future Work

Resulting from this chapter, my hypothesis as to why deletion of *TKL1* or *TAL1* causes suppression of the *cdc13-1* temperature-sensitive phenotype is based on alteration in nucleotide production. Specifically, I concluded that *cdc13-1 tkl1*Δ and *cdc13-1 tal1* strains are less temperature sensitive than *cdc13-1* strains due to an increase in the concentration ribose-5-phosphate, which in turn can aid an increase in dNTP levels.

In order to test this hypothesis, the dNTP levels in *cdc13-1*, *cdc13-1 tkl1*Δ and *cdc13-1 tal1*Δ strains could be measured to determine whether dNTP concentration is affected by telomere uncapping and disruption of the non-oxidative phase of the PPP in telomere capping mutants. The equivalent experiments could also be carried out in *yku70*Δ, *yku70*Δ *tkl1*Δ and *yku70*Δ *tal1*Δ strains, since I hypothesise that dNTP levels have a smaller effect on *yku70*Δ strains at restrictive temperatures than *cdc13-1* strains.

In this chapter I studied Zwf1 activity in *tkl1*Δ and *tal1*Δ strains. In order to ascertain whether any metabolic changes which occur in response to telomere uncapping are affected by *TKL1* and *TAL1* deletion, the activity of Zwf1 in *cdc13-1 tkl1*Δ and *cdc13-1 tal1*Δ strains could be examined using the same enzyme assay used in Chapter 4.2.6. Zwf1 activity in *cdc13-1* strains is investigated in Chapter 5.

TKL1 and *TAL1* do not encode the only yeast transketolase and transaldolase. Therefore the effects of *TKL1* and *TAL1* deletion explored in this chapter may rely on the activities of the secondary transketolase Tkl2 and the putative transaldolase Nqm1 (Huang et al., 2008; Schaaff-Gerstenschläger et al., 1993). Strains could be generated in which *TKL2* and *NQM1* are deleted along with *TKL1* and *TAL1* in the *cdc13-1* background. This would eliminate all transketolase and transaldolase activity and could support the hypothesis that disruption to the non-oxidative phase of the PPP results in suppression of *cdc13-1* temperature sensitivity.

5 Telomere uncapping leads to an increase in pentose phosphate pathway activity due to cell cycle arrest

5.1 Introduction

Metabolic flux is finely regulated and balanced. The increase in expression of a single enzyme can alter the chemical balance within a cell, and rapid switching between biochemical pathways means that responses to stresses or other environmental conditions, such as nutrient levels, are swift and effective. Flux through the pentose phosphate pathway under normal conditions in *Saccharomyces cerevisiae* is low, with the majority of glucose entering glycolysis (Frick and Wittmann, 2005). As little as 15% of glucose is diverted through the PPP; however, stressful conditions can alter this balance (Frick and Wittmann, 2005). One important metabolic switch in glucose metabolism is the inhbition of glyceraldehyde-3-phosphate dehydrogenase (GAPDH). The presence of oxidative species causes inactivation of GAPDH, blocking glycolysis and redirecting glucose into the PPP (Ralser et al., 2007).

The enzyme that catalyses the first step of the PPP also responds to environmental cues and alters flux into the pathway. Glucose-6-phosphate dehydrogenase (G6PDH, Zwf1 in budding yeast) is constitutively expressed in the manner of a housekeeping protein. G6PDH activity is regulated post-transcriptionally by various means, most significantly the $NADP^+$/NADPH ratio. NADPH is used as a reducing equivalent to reduce anti-oxidants which remove potentially harmful reactive oxygen species. Under oxidative stress conditions, reduced anti-oxidants become rapidly depleted and therefore NADPH levels drop. This change in the $NADP^+$/NADPH ratio increases G6PDH activity, which in turn increases NADPH production (Kotaka et al., 2005; Au et al., 2000; Luzzatto, 1967).

In a 2010 paper, Cosentino et al. demonstrated that G6PDH activity can also be regulated in response to DNA damage through the binding of a heat shock protein to the enzyme (Cosentino et al., 2010). Their work with *Xenopus laevis* and human cell lines explored the link between the activity of ATM, the kinase activity of which is

key to the DNA damage response and G6PDH activity. The group suggest that ATM, through a phosphorylation cascade, can stimulate an increase G6PDH activity in response to double strand breaks. This finding is significant, in that it suggests a role for the pentose phosphate pathway, or at least G6PDH activity, in the DNA damage response, and that increasing flux through the pathway could somehow be beneficial.

As I have already explored in previous chapters, the DNA damage response can be studied through use of the telomere capping mutant *cdc13-1*. The temperature-sensitive *cdc13-1* exhibits capping defects at restrictive temperatures which result in the initiation of a DNA damage response, leading to extensive resection and cell cycle arrest (Garvik et al., 1995). The presence of uncapped telomeres also stimulates transcriptional changes. A microarray carried out by Greenall et al. (2008) investigated the genome-wide transcriptional response to telomere uncapping in *cdc13-1*. RNA transcript levels in uncapped strains at permissive and restrictive temperatures were compared to those of wild type counterparts under the same conditions. Changes in transcript levels were monitored over a four-hour time course. The analysis revealed that NAD^+ metabolism potentially has a link with the response to telomere uncapping via increased expression of *BNA2*, which encodes an enzyme with a role in the *de novo* production of NAD^+ (Reaction 1 in Figure 1.6) (Panozzo et al., 2002). Interestingly, NAD^+ is linked to the pentose phosphate pathway via the NADP kinases Utr1 and Yef1 (the latter of which is also upregulated following telomere uncapping), which phosphorylate NAD^+ to $NADP^+$ (Reaction 2 in Figure 1.6) (Li and Shi, 2006). As described in Chapter 1.3.3, $NADP^+$ is reduced in the oxidative phase of the PPP to produce NADPH (Figure 1.6). The expression of two PPP genes, *SOL4* and *GND2*, also increases greatly upon telomere uncapping. Here, I investigate the relationship between telomere uncapping, the pentose phosphate pathway and Zwf1 activity further, beginning with additional analysis of the published Greenall et al. (2008) microarray data, and with the aim of studying flux through the pentose phosphate pathway and the possible mechanisms by which any changes come about.

5.2 Results

5.2.1 593 genes are differentially regulated following telomere uncapping

Analysis of microarray data can provide a large amount of information about gene regulation in response to changes in conditions or over a particular time period. The method by which microarray data is analysed can return different results depending on the statistical method used. In addition, other parameters imposed during data analysis such as normalisation and pair-wise correction can also alter the results. Greenall et al. (2008) investigated the genome-wide response to telomere uncapping using a microarray, the data from which was subsequently analysed using Bioconductor in R (a statistical programming language) (Gentleman et al., 2004). Figure 5.1a, taken from the Greenall et al. (2008) paper, describes the time course from which samples were collected for the microarray, where *CDC13+* and *cdc13-1* cultures were shifted from permissive to restrictive temperatures and samples taken every hour. This analysis identified 647 genes as being differentially regulated upon telomere uncapping – the definition of differentially regulated being at least a two-fold change in expression between $CDC13^{+}$ and *cdc13-1* strains during at least one time point in the 4 hour time course (in all three replicates), and a p-value of < 0.05.

In order to determine which genes were most likely to be differentially regulated following telomere uncapping, I used this definition and compared the results of three different statistical tests on the microarray data associated with the Greenall et al. (2008) paper. I analysed the raw CEL files produced following the microarray (available via the ArrayExpress website, accession number E-MEXP-1551) in GeneSpring and CARMAweb, using the unpaired t-test and the moderated t-statistic (*limma*) respectively (Rainer et al., 2006; Grewal and Conway, 2000). This resulted in a list of 664 differentially regulated genes from GeneSpring, and 658 differentially regulated genes following analysis using CARMAweb. Subsequent comparison of the three lists of genes (the results from GeneSpring, CARMAweb and the original analysis) gave 593 genes which appeared in all three lists (Figure 5.1b). Therefore I could be confident that these 593 genes were upregulated following telomere uncapping.

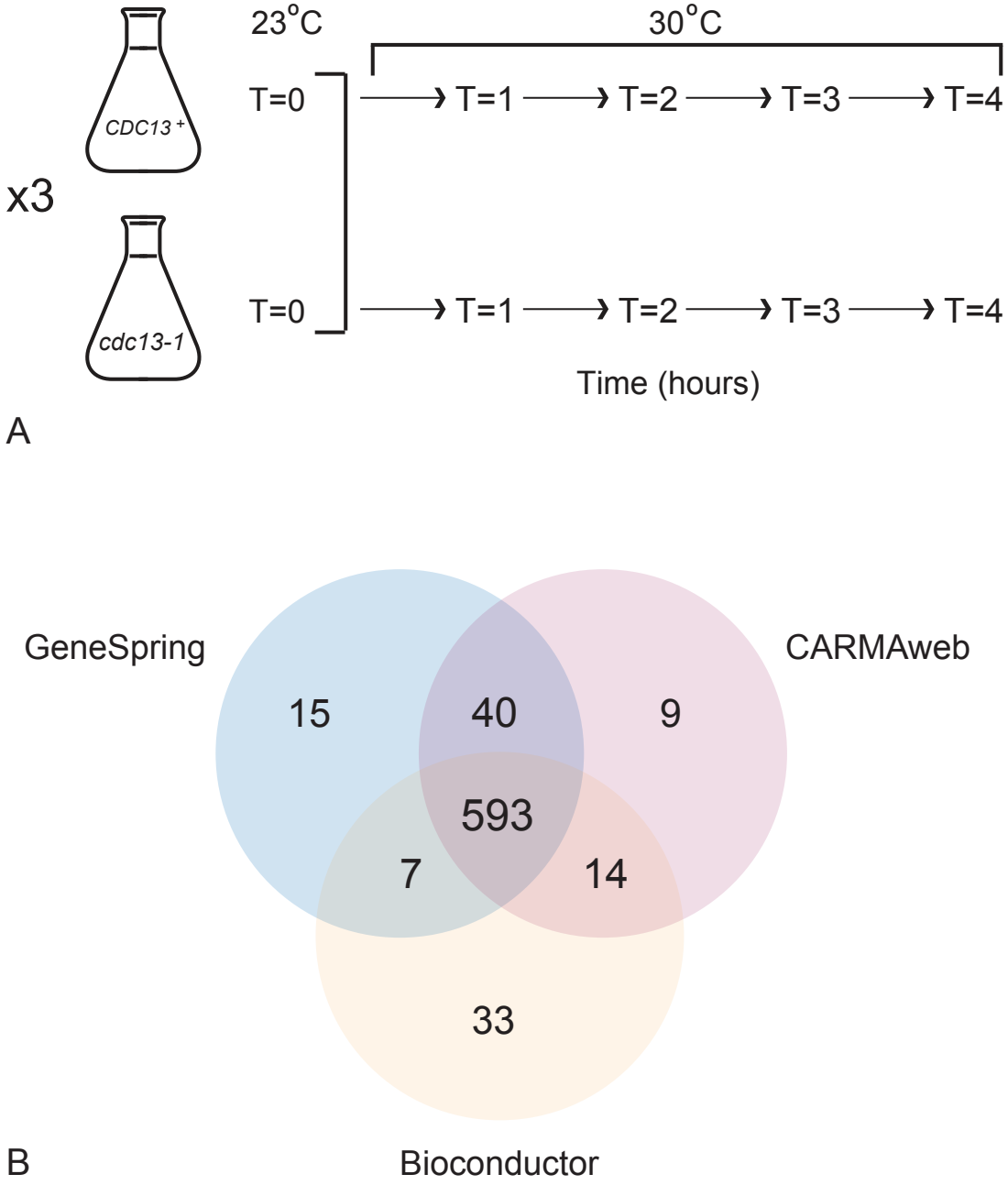

Figure 5.1: 593 genes are differentially expressed following telomere uncapping
(a) Experimental design of the Greenall et al. microarray (taken from the 2008 paper). *CDC13+* and *cdc13-1* strains were inoculated into liquid culture and grown at 23°C to early log phase. Samples were taken (T = 0) and cultures were shifted to 30°C. Samples taken every hour after the temperature shift (T = 1 - T = 4) were used for the microarray experiment. **(b)** Three different methods of data analysis identified 593 genes with at least two-fold changes in expression level between *cdc13-1* and *CDC13+* strains ($p \leq 0.05$). Statistical methods used are described in Chapter 2.1.7.

5.2.2 PPP-linked terms are over-represented among upregulated genes

I carried out Gene Ontology (GO) analysis on the genes which were identified as differentially regulated following telomere uncapping in my analysis of the microarray data. Prior to carrying out GO analysis, cell cycle regulated genes were removed from the list of genes identified as being differentially expressed, since a number of genes identified as differentially expressed following telomere uncapping are likely to be enriched or depleted due to the cell cycle arrest at G_2-M, which occurs in *cdc13-1* strains but not *CDC13*$^+$ strains (Greenall et al., 2008). GO analysis of the remaining 362 genes revealed that overrepresented GO terms related to differentially expressed genes following telomere uncapping include 'oxidoreductase activity' and 'pentose metabolic process' (Table 5.1).

Further analysis of the upregulated genes and downregulated genes in isolation found that many of the over-represented GO terms associated with upregulated genes were related to carbohydrate metabolism and the response to oxidative stress, whereas many GO terms associated with downregulated genes were related to the ribosome and RNA processing (Tables 5.2 and 5.3). A number of the upregulated genes related to carbohydrate metabolism were linked with the pentose metabolism, including *XKS1*, *GCY1*, *RBK1*, *YJR096W*, *GND2* and *SOL4*. *YEF1* and *BNA2* were also upregulated in response to telomere uncapping and both encode proteins with functions relating to the pentose phosphate pathway (Li and Shi, 2006; Panozzo et al., 2002). The GO analysis therefore indicates that the pentose phosphate pathway changes in response to telomere uncapping in *cdc13-1* strains following a shift to restrictive temperatures.

Gene Ontology Term	*p*-value
Biological Process	
Cellular carbohydrate metabolic process	5.85E-09
Carbohydrate metabolic process	6.10E-09
Oxidoreductase activity	9.21E-07
Monosaccharide metabolic process	8.11E-06
Generation of precursor metabolites and energy	5.61E-05
Alcohol metabolic process	1.02E-04
Energy derivation by oxidation of organic compounds	3.85E-04
Cellular carbohydrate catabolic process	3.95E-04
Carbohydrate catabolic process	3.95E-04
Pentose metabolic process	6.17E-04
Monosaccharide catabolic process	1.15E-03
Energy reserve metabolic process	1.94E-03
Alcohol catabolic process	1.94E-03
Amino acid biosynthetic process	2.09E-03
Glucose metabolic process	2.52E-03
Glutamine family amino acid biosynthetic process	3.11E-03
Glutamine family amino acid metabolic process	3.11E-03
Arginine biosynthetic process	4.04E-03
Amine biosynthetic process	7.34E-03
Nitrogen compound biosynthetic process	8.34E-03
Glycogen metabolic process	9.55E-03

Table 5.1: GO analysis of differentially expressed genes following telomere uncapping

Gene Ontology Term	*p*-value
Biological Process	
Carbohydrate metabolic process	7.49E-15
Cellular carbohydrate metabolic process	7.49E-15
Oxidoreductase activity	2.34E-10
Generation of precursor metabolites and energy	3.32E-08
Alcohol metabolic process	1.56E-06
Energy derivation by oxidation of organic compounds	2.28E-06
Monosaccharide metabolic process	8.99E-06
Cellular carbohydrate catabolic process	1.53E-05
Carbohydrate catabolic process	1.53E-05
Pentose metabolic process	4.32E-05
Energy reserve metabolic process	5.16E-05
Monosaccharide catabolic process	1.57E-04
Glucose metabolic process	2.07E-04
Alcohol catabolic process	2.74E-04
Glycogen metabolic process	5.84E-04
Hexose metabolic process	9.11E-04
Cellular glucan metabolic process	1.36E-03
Response to oxidative stress	1.92E-03
Carbohydrate kinase activity	5.45E-03
Glutamate metabolic process	5.45E-03
Carbohydrate biosynthetic process	6.20E-03
Catabolic process	6.50E-03
Succinate dehydrogenase (ubiquinone) activity	9.61E-03
Pentose catabolic process	9.61E-03
Oxidoreductase activity, acting on the CH-CH group of donors, quinone or related compound as acceptor	9.61E-03

Table 5.2: GO analysis of upregulated genes following telomere uncapping

Gene Ontology Term	*p*-value
Biological Process	
Ribosome biogenesis and assembly	1.16E-18
Ribonucleoprotein complex biogenesis	2.02E-17
rRNA metabolic process	1.00E-07
RNA processing	1.61E-07
rRNA processing	2.19E-07
Arginine biosynthetic process	1.81E-05
Cellular amino acid biosynthetic process	7.04E-05
Arginine metabolic process	1.07E-04
Urea cycle intermediate metabolic process	1.07E-04
Amine biosynthetic process	1.27E-04
Nitrogen compound biosynthetic process	1.30E-04
Organelle organisation and biogenesis	1.58E-04
Maturation of SSU-rRNA from tricistronic rRNA transcript (SSU-rRNA, 5.8S rRNA, LSU-rRNA)	3.13E-04
Maturation of SSU-rRNA	3.87E-04
RNA metabolic process	6.06E-04
Amino acid and derivative metabolic process	6.87E-04
Amino acid metabolic process	1.23E-03
Glutamine family amino acid biosynthetic process	1.60E-03
Cellular component organisation and biogenesis	4.92E-03
Nitrogen compound metabolic process	4.92E-03
Amine metabolic process	7.67E-03
Nucleobase-containing compound metabolic process	7.67E-03
Cellular Component	
Nucleolus	1.78E-18
Nuclear lumen	1.78E-10
Organelle lumen	1.08E-07
Membrane-enclosed lumen	1.08E-07
Nuclear part	1.21E-06
Nucleolar preribosome	3.87E-04
Non-membrane-bound organelle	3.87E-04
Intracellular non-membrane-bound organelle	3.87E-04
90S preribosome	4.13E-04
Preribosome	4.14E-04
Nucleus	4.87E-04
Small subunit processome	2.82E-03
Preribosome, large subunit precursor	7.18E-03

Table 5.3: GO analysis of downregulated following telomere uncapping

5.2.3 ZWF1 expression in uncapped strains and genetic interaction with cdc13-1

The large increases in *SOL4* and *GND2* levels observed following telomere uncapping (Figure 5.2) suggests that Sol4 and Gnd2 are required for the response to capping deficiencies. Sol4 and Gnd2 are enzymes which catalyse reactions of the oxidative phase of the pentose phosphate pathway (Reactions 4 and 5 in Figure 1.6). Therefore, their upregulation suggests that pentose phosphate pathway activity increases in response to telomere uncapping. Flux into the PPP in budding yeast is regulated in the main by the activity of Zwf1, a glucose-6-phosphate dehydrogenase (G6PDH), which catalyses the first step of the pathway (Figure 5.3a and Reaction 3 in Figure 1.6). Cosentino et al. (2011) demonstrated that G6PDH activity increases in response to the presence of double strand breaks (DSBs). Taking this into account, I hypothesised that if flux increases through the PPP as a response to telomere uncapping, the activity of Zwf1 should increase to facilitate this.

Therefore I decided to study Zwf1 activity in *cdc13-1* strains at permissive and restrictive temperatures compared with *CDC13*$^{+}$ strains. The microarray data from the Greenall et al. (2008) study suggests that there is a slight increase in *ZWF1* levels following telomere uncapping (Figure 5.3b); however, Zwf1 expression is constitutive and the activity of the enzyme is regulated post-transcriptionally (Greenall et al., 2008; Kletzien et al., 1994). The growth phenotype of *cdc13-1 zwf1*Δ is not altered in comparison with *cdc13-1* alone, which implies that *zwf1*Δ does not affect the growth defect of the mutant strain (Figure 5.4). Interestingly, in the S288C background as part of a genome wide screen, *cdc13-1 zwf1*Δ grows better at semi-permissive temperatures than *cdc13-1* alone (Figure 4.1 and (Addinall et al., 2011). However, as shown here, *ZWF1* expression does not increase significantly in response to telomere uncapping, nor does *ZWF1* deletion affect *cdc13-1* temperature sensitivity at semi-permissive temperatures in the W303 background.

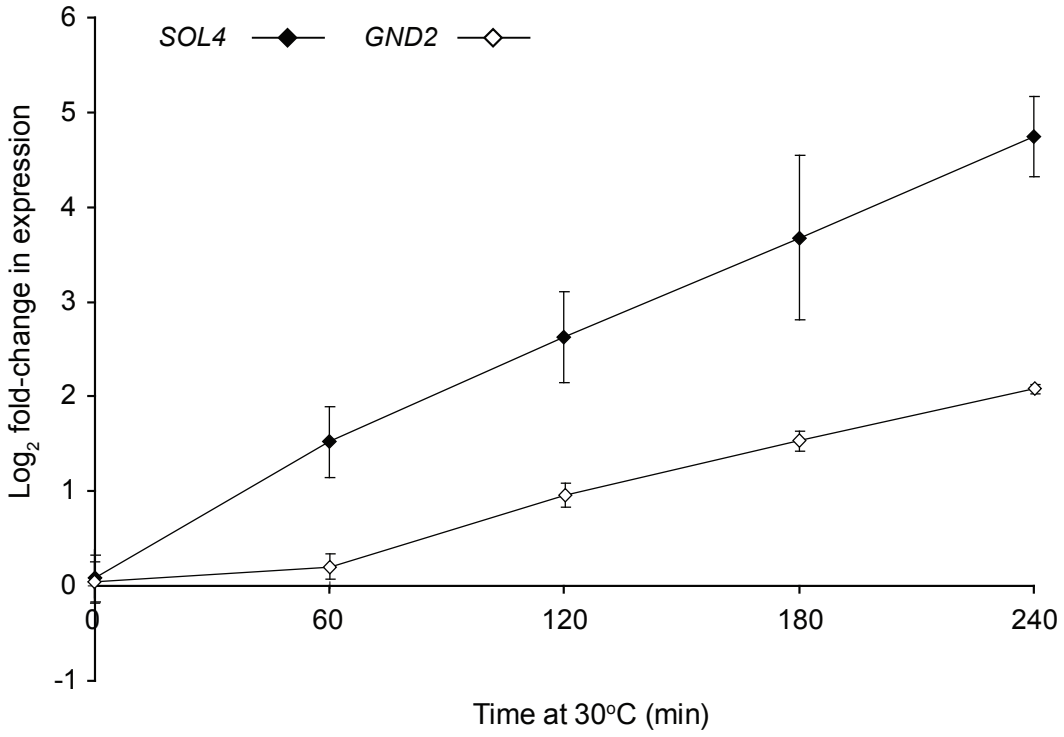

Figure 5.2: The expression of *SOL4* and *GND2* increases in response to telomere uncapping

Change in expression level of *SOL4* and *GND2* transcripts in *cdc13-1* strains in response to telomere uncapping, where $\log_2$ represents the log-fold change in expression when compared with *CDC13+* strains under the same conditions (data taken from Greenall et al. (2008)). Plotted values represent the means of three independent samples and error bars represent the standard deviations of the means.

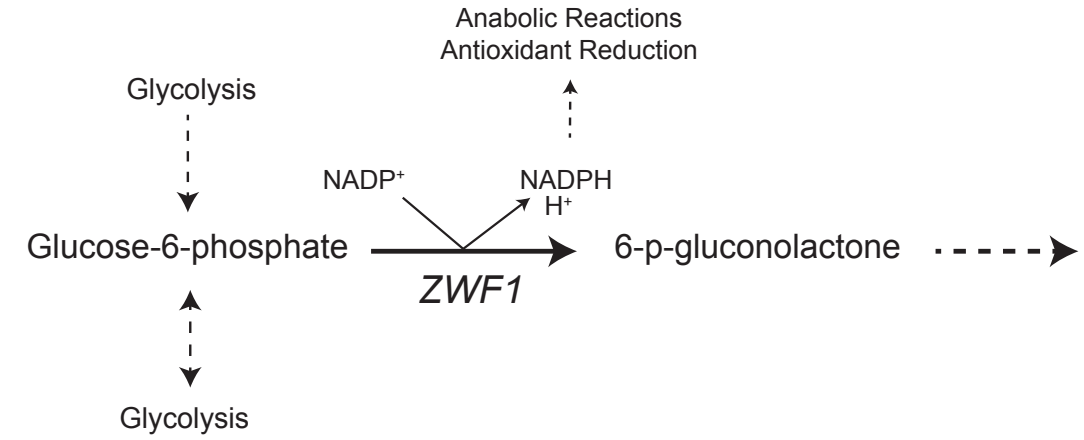

A

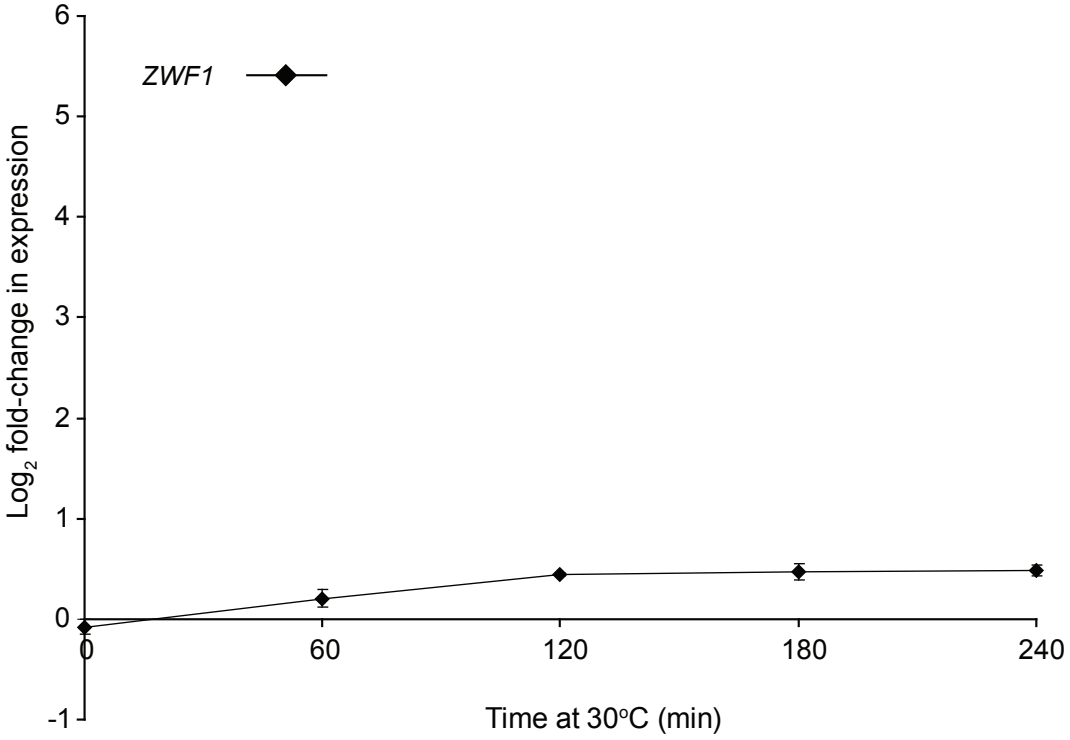

B

Figure 5.3: Change in *ZWF1* expression in response to telomere uncapping
(a) Zwf1 catalyses the conversion of glucose-6-phosphate to 6-p-gluconolactone in the first step of the oxidative phase of the pentose phosphate pathway, reducing $NADP^+$ to NADPH. **(b)** Change in expression level of *ZWF1* transcripts in *cdc13-1* strains in response to telomere uncapping, where $\log_2$ represents the log-fold change in expression when compared with *CDC13+* strains under the same conditions (data taken from Greenall et al. (2008)). Plotted values represent the means of three independent samples and error bars represent the standard deviations of the means.

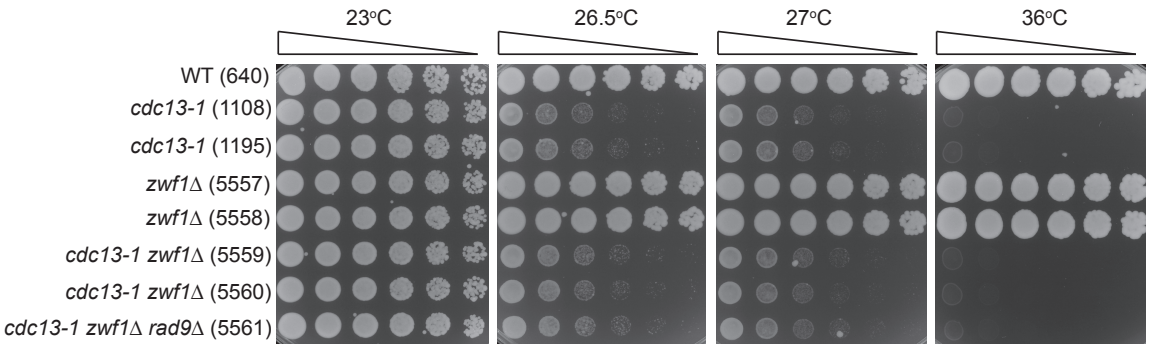

Figure 5.4: *cdc13-1* temperature sensitivity is not altered by *ZWF1* deletion
Spot test for temperature sensitivity of *cdc13-1* and *cdc13-1 zwf1*Δ. Strains were grown to saturation in YEPD before a 5-fold serial dilution and pinning onto solid agar plates. Plates were incubated at the indicated temperatures for 3 days.

5.2.4 G6PDH activity is absent in zwf1Δ strains

Zwf1 activity can be monitored by measuring NADPH accumulation in a controlled enzyme assay, in which all of the necessary reagents are added to saturation to cell lysate isolated from yeast cells. NADPH accumulation can be monitored by following changes in absorbance, since NADPH has an absorbance of 340 nm. Before testing *cdc13-1* strains for Zwf1 activity, I carried out the enzyme assay on a wild type strain alongside a *zwf1*Δ strain and a water control.

As the graph in Figure 5.5 demonstrates, Zwf1 activity can be observed in the wild type, but deletion of *ZWF1* results in an elimination of NADPH production by the particular reaction investigated. When compared to wild type, a *ZWF1* delete strain has virtually no specific activity whereas the specific activity of the wild type strain is over 800 μmol of NADPH/min/mg of protein (Table 5.4).

	Wild Type	***zwf1*Δ**
Specific Activity (μmol/min/mg)	817 ± 66	9.5 ± 9.6

Table 5.4: Specific activity of Zwf1 in *zwf1*Δ strains

The results from this experiment therefore suggest that I can be confident that the assay is indeed measuring amount of NADPH produced by the reaction catalysed by Zwf1, and that deletion of *ZWF1* eliminates G6PDH activity. However, since the assay cannot be corrected for enzyme co-factors, the enzyme assay can be used to measure Zwf1 activity but it cannot be used to measure flux through the reaction.

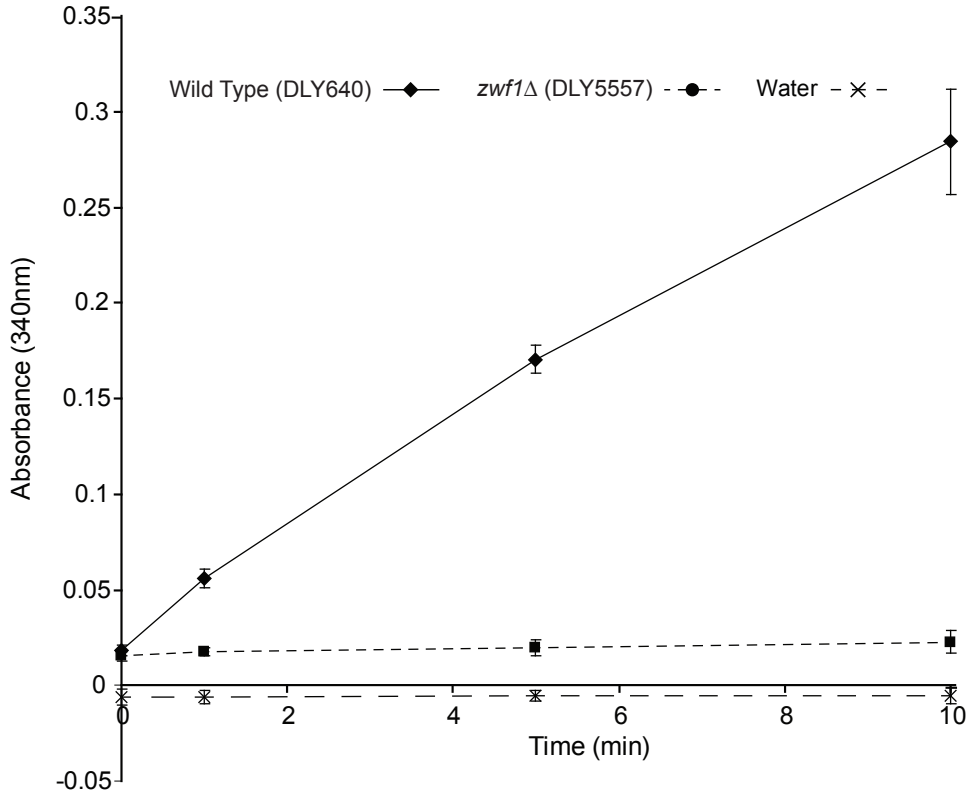

Figure 5.5: Deletion of *ZWF1* eliminates NADPH production in a G6PDH assay
Measurement of Zwf1 (G6PDH) activity in wild type and *zwf1*Δ strains by measuring NADPH generation. NADPH generation was determined by measuring absorbance at 340 nm before and 1, 5 and 10 minutes after the addition of glucose-6-phosphate to the reaction mixture. In the water control, water was added to the reaction mixture in place of cell lysate.

5.2.5 G6PDH activity in cdc13-1 increases at restrictive temperatures

I hypothesised that an increase in flux through the pentose phosphate pathway occurs following telomere uncapping and that this increase in flux could, in part, be identified by an increase in Zwf1 activity. As demonstrated in 5.2.4, Zwf1 activity can be monitored using a G6PDH activity assay in which NADPH concentration in followed through absorbance measurements. In order to observe the response of Zwf1 activity to telomere uncapping, I carried out a time course, represented diagrammatically in Figure 5.6. Samples of *CDC13*$^{+}$ and *cdc13-1* cultures were taken at T = 0, then cultures were split and placed at 23^{o}C or 36^{o}C. Further samples were taken at 15, 60, 120, 180 and 240 minutes following the shift from permissive to non-permissive temperature.

As Figure 5.7 demonstrates, Zwf1 activity remains at a constant level at 23^{o}C in both *CDC13*$^{+}$ and *cdc13-1* strains. At 36^{o}C, Zwf1 activity is elevated after 60 minutes in both *CDC13*$^{+}$ and *cdc13-1* strains, when compared to activity at 23^{o}C. However, whereas Zwf1 activity in *CDC13*$^{+}$ strains remains the same over the remainder of the time course, the activity of Zwf1 in uncapped *cdc13-1* strains continues to rise (Table 5.5).

	Specific Activity (µmol/min/mg)			
Incubation Temperature	**23^{o}C**		**36^{o}C**	
Time (mins)	***CDC13+***	***cdc13-1***	***CDC13+***	***cdc13-1***
0	261.5 ± 86	306 ± 66	261.5 ± 86	306 ± 66
15	252.5 ± 16	277 ± 44	279 ± 54	330.5 ± 32
60	298 ± 0	264.5 ± 60	457 ± 16	505.5 ± 9
120	284.5 ± 6	247 ± 16	443.5 ± 35	664.5 ± 32
180	259 ± 13	270 ± 28	462.5 ± 35	699 ± 85
240	272.5 ± 25	333 ± 28	404.5 ± 4	873.5 ± 117

Table 5.5: Specific activity of Zwf1 in *CDC13+* and *cdc13-1* strains

I determined the cell cycle position of 100 cells from each sample at each time point using DAPI staining. The results indicate that after 60 minutes there is little difference between the percentage of cells in each stage between wild type and *cdc13-1* strains (Figure 5.8). However, as the time course progresses the number of *cdc13-1* cells arrested at G_2-M increases significantly, peaking at almost 90% of cells after four hours at 36^{o}C. The *cdc13-1* strains kept at 23^{o}C, along with the wild

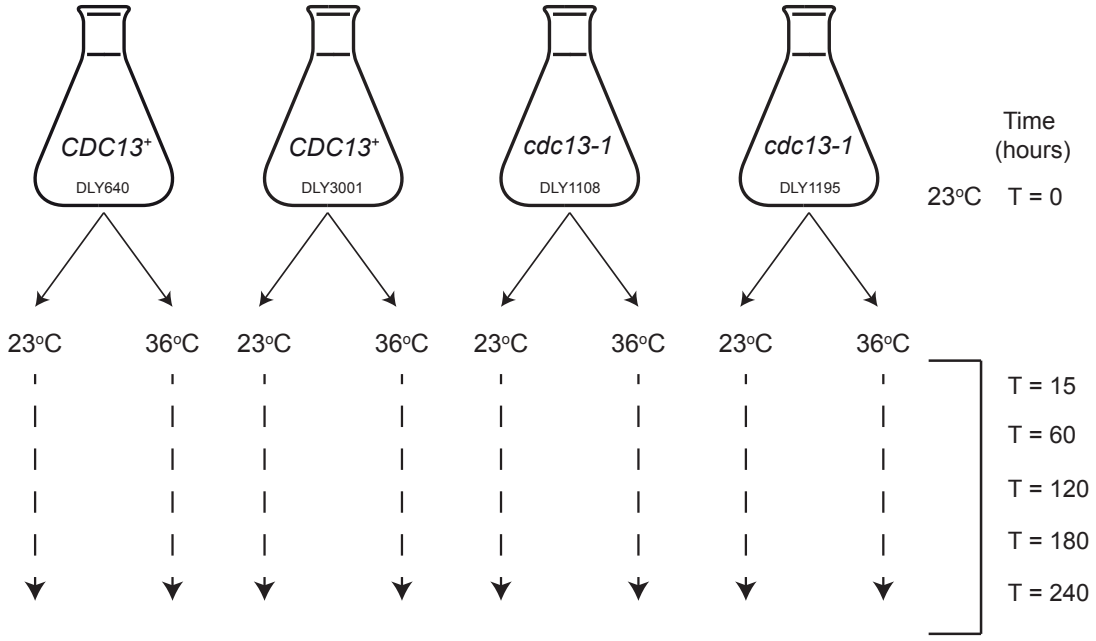

Figure 5.6: Experimental design of Zwf1 activity measurement time-course
CDC13+ and *cdc13-1* strains were inoculated into liquid culture and grown at 23°C for four hours, samples taken then the cultures were diluted with fresh YEPD and divided into two separate flasks. One flask of each culture was placed at 23°C and the other at 36°C. Samples were taken after 15, 60, 120, 180 and 240 minutes.

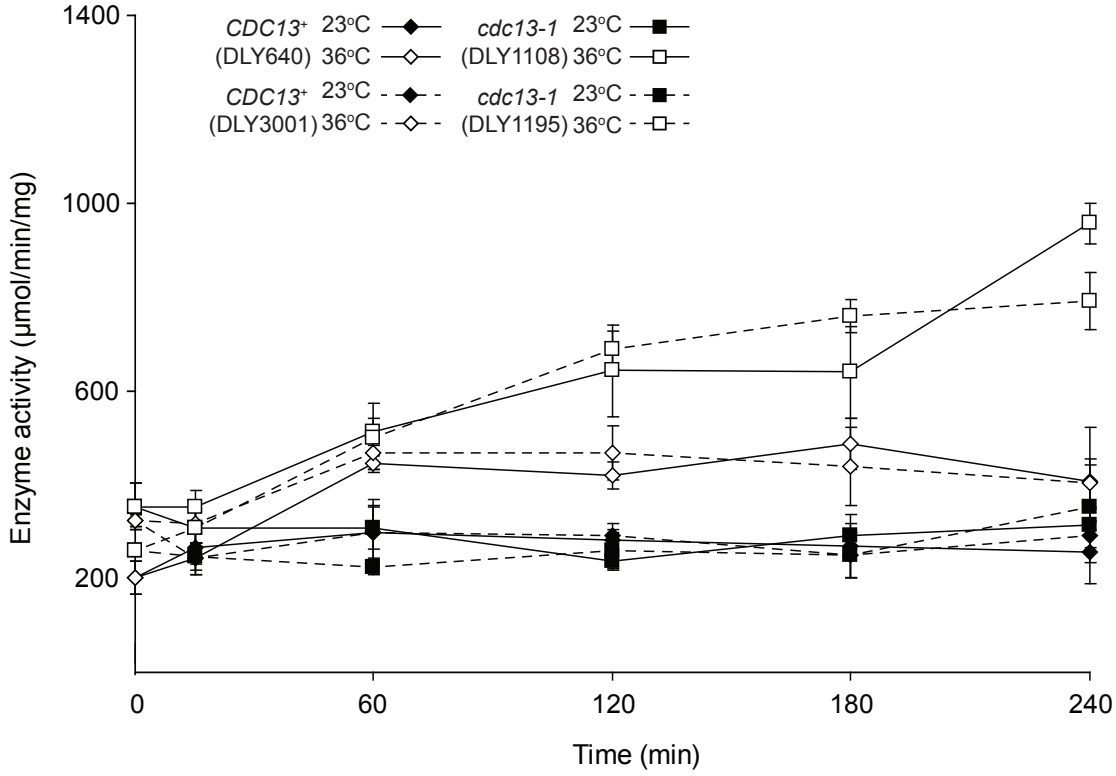

Figure 5.7: Change in the specific activity of Zwf1 in wild type and *cdc13-1* strains
Measurement of Zwf1 (G6PDH) activity in wild type and *cdc13-1* strains by measuring NADPH generation. NADPH generation was determined as in Figure 5.5. Change in absorbance over 5 minutes was used to calculate specific activity. Plotted values indicate mean specific activities of Zwf1 in three independent measurements of each sample and error bars represent the standard deviations of the means.

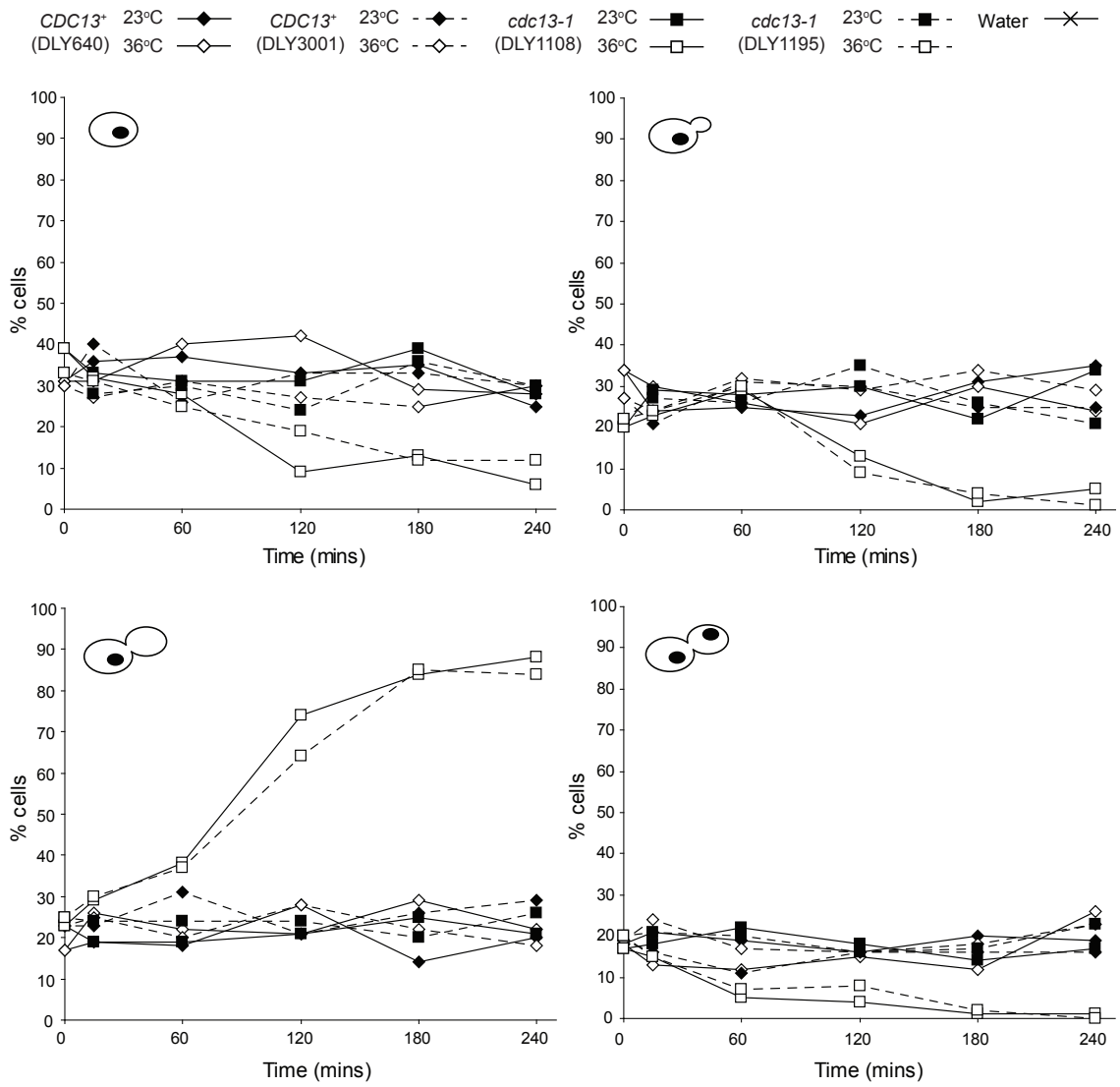

Figure 5.8: Cell cycle arrest of *cdc13-1* cells correlates with increase in Zwf1 activity

Cell cycle position of strains tested in Figure 5.7, determined using DAPI staining. Samples were taken at the same time as enzyme activity analysis samples. % cells indicates the proportion of cells in the indicated stage of the cell cycle (see Chapter 2.3.4 for cell classifications).

type strains at both temperatures, demonstrate an even distribution of cells in each cell cycle stage at all time points. The data therefore indicates that the increase in Zwf1 activity observed in *cdc13-1* strains at restrictive temperatures correlates with cell cycle arrest at G_2-M.

5.2.6 G6PDH activity increase in cdc13-1 is dependent on Rad9 activity

An increase in Zwf1 activity in *cdc13-1* strains appears to correspond with cell cycle arrest at G_2-M. The proportion of arrested cells increases throughout the time course, following a shift to a restrictive temperature (Figure 5.8). Similarly, as the time course continues, the specific activity of Zwf1 in *cdc13-1* cultures gradually increases. Cell cycle arrest in *cdc13-1* strains at restrictive temperatures is dependent on Rad9 activity (Garvik et al., 1995). Rad9 activity initiates cell cycle checkpoints and stimulates downstream effectors which bring about the arrest. Therefore, deleting *RAD9* in the *cdc13-1* background prevents the cell cycle arrest aspect of the response to telomere uncapping. In *cdc13-1 rad9*Δ strains, cells progress through the G_2-M checkpoint and continue to divide for several generations, in spite of the presence of uncapped telomeres (Garvik et al., 1995). This means that *cdc13-1 rad9*Δ strains display improved growth at non-permissive temperatures compared to *cdc13-1* alone; however, the problems which stem from the presence of uncapped telomeres, such as loss of essential genes, accumulation of single-stranded DNA and homologous recombination, eventually result in too much damage to sustain growth, and as a consequence, *cdc13-1 rad9*Δ strains do not grow over 28^{o}C (Garvik et al., 1995).

Since an increase in Zwf1 activity in *cdc13-1* strains appears to correspond with cell cycle arrest at G_2-M, I investigated whether preventing arrest from occurring would prevent the observed Zwf1 activity increase. Following the same 4-hour time course utilised in 5.2.6, the activity of Zwf1 in *cdc13-1 rad9*Δ strains was measured, alongside Zwf1 activity in *CDC13+ RAD9+* strains (Figure 5.9 and Table 5.6).

	Specific Activity (µmol/min/mg)			
Incubation Temperature	**23^{o}C**		**36^{o}C**	
Time (mins)	***CDC13+ RAD9***	***cdc13-1 rad9*Δ**	***CDC13+ RAD9***	***cdc13-1 rad9*Δ**
0	201 ± 54	121 ± 174	259.5 ± 22	241.5 ± 4
15	252.5 ± 6	217 ± 38	201 ± 54	174.5 ± 22
60	274.5 ± 19	301.5 ± 32	457.5 ± 45	384 ± 16
120	174 ± 92	225 ± 25	379.5 ± 168	473 ± 54
180	233 ± 0	240 ± 66	441 ± 117	432 ± 35
240	236 ± 41	327 ± 18	474.5 ± 57	497 ± 25

Table 5.6: Specific activity of Zwf1 in *CDC13+ RAD9* and *cdc13-1 rad9*Δ strains

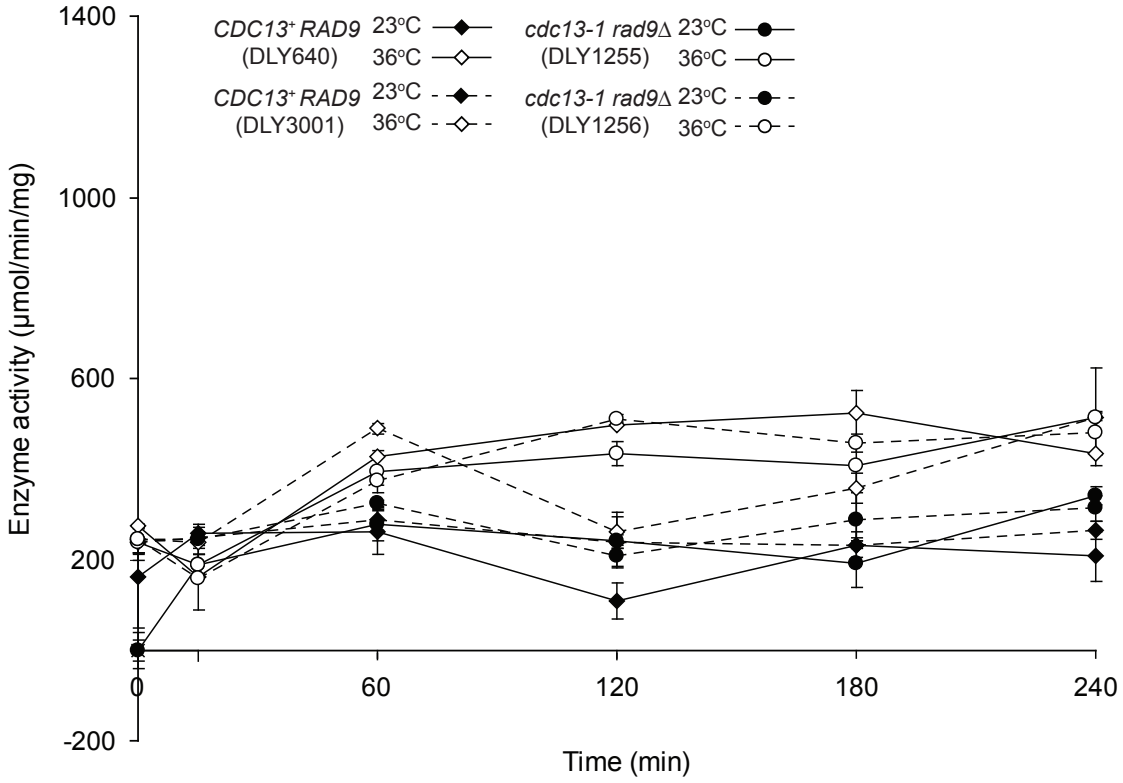

Figure 5.9: Specific activity of Zwf1 in wild type and *cdc13-1 rad9*Δ strains
Measurement of Zwf1 (G6PDH) activity in wild type and *cdc13-1 rad9*Δ strains by measuring NADPH generation. NADPH generation was determined as in Figure 5.5. Change in absorbance over 5 minutes was used to calculate specific activity. Plotted values indicate mean specific activities of Zwf1 in three independent measurements of each sample and error bars represent the standard deviations of the means.

As noted in 5.2.5, Zwf1 activity in wild type strains remains fairly constant over the 4 hour time course. An increase in Zwf1 activity after 60 minutes is again observed in both *CDC13+ RAD9+* and *cdc13-1 rad9*Δ strains. As reported previously, the activity of Zwf1 in wild type strains at 36^{o}C remains at a constant level for the remainder of the time course. Interestingly, unlike in *cdc13-1* strains (Figure 5.7 and Table 5.5), Zwf1 activity in *cdc13-1 rad9*Δ strains is similar to that in wild type. Where the activity of the enzyme increases further as the time course progresses in *cdc13-1* strains, in *cdc13-1 rad9*Δ, enzyme activity remains at a similar level.

This result suggests that the increase in Zwf1 activity observed following telomere uncapping in *cdc13-1* strains incubated at restrictive temperatures is due to cell cycle arrest and is dependent on Rad9 activity. As the determination of cell cycle position in the samples shows, no cell cycle arrest is occurring in *cdc13-1 rad9*Δ strains. (Figure 5.10) Both wild type and *cdc13-1 rad9*Δ strains demonstrate even distribution of cells in each cell cycle stage at each time point across the time course. Therefore I conclude that the increase in Zwf1 activity observed in *cdc13-1* strains is due to cell cycle arrest, which does not occur in *cdc13-1 rad9*Δ strains and therefore does not lead to a change in Zwf1 activity.

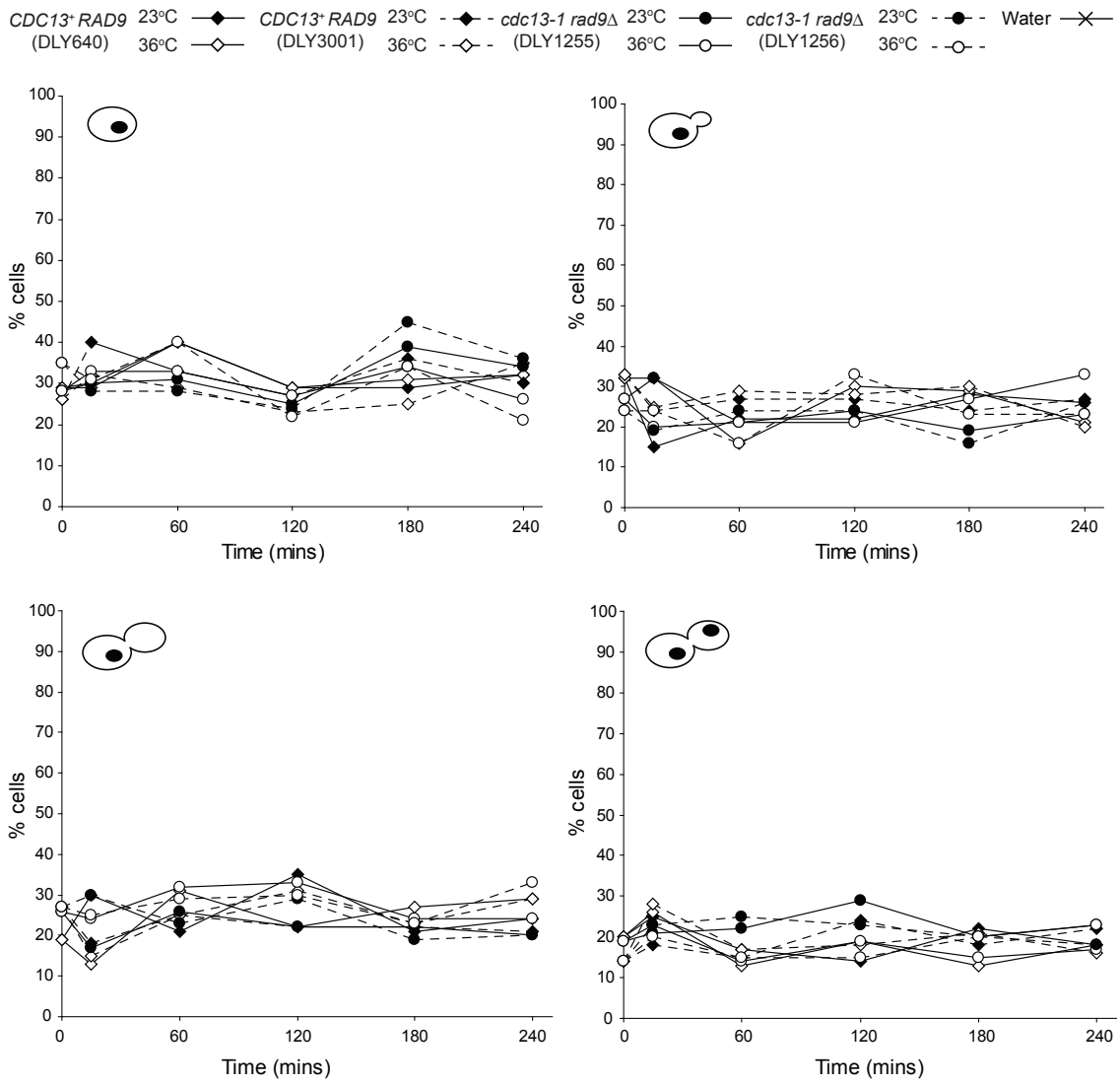

Figure 5.10: Cell cycle arrest did not occur in *cdc13-1 rad9*Δ cells
Cell cycle position of strains tested in Figure 5.9, determined using DAPI staining. Samples were taken at the same time as enzyme activity analysis samples. % cells indicates the proportion of cells in the indicated stage of the cell cycle (see Chapter 2.3.4 for cell classifications).

5.2.7 Cell-cycle arrest affects G6PDH activity

The above results suggest that the increase in Zwf1 activity observed in *cdc13-1* strains is due to Rad9 activity and the cell cycle arrest which occurs in response to telomere uncapping. If the cause of the increase in Zwf1 activity were due primarily to the G_2-M cell cycle arrest rather than telomere uncapping, Zwf1 activity in other strains which arrest in the cell cycle may display similar changes. Mutations in other *CDC* genes can cause arrest at different points in the cell cycle. For example, *cdc15-2* arrests in late mitosis at restrictive temperatures (Jaspersen et al., 1998). Using the same time course experiment, I studied Zwf1 activity in wild type and *cdc15-2* strains over a 4-hour period following a shift to restrictive temperatures (Figure 5.11 and Table 5.7).

	Specific Activity (µmol/min/mg)			
Incubation Temperature	**23°C**		**36°C**	
Time (mins)	***CDC15+***	***cdc15-2***	***CDC15+***	***cdc15-2***
0	212 ± 13	301 ± 25	156 ± 66	301 ± 25
15	192 ± 41	230 ± 95	194 ± 95	227.5 ± 35
60	291.5 ± 32	262.5 ± 47	441 ± 16	392 ± 98
120	240 ± 16	331 ± 0	401 ± 41	715.5 ± 94
180	307 ± 31	340.5 ± 16	582 ± 110	923.5 ± 57
240	337 ± 42	329.5 ± 50	501 ± 28	1064 ± 54

Table 5.7: Specific activity of Zwf1 in *CDC15+* and *cdc15-2* strains

Zwf1 activity in *cdc15-2* strains increases significantly over the time course, compared to wild type, in which Zwf1 activity increases within the first 60 minutes then remains at the same level for the remaining 3 hours. Comparing changes in the specific activity of Zwf1 in *cdc15-2* to those in *cdc13-1*, the increase observed in activity in the former is greater than in the latter. And as the cell cycle position results indicate, a majority (over 90%) of cells in *cdc15-2* strains at restrictive temperatures are arrested in late anaphase/cytokinesis (Figure 5.12).

Cells can also be arrested in the G_1 phase of the cell cycle using the mating pheromone α-factor. Exposure of strains containing the *bar1*Δ mutation to low levels of α-factor results in arrest in the G_1 phase of the cell cycle, since *BAR1* encodes a protease which can cleave and inactivate the mating pheromone. Since I

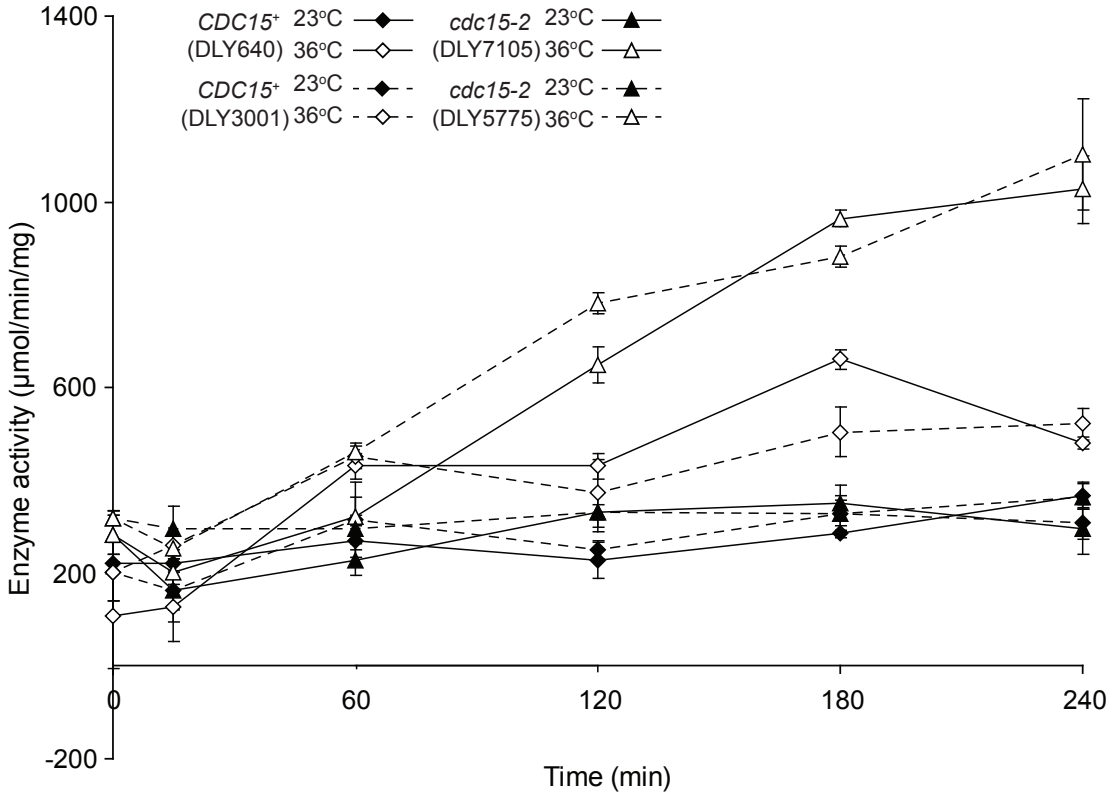

Figure 5.11: **The change in the specific activity of Zwf1 in wild type and *cdc15-2* strains**

Measurement of Zwf1 (G6PDH) activity in wild type and *cdc15-2* strains by measuring NADPH generation. NADPH generation was determined as in Figure 5.5. Change in absorbance over 5 minutes was used to calculate specific activity. Plotted values indicate mean specific activities of Zwf1 in three independent measurements of each sample and error bars represent the standard deviations of the means.

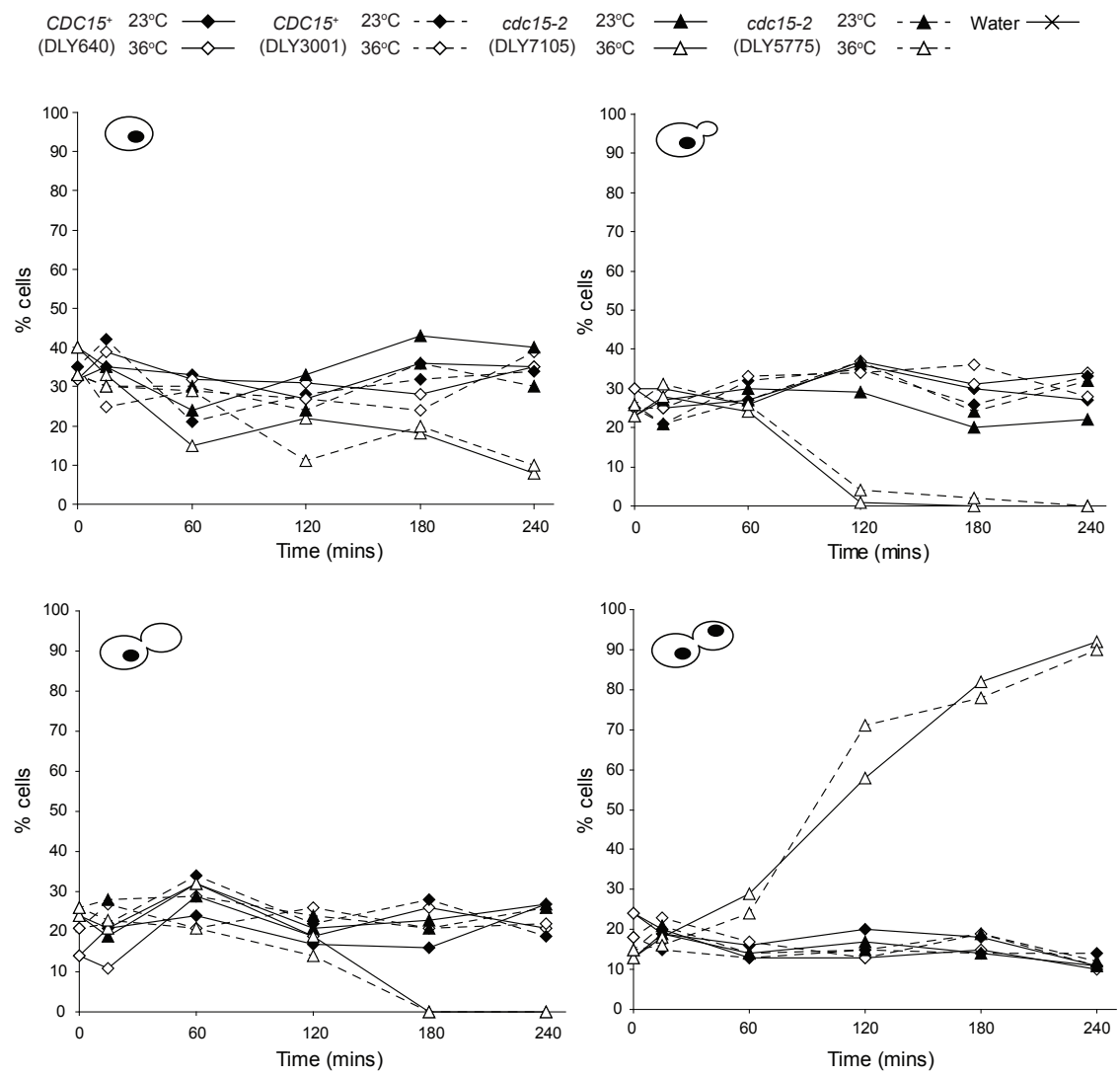

Figure 5.12: Cell cycle arrest of *cdc15-2* cells correlates with increase in Zwf1 activity

Cell cycle position of strains tested in Figure 5.11, determined using DAPI staining. Samples were taken at the same time as enzyme activity analysis samples. % cells indicates the proportion of cells in the indicated stage of the cell cycle (see Chapter 2.3.4 for cell classifications).

had previously only tested strains arrested later on the cell cycle, I decided to study the effect of arresting cells in G_1. I wanted to determine whether the effect on Zwf1 activity seen in the previous experiments was specific to cells arrested later on in the cell cycle, or whether it was part of a general cell cycle arrest response. A similar assay to those above was carried out, but instead of shifting half of the cultures to a restrictive temperature, half of the cultures were incubated with α-factor and half without, both at 23°C. As demonstrated in Figure 5.13, Zwf1 activity remains similar between strains incubated with α-factor and those without across the 4-hour time course (Table 5.6).

	Specific Activity (µmol/min/mg)	
α-factor	**-**	+
Time (mins)	***bar1*Δ**	***bar1*Δ**
0	447 ± 136	447 ± 136
15	407 ± 3	342 ± 64
60	442 ± 23	406 ± 54
120	339.5 ± 101	366.5 ± 19
180	373 ± 41	460 ± 13
240	362 ± 25	500.5 ± 6

Table 5.8: Specific activity of Zwf1 in α-factor arrested strains

Cell cycle position determination indicates that, in one strain at least, virtually all of cells in the cultures incubated with α-factor were arrested in G_1 by 4 hours (Figure 5.14), which suggests that in spite of cell cycle arrest taking place, there is no alteration in Zwf1 activity in response, as viewed in arrested *cdc13-1* and *cdc15-2* strains. Therefore it appears that the increase in Zwf1 activity seen in *cdc13-1* and *cdc15-2* strains is specific to arrest late in the cell cycle.

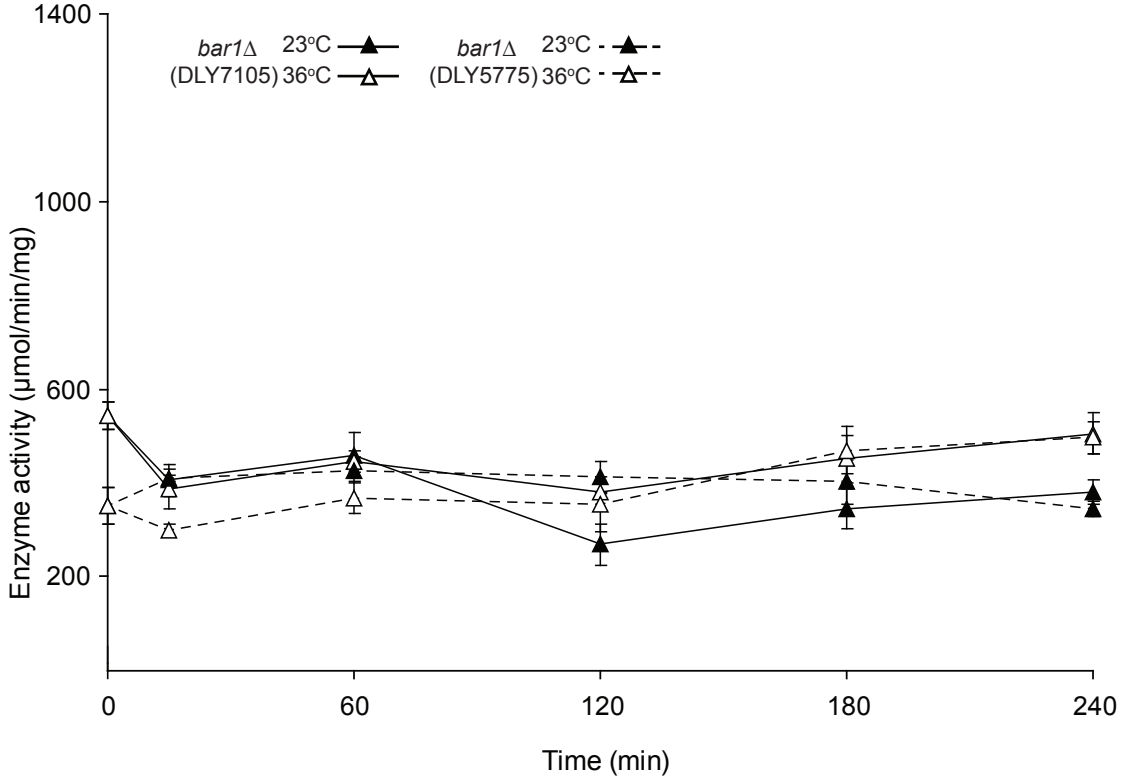

Figure 5.13: Change in the specific activity of Zwf1 in α-factor arrested strains
Measurement of Zwf1 (G6PDH) activity in wild type and α-factor arrested strains by measuring NADPH generation. NADPH generation was determined as in Figure 5.5. Change in absorbance over 5 minutes was used to calculate specific activity. Plotted values indicate mean specific activities of Zwf1 in three independent measurements of each sample and error bars represent the standard deviations of the means.

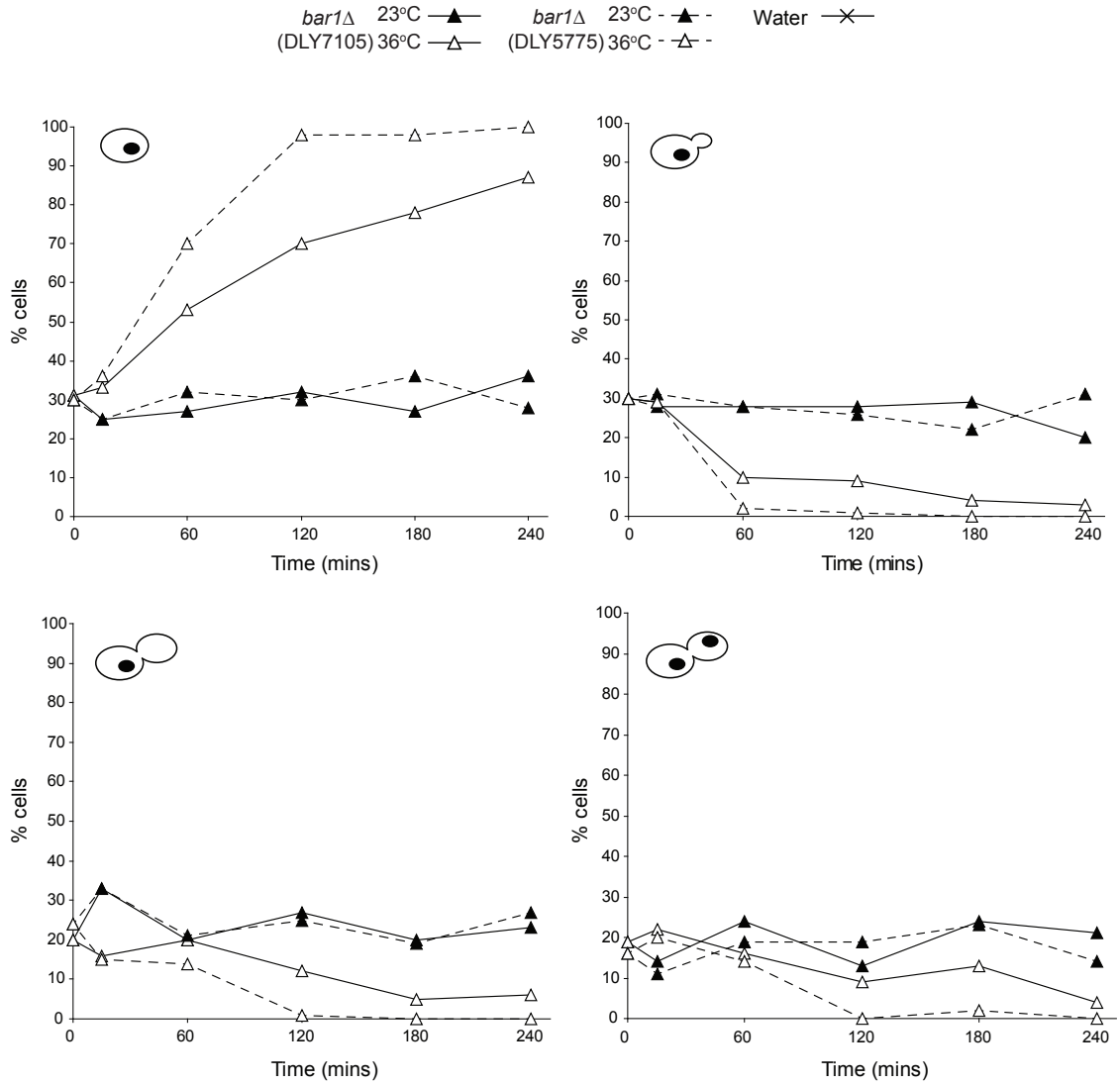

Figure 5.14: Cell cycle arrest of α-factor treated strains
Cell cycle position of strains tested in Figure 5.13, determined using DAPI staining. Samples were taken at the same time as enzyme activity analysis samples. % cells indicates the proportion of cells in the indicated stage of the cell cycle (see Chapter 2.3.4 for cell classifications).

5.3 Discussion

In this chapter I have demonstrated that Zwf1 activity increases in *cdc13-1* strains incubated at restrictive temperatures over a 4-hour time period. I studied Zwf1 activity with the aim of discerning whether flux through the pentose phosphate pathway (PPP) increases in *cdc13-1* strains, as suggested by transcription data. The results from the Greenall et al. (2008) microarray indicated that telomere uncapping in *cdc13-1* strains results in an increase in pentose phosphate pathway activity. The transcript abundance of *SOL4* and *GND2* (Reactions 4 and 5 in Figure 1.6), along with the transcript levels of other PPP-related genes, increased upon shifting temperature-sensitive *cdc13-1* mutants to restrictive temperatures. However, the expression of *ZWF1* did not increase to a significant extent, which I attributed to the constitutive expression of the gene. Zwf1 activity is instead regulated post-transcriptionally, and it is this activity which I aimed to investigate.

My original hypothesis was that the observed increase in Zwf1 activity was due to the DNA damage response which occurs following telomere uncapping in *cdc13-1*, similar to the findings of Cosentino et al. (2010) in their study of G6PDH activity in *Xenopus* and human cell lines in response to double strand breaks. However, upon study of other cell cycle arrest mutants I found that the increase in Zwf1 activity observed in *cdc13-1* strains arrested at G_2-M was also observable in *cdc15-2* strains, which arrest later in the cell cycle during late anaphase. Zwf1 activity in cells arrested in G_1, such as those treated with α-factor, did not increase in a similar fashion which led me to conclude that the stage of the cell cycle in which cells are arrested is the important factor when studying Zwf1 activity.

Without studying the flux through the PPP, it is hard to conclude whether activity of the pentose phosphate pathway as a whole increases in response to cell cycle arrest in these strains. However, given the main roles of the PPP in generation of NADPH and ribose-5-phosphate, it is conceivable that an increase in PPP flux in cells arrested at G_2-M and late anaphase would aid defence against oxidative stress and contribute to repair following DNA damage. Alternatively, cell cycle arrest may lead to an increase in flux through glycolysis and therefore an increase in flux through the PPP, in a metabolic change similar to that seen in cancer cells as part of

the Warburg effect (Dickens, 1938; Warburg and Christian, 1937; Lipmann, 1936; Warburg et al., 1935). Indeed, carbohydrate metabolism features prominently amongst the GO terms linked to genes upregulated following telomere uncapping (Table 5.2).

And so the increase in Zwf1 activity observed in *cdc13-1* and *cdc15-2* strains may be part of a generic stress response or metabolic change. However, it still remains unclear as to why this effect is dependent upon the stage of the cell cycle in which arrest is occurring, since Zwf1 displayed similar activity in both cells arrested in G_1 and cells which were not exposed to α-factor.

5.4 Future Work

My research found that cell cycle arrest in G_2-M and late anaphase results in increased glucose-6-phosphate dehydrogenase (Zwf1) activity. The data suggests that this increase is only observed when cells are arrested later on the cell cycle, as a change in activity is not seen in cells arrested in G_1. I hypothesise that this increase is due to a stress response or a metabolic change caused by the arrest.

The change in G6PDH activity observed appears to be dependent on the stage of the cell cycle in which cells are arrested. In order to confirm my results, Zwf1 activity could be explored in a number of other strains which arrest at different stages in the cell cycle. Here, I have only tested 3 strains which arrest at specific points; the investigation of Zwf1 in other strains could further support my hypothesis and provide information as to how Zwf1 activity changes throughout the cell cycle.

The work by Cosentino et al. (2010) indicates that G6PDH activity can be regulated by means other than NADP/NADPH ratio, such as ATM activity in response to DNA damage. Therefore the regulation of Zwf1 activity in response to cell cycle arrest could be explored. This could be carried out by genetic means, such as deletion of the ATM homolog, Tel1, followed by monitoring of Zwf1 activity.

Studying Zwf1 activity does not give a complete picture of flux through the PPP. Therefore to investigate whether the increase in Zwf1 activity translates into an increase in flux through the PPP in response to cell cycle arrest, the concentrations of PPP intermediates in arrested strains could be measured using liquid chromatography-tandem mass spectrometry (LC-MS/MS).

6 General Discussion

In this thesis I set out to examine the cellular response of yeast to treatment with a G-quadruplex binding ligand through utilising a single gene deletion library and monitoring strain fitness. Due to the relationship between the G-rich telomeres, G-quadruplexes and telomerase, I expected to find that mutants with deficiencies in telomere-, telomerase- and DNA damage-related genes had differential sensitivity to the ligand tested, TMPyP4. However, the results of my screen indicated that the greatest sensitivity to TMPyP4 occurs when there are deficiencies in the oxidative stress response, and in particular, the pentose phosphate pathway (PPP). Further investigations into the TMPyP4-sensitive strains revealed that the sensitivity of the strains to the porphyrin was most likely due to the inability to remove reactive oxygen species efficiently. TMPyP4 treatment of mammalian cell lines results in the upregulation of oxidative stress response genes, and is a member of the porphyrin family, a group of compounds which are capable of generating ROS upon exposure to light (Grand et al., 2002; Granville et al., 2001). Porphyrins are also used in the treatment of cancer, whereby the photosensitising agent is administered intravenously, accumulates in most cells and is exposed to light in the target region, producing ROS and inducing apoptosis (Granville et al., 2001). Therefore the efficacy of TMPyP4 against cancer cell lines could be attributed to either its G-quadruplex binding ability or relationship with the porphyrin family.

High-throughput screening of the yeast gene deletion collection has also been used to determine genetic interactions between deletion strains and the telomere capping mutant *cdc13-1* (Addinall et al., 2011; Addinall et al., 2008). The deletion of *TKL1* and *TAL1*, genes which encode key enzyme in the non-oxidative phase of the PPP, suppresses the temperature sensitivity of *cdc13-1* strains. I originally hypothesised that this suppression was attributable to alterations in NADPH levels and that telomere uncapping in *cdc13-1* strains were causing oxidative stress. However, further investigations into the effects of deleting *TAL1* and *TKL1* on Zwf1 activity suggested that NADPH production and a response to oxidative stress were unlikely to be the cause of the observed phenotypic suppression. Instead I hypothesise that deletion of TKL1 and TAL1 cause an accumulation of the nucleotide precursor ribose-5-phosphate and that this increase enhances growth of *cdc13-1* at semi-

permissive temperatures. Other data suggests that nucleotide production increases in *cdc13-1* strains and that this is beneficial to the telomere capping mutants, including transcription data which demonstrates an increase in the expression of RNR subunits, the relocation of RNR subunits following telomere uncapping and the suppression of temperature sensitivity of *cdc13-1* strains by deletion of the RNR inhibitor *SML1* (Greenall et al., 2008; Tsolou and Lydall, 2007; Yao et al., 2003).

I also hypothesised that flux through the pentose phosphate pathway changes in response to telomere uncapping. Studies into transcript expression changes in *cdc13-1* in response to a shift to restrictive temperatures indicate that there is an increase in the expression of several PPP and PPP-related genes. A recently study by Cosentino et al. (2010) has also indicated that G6PDH activity can be altered in response to the presence of double strand breaks via the activity of ATM. Taking this data into account, I sought to monitor the activity of the enzyme which catalyses the first rate limiting step of the PPP – Zwf1. I found that while Zwf1 activity did indeed increase in *cdc13-1* strains following telomere uncapping, it also increased in strains arrested in late anaphase (*cdc15-2*). Since this increase was not observed in cells arrested in G_1, I concluded that increase in Zwf1 is caused by arrest late in the cell cycle. It is likely that Zwf1 activity and NADPH production increases in G_2-M and late anaphase due to a general alteration in cellular metabolism or in order to protect against oxidative damage, as a result of a general stress response to cell cycle arrest.

Overall I have demonstrated that the pentose phosphate pathway is key for the response to environmental changes that cells may encounter, from effect of drug treatment to telomere uncapping and cell cycle arrest. The methods by which pentose phosphate pathway activity is regulated and modified have in recent times been revealed to be more complex than previously thought. Indeed, recent studies into the effect of the upregulation of the PPP have also revealed a transcriptional role for the non-oxidative phase of the pathway, particularly in the response to oxidative stress (Krüger et al., 2011). Since the PPP is intrinsically linked to cancer cell metabolism and tumour proliferation, any further knowledge on its regulation and the effects of increase in flux through the pathway will be useful.

7 Publications

Andrew, E.J., Merchan, S., Lawless, C., Banks, A.P., Wilkinson, D.J. and Lydall, D. (under review) 'Pentose phosphate pathway function affects sensitivity to the G-quadruplex binder TMPyP4'

8 References

Addinall, S. G., Downey, M., Yu, M., Zubko, M. K., Dewar, J., Leake, A., Hallinan, J., Shaw, O., James, K., Wilkinson, D. J., Wipat, A., Durocher, D. and Lydall, D. (2008) 'A genomewide suppressor and enhancer analysis of cdc13-1 reveals varied cellular processes influencing telomere capping in Saccharomyces cerevisiae', *Genetics,* 180, (4), pp. 2251-2266.

Addinall, S. G., Holstein, E. M., Lawless, C., Yu, M., Chapman, K., Banks, A. P., Ngo, H. P., Maringele, L., Taschuk, M., Young, A., Ciesiolka, A., Lister, A. L., Wipat, A., Wilkinson, D. and Lydall, D. (2011) 'Quantitative fitness analysis shows that NMD proteins and many other protein complexes suppress or enhance distinct telomere cap defects', *PLoS Genetics,* 7, (4), pp. e1001362.

Allsopp, R. C., Vaziri, H., Patterson, C., Goldstein, S., Younglai, E. V., Futcher, A. B., Greider, C. W. and Harley, C. B. (1992) 'Telomere length predicts replicative capacity of human fibroblasts', *Proceedings of the National Academy of Sciences,* 89, (21), pp. 10114.

Ambrus, A., Chen, D., Dai, J., Jones, R. A. and Yang, D. (2005) 'Solution structure of the biologically relevant G-quadruplex element in the human c-MYC promoter. Implications for G-quadruplex stabilization', *Biochemistry,* 44, (6), pp. 2048-2058.

An, X., Zhang, Z., Yang, K. and Huang, M. (2006) 'Cotransport of the heterodimeric small subunit of the Saccharomyces cerevisiae ribonucleotide reductase between the nucleus and the cytoplasm', *Genetics,* 173, (1), pp. 63-73.

Arora, A., Dutkiewicz, M., Scaria, V., Hariharan, M., Maiti, S. and Kurreck, J. (2008) 'Inhibition of translation in living eukaryotic cells by an RNA G-quadruplex motif', *RNA,* 14, (7), pp. 1290-1296.

Artandi, S. E. and DePinho, R. A. (2000) 'A critical role for telomeres in suppressing and facilitating carcinogenesis', *Current Opinion in Genetics & Development,* 10, (1), pp. 39-46.

Au, S. W. N., Gover, S., Lam, V. M. S. and Adams, M. J. (2000) 'Human glucose-6-phosphate dehydrogenase: the crystal structure reveals a structural NADP+ molecule and provides insights into enzyme deficiency', *Structure,* 8, pp. 293-303.

Auriche, C., Di Domenico, E. G. and Ascenzioni, F. (2008) 'Budding yeast with human telomeres: A puzzling structure', *Biochimie,* 90, (1), pp. 108-115.

Back, D. W., Sohal, P. S. and Angel, J. F. (1985) 'Effects of diet and selected hormones on the activities of hepatic malic enzyme and glucose-6-phosphate dehydrogenase in infant, prematurely weaned rats', *The Journal of Nutrition,* 115, (5), pp. 625.

Balagurumoorthy, P. and Brahmachari, S. K. (1994) 'Structure and stability of human telomeric sequence', *Journal of Biological Chemistry,* 269, (34), pp. 21858-21869.

Balasubramanian, S., Hurley, L. H. and Neidle, S. (2011) 'Targeting G-quadruplexes in gene promoters: a novel anticancer strategy?', *Nature Reviews Drug Discovery,* 10, (4), pp. 261-275.

Barnes, G. and Rio, D. (1997) 'DNA double-strand-break sensitivity, DNA replication, and cell cycle arrest phenotypes of Ku-deficient Saccharomyces cerevisiae', *Proceedings of the National Academy of Sciences,* 94, (3), pp. 867.

Beißbarth, T. and Speed, T. P. (2004) 'GOstat: find statistically overrepresented Gene Ontologies within a group of genes', *Bioinformatics,* 20, (9), pp. 1464-1465.

Bensaad, K., Tsuruta, A., Selak, M. A., Vidal, M., Nakano, K., Bartrons, R., Gottlieb, E. and Vousden, K. H. (2006) 'TIGAR, a p53-inducible regulator of glycolysis and apoptosis', *Cell,* 126, (1), pp. 107-120.

Bianchi, A., Negrini, S. and Shore, D. (2004) 'Delivery of yeast telomerase to a DNA break depends on the recruitment functions of Cdc13 and Est1', *Molecular Cell,* 16, (1), pp. 139-146.

Biessmann, H., Champion, L. E., O'Hair, M., Ikenaga, K., Kasravi, B. and Mason, J. M. (1992) 'Frequent transpositions of Drosophila melanogaster HeT-A transposable elements to receding chromosome ends', *The EMBO Journal,* 11, (12), pp. 4459.

Biessmann, H. and Mason, J. M. (1994) 'Telomeric repeat sequences', *Chromosoma,* 103, (3), pp. 154-161.

Blackburn, E. H. (1991) 'Structure and function of telomeres', *Nature,* 350, (6319), pp. 569.

Blankley, R. T. and Lydall, D. (2004) 'A domain of Rad9 specifically required for activation of Chk1 in budding yeast', *Journal of Cell Science,* 117, (4), pp. 601-608.

Blasco, M. A. (2005) 'Telomeres and human disease: ageing, cancer and beyond', *Nature Reviews Genetics,* 6, (8), pp. 611-622.

Boros, L. G., Torday, J. S., Lim, S., Bassilian, S., Cascante, M. and Lee, W. N. P. (2000) 'Transforming growth factor β2 promotes glucose carbon incorporation into nucleic acid ribose through the nonoxidative pentose cycle in lung epithelial carcinoma cells', *Cancer Research,* 60, (5), pp. 1183.

Boulton, S. J. and Jackson, S. P. (1996a) 'Identification of a Saccharomyces cerevisiae Ku80 homologue: roles in DNA double strand break rejoining and in telomeric maintenance', *Nucleic Acids Research,* 24, (23), pp. 4639.

Boulton, S. J. and Jackson, S. P. (1996b) 'Saccharomyces cerevisiae Ku70 potentiates illegitimate DNA double-strand break repair and serves as a barrier to error-prone DNA repair pathways', *The EMBO Journal,* 15, (18), pp. 5093.

Boulton, S. J. and Jackson, S. P. (1998) 'Components of the Ku-dependent non-homologous end-joining pathway are involved in telomeric length maintenance and telomeric silencing', *The EMBO Journal,* 17, (6), pp. 1819-1828.

Bradford, M. M. (1976) 'A rapid and sensitive method for the quantitation of microgram quantities of protein utilizing the principle of protein-dye binding', *Analytical Biochemistry,* 72, (1-2), pp. 248-254.

Bryce, L. A., Morrison, N., Hoare, S. F., Muir, S. and Keith, W. N. (2000) 'Mapping of the gene for the human telomerase reverse transcriptase, hTERT, to chromosome 5p15. 33 by fluorescence in situ hybridization', *Neoplasia (New York, NY),* 2, (3), pp. 197.

Burger, A. M., Dai, F., Schultes, C. M., Reszka, A. P., Moore, M. J., Double, J. A. and Neidle, S. (2005) 'The G-quadruplex-interactive molecule BRACO-19 inhibits tumor growth, consistent with telomere targeting and interference with telomerase function', *Cancer Research,* 65, (4), pp. 1489.

Cadière, A., Galeote, V. and Dequin, S. (2010) 'The Saccharomyces cerevisiae zinc factor protein Stb5p is required as a basal regulator of the pentose phosphate pathway', *FEMS Yeast Research,* 10, (7), pp. 819-827.

Cadière, A., Ortiz-Julien, A., Camarasa, C. and Dequin, S. (2011) 'Evolutionary engineered Saccharomyces cerevisiae wine yeast strains with increased in vivo flux through the pentose phosphate pathway', *Metabolic Engineering*.

Cappellini, M. D. and Fiorelli, G. (2008) 'Glucose-6-phosphate dehydrogenase deficiency', *The Lancet,* 371, (9606), pp. 64-74.

Carter, C. D., Kitchen, L. E., Au, W. C., Babic, C. M. and Basrai, M. A. (2005) 'Loss of SOD1 and LYS7 sensitizes Saccharomyces cerevisiae to hydroxyurea and DNA damage agents and downregulates MEC1 pathway effectors', *Molecular and Cellular Biology,* 25, (23), pp. 10273-10285.

Cascante, M., Centelles, J. J., Veech, R. L., Lee, W. N. P. and Boros, L. G. (2000) 'Role of thiamin (vitamin B-1) and transketolase in tumor cell proliferation', *Nutrition and Cancer,* 36, (2), pp. 150-154.

Celton, M., Goelzer, A., Camarasa, C., Fromion, V. and Dequin, S. (2012) 'A constraint-based model analysis of the metabolic consequences of increased NADPH oxidation in Saccharomyces cerevisiae', *Metabolic engineering*.

Cesare, A. J., Quinney, N., Willcox, S., Subramanian, D. and Griffith, J. D. (2003) 'Telomere looping in P. sativum (common garden pea)', *The Plant Journal,* 36, (2), pp. 271-279.

Chabes, A., Domkin, V., Larsson, G., Liu, A., Gräslund, A., Wijmenga, S. and Thelander, L. (2000) 'Yeast ribonucleotide reductase has a heterodimeric iron-radical-containing subunit', *Proceedings of the National Academy of Sciences,* 97, (6), pp. 2474.

Chabes, A., Domkin, V. and Thelander, L. (1999) 'Yeast Sml1, a protein inhibitor of ribonucleotide reductase', *Journal of Biological Chemistry,* 274, (51), pp. 36679-36683.

Chabes, A., Georgieva, B., Domkin, V., Zhao, X., Rothstein, R. and Thelander, L. (2003) 'Survival of DNA damage in yeast directly depends on increased dNTP levels allowed by relaxed feedback inhibition of ribonucleotide reductase', *Cell,* 112, (3), pp. 391-401.

Chan, C. S. M. and Tye, B. K. (1983) 'Organization of DNA sequences and replication origins at yeast telomeres', *Cell,* 33, (2), pp. 563-573.

Chance, B., Sies, H. and Boveris, A. (1979) 'Hydroperoxide metabolism in mammalian organs', *Physiological reviews,* 59, (3), pp. 527-605.

Chandra, A., Hughes, T. R., Nugent, C. I. and Lundblad, V. (2001) 'Cdc13 both positively and negatively regulates telomere replication', *Genes & Development,* 15, (4), pp. 404.

Chen, H., Yue, J. X., Yang, S. H., Ding, H., Zhao, R. W. and Zhang, S. (2009) 'Overexpression of transketolase-like gene 1 is associated with cell proliferation in uterine cervix cancer', *Journal of Experimental & Clinical Cancer Research,* 28, (1), pp. 43.

Chen, Z., Odstrcil, E. A., Tu, B. P. and McKnight, S. L. (2007) 'Restriction of DNA replication to the reductive phase of the metabolic cycle protects genome integrity', *Science's STKE,* 316, (5833), pp. 1916.

Christofk, H. R., Vander Heiden, M. G., Harris, M. H., Ramanathan, A., Gerszten, R. E., Wei, R., Fleming, M. D., Schreiber, S. L. and Cantley, L. C. (2008a) 'The M2 splice isoform of pyruvate kinase is important for cancer metabolism and tumour growth', *Nature,* 452, (7184), pp. 230-233.

Christofk, H. R., Vander Heiden, M. G., Wu, N., Asara, J. M. and Cantley, L. C. (2008b) 'Pyruvate kinase M2 is a phosphotyrosine-binding protein', *Nature,* 452, (7184), pp. 181-186.

Chung, S., Arrell, D. K., Faustino, R. S., Terzic, A. and Dzeja, P. P. (2010) 'Glycolytic network restructuring integral to the energetics of embryonic stem cell cardiac differentiation', *Journal of Molecular and Cellular Cardiology,* 48, (4), pp. 725-734.

Clarke, J. L., Scopes, D. A., Sodeinde, O. and Mason, P. J. (2001) 'Glucose-6-phosphate dehydrogenase-6-phosphogluconolactonase', *European Journal of Biochemistry,* 268, (7), pp. 2013-2019.

Clasquin, M. F., Melamud, E., Singer, A., Gooding, J. R., Xu, X., Dong, A., Cui, H., Campagna, S. R., Savchenko, A. and Yakunin, A. F. (2011) 'Riboneogenesis in yeast', *Cell,* 145, (6), pp. 969-980.

Cogoi, S. and Xodo, L. E. (2006) 'G-quadruplex formation within the promoter of the KRAS proto-oncogene and its effect on transcription', *Nucleic Acids Research,* 34, (9), pp. 2536-2549.

Colgin, L. M., Baran, K., Baumann, P., Cech, T. R. and Reddel, R. R. (2003) 'Human POT1 facilitates telomere elongation by telomerase', *Current Biology,* 13, (11), pp. 942-946.

Cookson, J. C., Dai, F., Smith, V., Heald, R. A., Laughton, C. A., Stevens, M. F. G. and Burger, A. M. (2005) 'Pharmacodynamics of the G-quadruplex-stabilizing telomerase inhibitor 3, 11-difluoro-6, 8, 13-trimethyl-8H-quino [4, 3, 2-kl] acridinium methosulfate (RHPS4) in vitro: activity in human tumor cells correlates with telomere length and can be enhanced, or antagonized, with cytotoxic agents', *Molecular pharmacology,* 68, (6), pp. 1551-1558.

Cosentino, C., Grieco, D. and Costanzo, V. (2010) 'ATM activates the pentose phosphate pathway promoting anti-oxidant defence and DNA repair', *The EMBO Journal,* 30, (3), pp. 546-555.

Coy, J. F., Dressler, D., Wilde, J. and Schubert, P. (2005) 'Mutations in the transketolase-like gene TKTL1: clinical implications for neurodegenerative diseases, diabetes and cancer', *Clinical laboratory,* 51, (5-6), pp. 257-274.

Culotta, V. C., Klomp, L. W., Strain, J., Casareno, R. L., Krems, B. and Gitlin, J. D. (1997) 'The copper chaperone for superoxide dismutase', *Journal of Biological Chemistry,* 272, (38), pp. 23469-72.

D'Amours, D. and Jackson, S. P. (2002) 'The Mre11 complex: at the crossroads of DNA repair and checkpoint signalling', *Nature Reviews Molecular Cell Biology,* 3, (5), pp. 317-327.

Dai, J., Chen, D., Jones, R. A., Hurley, L. H. and Yang, D. (2006a) 'NMR solution structure of the major G-quadruplex structure formed in the human BCL2 promoter region', *Nucleic Acids Research,* 34, (18), pp. 5133-5144.

Dai, J., Dexheimer, T. S., Chen, D., Carver, M., Ambrus, A., Jones, R. A. and Yang, D. (2006b) 'An intramolecular G-quadruplex structure with mixed

parallel/antiparallel G-strands formed in the human BCL-2 promoter region in solution', *Journal of the American Chemical Society,* 128, (4), pp. 1096-1098.

De Cian, A., Gros, J., Guédin, A., Haddi, M., Lyonnais, S., Guittat, L., Riou, J.-F., Trentesaux, C., Saccà , B., Lacroix, L., Alberti, P. and Mergny, J.-L. (2008) 'DNA and RNA Quadruplex ligands', *Nucleic Acids Symposium Series,* 52, (1), pp. 7-8.

De Lange, T. (2005) 'Shelterin: the protein complex that shapes and safeguards human telomeres', *Genes & Development,* 19, (18), pp. 2100.

De Lange, T., Shiue, L., Myers, R. M., Cox, D. R., Naylor, S. L., Killery, A. M. and Varmus, H. E. (1990) 'Structure and variability of human chromosome ends', *Molecular and Cellular Biology,* 10, (2), pp. 518.

Deutscher, D., Meilijson, I., Kupiec, M. and Ruppin, E. (2006) 'Multiple knockout analysis of genetic robustness in the yeast metabolic network', *Nature Genetics,* 38, (9), pp. 993-998.

Dexheimer, T. S., Fry, M. and Hurley, L. H. (2006) 'DNA quadruplexes and gene regulation', *Quadruplex Nucleic Acids*, pp. 180-207.

di Fagagna, F. A., Reaper, P. M., Clay-Farrace, L., Fiegler, H., Carr, P., von Zglinicki, T., Saretzki, G., Carter, N. P. and Jackson, S. P. (2003) 'A DNA damage checkpoint response in telomere-initiated senescence', *Nature,* 426, (6963), pp. 194-198.

di Fagagna, F. A., Teo, S. H. and Jackson, S. P. (2004) 'Functional links between telomeres and proteins of the DNA-damage response', *Genes & development,* 18, (15), pp. 1781-1799.

Dickens, F. (1938) 'Oxidation of phosphohexonate and pentose phosphoric acids by yeast enzymes: Oxidation of phosphohexonate. II. Oxidation of pentose phosphoric acids', *Biochemical Journal,* 32, (9), pp. 1626.

Diede, S. J. and Gottschling, D. E. (2001) 'Exonuclease activity is required for sequence addition and Cdc13p loading at a de novo telomere', *Current Biology,* 11, (17), pp. 1336-1340.

Domkin, V., Thelander, L. and Chabes, A. (2002) 'Yeast DNA damage-inducible Rnr3 has a very low catalytic activity strongly stimulated after the formation of a cross-talking Rnr1/Rnr3 complex', *Journal of Biological Chemistry,* 277, (21), pp. 18574.

Drygin, D., Siddiqui-Jain, A., O'Brien, S., Schwaebe, M., Lin, A., Bliesath, J., Ho, C. B., Proffitt, C., Trent, K. and Whitten, J. P. (2009) 'Anticancer activity of CX-3543: a direct inhibitor of rRNA biogenesis', *Cancer research,* 69, (19), pp. 7653.

Eggleston, L. V. and Krebs, H. A. (1974) 'Regulation of the pentose phosphate cycle', *Biochemical Journal,* 138, (3), pp. 425.

El-Hassan, A., Zubairu, S., Hothersall, J. S. and Greenbaum, A. L. (1981) 'Age-related changes in enzymes of rat brain. 1. Enzymes of glycolysis, the pentose phosphate pathway and lipogenesis', *Enzyme,* 26, (2), pp. 107.

Elledge, S. J. (1996) 'Cell cycle checkpoints: preventing an identity crisis', *Science,* 274, (5293), pp. 1664.

Elledge, S. J., Zhou, Z., Allen, J. B. and Navas, T. A. (2005) 'DNA damage and cell cycle regulation of ribonucleotide reductase', *Bioessays,* 15, (5), pp. 333-339.

Emili, A. (1998) 'MEC1-Dependent Phosphorylation of Rad9p in Response to DNA Damage', *Molecular Cell,* 2, (2), pp. 183-189.

Evans, S. K. and Lundblad, V. (1999) 'Est1 and Cdc13 as comediators of telomerase access', *Science,* 286, (5437), pp. 117.

Faure, V., Coulon, S., Hardy, J. and Géli, V. (2010) 'Cdc13 and telomerase bind through different mechanisms at the lagging-and leading-strand telomeres', *Molecular cell,* 38, (6), pp. 842-852.

Feierbach, B., Nogales, E., Downing, K. H. and Stearns, T. (1999) 'Alf1p, a CLIP-170 domain-containing protein, is functionally and physically associated with α-tubulin', *Journal of Cell Biology,* 144, (1), pp. 113-124.

Feldmann, H., Driller, L., Meier, B., Mages, G., Kellermann, J. and Winnacker, E. L. (1996) 'HDF2, the second subunit of the Ku homologue from Saccharomyces cerevisiae', *Journal of Biological Chemistry,* 271, (44), pp. 27765.

Feng, J., Funk, W. D., Wang, S. S., Weinrich, S. L., Avilion, A. A., Chiu, C. P., Adams, R. R., Chang, E., Allsopp, R. C. and Yu, J. (1995) 'The RNA component of human telomerase', *Science,* 269, (5228), pp. 1236.

Finkel, T. and Holbrook, N. J. (2000) 'Oxidants, oxidative stress and the biology of ageing', *Nature*, pp. 239-247.

Fisher, T. S., Taggart, A. K. P. and Zakian, V. A. (2004) 'Cell cycle-dependent regulation of yeast telomerase by Ku', *Nature Structural & Molecular Biology,* 11, (12), pp. 1198-1205.

Foster, S. S., Zubko, M. K., Guillard, S. and Lydall, D. (2006) 'MRX protects telomeric DNA at uncapped telomeres of budding yeast cdc13-1 mutants', *DNA repair,* 5, (7), pp. 840-851.

Frank-Vaillant, M. and Marcand, S. (2002) 'Transient stability of DNA ends allows nonhomologous end joining to precede homologous recombination', *Molecular Cell,* 10, (5), pp. 1189-1199.

Freyer, M. W., Buscaglia, R., Kaplan, K., Cashman, D., Hurley, L. H. and Lewis, E. A. (2007) 'Biophysical studies of the c-MYC NHE III1 promoter: model quadruplex interactions with a cationic porphyrin', *Biophysical journal,* 92, (6).

Frick, O. and Wittmann, C. (2005) 'Characterization of the metabolic shift between oxidative and fermentative growth in Saccharomyces cerevisiae by comparative 13C flux analysis', *Microbial Cell Factories,* 4, (1), pp. 30.

Fry, M. and Loeb, L. A. (1999) 'Human Werner syndrome DNA helicase unwinds tetrahelical structures of the fragile X syndrome repeat sequence d (CGG) n', *Journal of Biological Chemistry,* 274, (18), pp. 12797-12802.

Fu, Y., Pastushok, L. and Xiao, W. (2008) 'DNA damage-induced gene expression in Saccharomyces cerevisiae', *FEMS Microbiology Reviews,* 32, (6), pp. 908-926.

Futcher, B. (2006) 'Metabolic cycle, cell cycle, and the finishing kick to Start', *Genome biology,* 7, (4), pp. 107.

Gardner, R., Putnam, C. W. and Weinert, T. (1999) 'RAD53, DUN1 and PDS1 define two parallel G2/M checkpoint pathways in budding yeast', *The EMBO journal,* 18, (11), pp. 3173-3185.

Garvik, B., Carson, M. and Hartwell, L. (1995) 'Single-stranded DNA arising at telomeres in cdc13 mutants may constitute a specific signal for the RAD9 checkpoint', *Molecular and Cellular Biology,* 15, (11), pp. 6128-6138.

Gasch, A. P., Spellman, P. T., Kao, C. M., Carmel-Harel, O., Eisen, M. B., Storz, G., Botstein, D. and Brown, P. O. (2000) 'Genomic expression programs in the response of yeast cells to environmental changes', *Science's STKE,* 11, (12), pp. 4241.

Gavathiotis, E., Heald, R. A., Stevens, M. F. G. and Searle, M. S. (2001) 'Recognition and stabilization of quadruplex DNA by a potent new telomerase inhibitor: NMR studies of the 2:1 complex of a pentacyclic methylacridinium cation with d (TTAGGGT)4', *Angewandte Chemie,* 113, (24), pp. 4885-4887.

Gavathiotis, E., Heald, R. A., Stevens, M. F. G. and Searle, M. S. (2003) 'Drug recognition and stabilisation of the parallel-stranded DNA quadruplex d

(TTAGGGT) 4 containing the human telomeric repeat', *Journal of Molecular Biology,* 334, (1), pp. 25-36.

Geissler, S., Siegers, K. and Schiebel, E. (1998) 'A novel protein complex promoting formation of functional α-and γ-tubulin', *The EMBO Journal,* 17, (4), pp. 952-966.

Gellert, M., Lipsett, M. N. and Davies, D. R. (1962) 'Helix formation by guanylic acid', *Proceedings of the National Academy of Sciences of the United States of America,* 48, (12), pp. 2013.

Gentleman, R., Carey, V., Bates, D., Bolstad, B., Dettling, M., Dudoit, S., Ellis, B., Gautier, L., Ge, Y., Gentry, J., Hornik, K., Hothorn, T., Huber, W., Iacus, S., Irizarry, R., Leisch, F., Li, C., Maechler, M., Rossini, A. J., Sawitzki, G., Smith, C., Smyth, G., Tierney, L., Yang, J. Y. and Zhang, J. (2004) 'Bioconductor: open software development for computational biology and bioinformatics', *Genome Biology,* 5, (10), pp. R80.

Gilbert, C. S., Green, C. M. and Lowndes, N. F. (2001) 'Budding yeast Rad9 is an ATP-dependent Rad53 activating machine', *Molecular cell,* 8, (1), pp. 129-136.

Giraldo, R. and Rhodes, D. (1994) 'The yeast telomere-binding protein RAP1 binds to and promotes the formation of DNA quadruplexes in telomeric DNA', *The EMBO Journal,* 13, (10), pp. 2411.

Gottschling, D. E. and Zakian, V. A. (1986) 'Telomere proteins: specific recognition and protection of the natural termini of Oxytricha macronuclear DNA', *Cell,* 47, (2), pp. 195.

Grabowska, D. and Chelstowska, A. (2003) 'The ALD6 gene product is indispensable for providing NADPH in yeast cells lacking glucose-6-phosphate dehydrogenase activity', *Journal of Biological Chemistry,* 278, (16), pp. 13984.

Grand, C. L., Han, H., Muñoz, R. M., Weitman, S., Von Hoff, D. D., Hurley, L. H. and Bearss, D. J. (2002) 'The Cationic Porphyrin TMPyP4 Down-Regulates c-MYC

and Human Telomerase Reverse Transcriptase Expression and Inhibits Tumor Growth in Vivo 1', *Molecular Cancer Therapeutics,* 1, (8), pp. 565.

Grandin, N., Damon, C. and Charbonneau, M. (2000) 'Cdc13 cooperates with the yeast Ku proteins and Stn1 to regulate telomerase recruitment', *Molecular and Cellular Biology,* 20, (22), pp. 8397.

Grandin, N., Damon, C. and Charbonneau, M. (2001) 'Ten1 functions in telomere end protection and length regulation in association with Stn1 and Cdc13', *The EMBO Journal,* 20, (5), pp. 1173-1183.

Grant, C. M., Quinn, K. A. and Dawes, I. W. (1999) 'Differential protein S-thiolation of glyceraldehyde-3-phosphate dehydrogenase isoenzymes influences sensitivity to oxidative stress', *Molecular and Cellular Biology,* 19, (4), pp. 2650-2656.

Granville, D. J., McManus, B. M. and Hunt, D. W. C. (2001) 'Photodynamic therapy: shedding light on the biochemical pathways regulating porphyrin-mediated cell death', *Histology and Histopathology,* 16, pp. 309-317.

Gray, J. T., Celander, D. W., Price, C. M. and Cech, T. R. (1991) 'Cloning and expression of genes for the Oxytricha telomere-binding protein: specific subunit interactions in the telomeric complex', *Cell,* 67, (4), pp. 807-814.

Green, C. M., Erdjument-Bromage, H., Tempst, P. and Lowndes, N. F. (2000) 'A novel Rad24 checkpoint protein complex closely related to replication factor C', *Current Biology,* 10, (1), pp. 39-42.

Greenall, A., Lei, G., Swan, D. C., James, K., Wang, L., Peters, H., Wipat, A., Wilkinson, D. J. and Lydall, D. (2008) 'A genome wide analysis of the response to uncapped telomeres in budding yeast reveals a novel role for the NAD+ biosynthetic gene BNA2 in chromosome end protection', *Genome Biology,* 9, (10), pp. R146.

Greider, C. W. and Blackburn, E. H. (1985) 'Identification of a specific telomere terminal transferase activity in Tetrahymena extracts', *Cell,* 43, (2), pp. 405-413.

Grewal, A. and Conway, A. (2000) 'Tools for analyzing microarray expression data', *Journal of the Association for Laboratory Automation,* 5, (5), pp. 62-64.

Griffith, J. D., Comeau, L., Rosenfield, S., Stansel, R. M., Bianchi, A., Moss, H. and De Lange, T. (1999) 'Mammalian telomeres end in a large duplex loop', *Cell,* 97, pp. 503-514.

Guo, K. (2008) 'DNA secondary structures in the promoters of human VEGF and RET genes and their roles in gene transcriptional regulation', in ProQuest.

Guschlbauer, W., Chantot, J. F. and Thiele, D. (1990) 'Four-stranded nucleic acid structures 25 years later: from guanosine gels to telomer DNA', *Journal of biomolecular structure & dynamics,* 8, (3), pp. 491.

Hahn, W. C., Stewart, S. A., Brook, M. W., York, S. G., Eaton, E., Kurachi, A., Beijersbergen, R. L., Knoll, J. H. M., Meyerson, M. and Weinberg, R. A. (1999) 'Inhibition of telomerase limits the growth of human cancer cells', *Nature Medicine,* 5, (10), pp. 1164-1170.

Haq, I., Trent, J. O., Chowdhry, B. Z. and Jenkins, T. C. (1999) 'Intercalative G-tetraplex stabilization of telomeric DNA by a cationic porphyrin', *Journal of the American Chemical Society,* 121, (9), pp. 1768-1779.

Hara, E., Tsurui, H., Shinozaki, A., Nakada, S. and Oda, K. (1991) 'Cooperative effect of antisense-Rb and antisense-p53 oligomers on the extension of life span in human diploid fibroblasts, TIG-1', *Biochemical and biophysical research communications,* 179, (1), pp. 528-534.

Harley, C. B., Futcher, A. B. and Greider, C. W. (1990) 'Telomeres shorten during ageing of human fibroblasts', *Nature*.

Harley, C. B., Kim, N. W., Prowse, K. R., Weinrich, S. L., Hirsch, K. S., West, M. D., Bacchetti, S., Hirte, H. W., Counter, C. M. and Greider, C. W. (1994):Cold Spring Harbor Laboratory Press.

Harrison, R. J., Gowan, S. M., Kelland, L. R. and Neidle, S. (1999) 'Human telomerase inhibition by substituted acridine derivatives', *Bioorganic & medicinal chemistry letters,* 9, (17), pp. 2463-2468.

Hayflick, L. and Moorhead, P. S. (1961) 'The serial cultivation of human diploid cell strains* 1', *Experimental Cell Research,* 25, (3), pp. 585-621.

Henderson, E., Hardin, C. C., Walk, S. K., Tinoco Jr, I. and Blackburn, E. H. (1987) 'Telomeric DNA oligonucleotides form novel intramolecular structures containing guanine-guanine base pairs', *Cell,* 51, (6), pp. 899.

Henderson, E. R. and Blackburn, E. H. (1989) 'An overhanging 3' terminus is a conserved feature of telomeres', *Molecular and Cellular Biology,* 9, (1), pp. 345.

Hershman, S. G., Chen, Q., Lee, J. Y., Kozak, M. L., Yue, P., Wang, L.-S. and Johnson, F. B. (2008) 'Genomic distribution and functional analyses of potential G-quadruplex-forming sequences in Saccharomyces cerevisiae', *Nucleic Acids Research,* 36, (1), pp. 144-56.

Ho, H., Cheng, M. and Chiu, D. T. (2007) 'Glucose-6-phosphate dehydrogenase - from oxidative stress to cellular functions and degenerative diseases', *Redox Report,* 12, (3), pp. 109-118.

Holmgren, A. (1989) 'Thioredoxin and glutaredoxin systems', *Journal of Biological Chemistry,* 264, (24), pp. 13963-13966.

Holten, D., Procsal, D. and Chang, H. L. (1976) 'Regulation of pentose phosphate pathway dehydrogenases by NADP+/NADPH ratios', *Biochemical and biophysical research communications,* 68, (2), pp. 436-441.

Hoyt, M. A., Macke, J. P., Roberts, B. T. and Geiser, J. R. (1997) 'Saccharomyces cerevisiae PAC2 functions with CIN1, 2 and 4 in a pathway leading to normal microtubule stability', *Genetics,* 146, (3), pp. 849-857.

Huang, H., Rong, H., Li, X., Tong, S., Zhu, Z., Niu, L. and Teng, M. (2008) 'The crystal structure and identification of NQM1/YGR043C, a transaldolase from Saccharomyces cerevisiae', *Proteins: Structure, Function, and Bioinformatics,* 73, (4), pp. 1076-1081.

Huang, M. and Elledge, S. J. (1997) 'Identification of RNR4, encoding a second essential small subunit of ribonucleotide reductase in Saccharomyces cerevisiae', *Molecular and Cellular Biology,* 17, (10), pp. 6105.

Huang, M., Zhou, Z. and Elledge, S. J. (1998) 'The DNA replication and damage checkpoint pathways induce transcription by inhibition of the Crt1 repressor', *Cell,* 94, (5), pp. 595-605.

Huber, M. D., Duquette, M. L., Shiels, J. C. and Maizels, N. (2006) 'A conserved G4 DNA binding domain in RecQ family helicases', *Journal of molecular biology,* 358, (4), pp. 1071-1080.

Huck, J. H. J., Verhoeven, N. M., Struys, E. A., Salomons, G. S., Jakobs, C. and Van der Knaap, M. S. (2004) 'Ribose-5-phosphate isomerase deficiency: new inborn error in the pentose phosphate pathway associated with a slowly progressive leukoencephalopathy', *The American Journal of Human Genetics,* 74, (4), pp. 745-751.

Hughes, T. R., Weilbaecher, R. G., Walterscheid, M. and Lundblad, V. (2000) 'Identification of the single-strand telomeric DNA binding domain of the Saccharomyces cerevisiae Cdc13 protein', *Proceedings of the National Academy of Sciences,* 97, (12), pp. 6457.

Huppert, J. L. (2008) 'Hunting G-quadruplexes', *Biochimie,* 90, (8), pp. 1140-1148.

Huppert, J. L. and Balasubramanian, S. (2005) 'Prevalence of quadruplexes in the human genome', *Nucleic Acids Research,* 33, (9), pp. 2908-2916.

Huppert, J. L. and Balasubramanian, S. (2007) 'G-quadruplexes in promoters throughout the human genome', *Nucleic Acids Research,* 35, (2), pp. 406-413.

Izbicka, E., Nishioka, D., Marcell, V., Raymond, E., Davidson, K., Lawrence, R., Wheelhouse, R., Hurley, L., Wu, R. and Von Hoff, D. (1999) 'Telomere-interactive agents affect proliferation rates and induce chromosomal destabilization in sea urchin embryos', *Anti-Cancer Drug Design,* 14, (4), pp. 355-365.

Jain, D. and Cooper, J. P. (2010) 'Telomeric strategies: means to an end', *Annual Review of Genetics,* 44, pp. 243-269.

Jaspersen, S. L., Charles, J. F., Tinker-Kulberg, R. L. and Morgan, D. O. (1998) 'A late mitotic regulatory network controlling cyclin destruction in Saccharomyces cerevisiae', *Molecular Biology of the Cell,* 9, (10), pp. 2803-2817.

Jia, X., Weinert, T. and Lydall, D. (2004) 'Mec1 and Rad53 inhibit formation of single-stranded DNA at telomeres of Saccharomyces cerevisiae cdc13-1 mutants', *Genetics,* 166, (2), pp. 753-764.

Jiang, P., Du, W., Wang, X., Mancuso, A., Gao, X., Wu, M. and Yang, X. (2011) 'p53 regulates biosynthesis through direct inactivation of glucose-6-phosphate dehydrogenase', *Nature cell biology,* 13, (3), pp. 310-316.

Jonas, S. K., Benedetto, C., Flatman, A., Hammond, R. H., Micheletti, L., Riley, C., Riley, P. A., Spargo, D. J., Zonca, M. and Slater, T. F. (1992) 'Increased activity of 6-phosphogluconate dehydrogenase and glucose-6-phosphate dehydrogenase in purified cell suspensions and single cells from the uterine cervix in cervical intraepithelial neoplasia', *British Journal of Cancer,* 66, (1), pp. 185.

Juhnke, H., Krems, B., Kötter, P. and Entian, K. D. (1996) 'Mutants that show increased sensitivity to hydrogen peroxide reveal an important role for the pentose phosphate pathway in protection of yeast against oxidative stress', *Molecular and General Genetics MGG,* 252, (4), pp. 456-464.

Kang, C. H., Zhang, X., Ratliff, R., Moyzis, R. and Rich, A. (1992) 'Crystal structure of four-stranded Oxytricha telomeric DNA', *Nature,* 356, (6365), pp. 126-131.

Katsurada, A., Iritani, N., Fukuda, H., Matsumura, Y., Noguchi, T. and Tanaka, T. (1989) 'Effects of nutrients and insulin on transcriptional and post-transcriptional regulation of glucose-6-phosphate dehydrogenase synthesis in rat liver', *Biochimica et Biophysica Acta (BBA)-Lipids and Lipid Metabolism,* 1006, (1), pp. 104-110.

Kawanishi, S. and Oikawa, S. (2004) 'Mechanism of telomere shortening by oxidative stress', *Annals of the New York Academy of Sciences,* 1019, (1), pp. 278-284.

Kerwin, S. M. (2000) 'G-quadruplex DNA as a target for drug design', *Current Pharmaceutical Design,* 6, (4), pp. 441-471.

Kim, J. S., Krasieva, T. B., Kurumizaka, H., Chen, D. J., Taylor, A. M. R. and Yokomori, K. (2005) 'Independent and sequential recruitment of NHEJ and HR factors to DNA damage sites in mammalian cells', *Journal of Cell Biology,* 170, (3), pp. 341.

Kim, N. W., Piatyszek, M. A., Prowse, K. R., Harley, C. B., West, M. D., Ho, P. L., Coviello, G. M., Wright, W. E., Weinrich, S. L. and Shay, J. W. (1994) 'Specific association of human telomerase activity with immortal cells and cancer', *Science,* 266, (5193), pp. 2011-2015.

Kletzien, R. F. and Berdanier, C. D. (1993) 'Glucose-6-phosphate dehydrogenase: diet and hormonal influences on de novo enzyme synthesis', in JL.(eds), B. C. a. H.(ed), *Nutrition and Gene Expression.* pp. 187-206.

Kletzien, R. F., Harris, P. K. and Foellmi, L. A. (1994) 'Glucose-6-phosphate dehydrogenase: a" housekeeping" enzyme subject to tissue-specific regulation by hormones, nutrients, and oxidant stress', *The FASEB Journal,* 8, (2), pp. 174.

Kotaka, M., Gover, S., Vandeputte-Rutten, L., Au, S. W. N., Lam, V. M. S. and Adams, M. J. (2005) 'Structural studies of glucose-6-phosphate and NADP+ binding to human glucose-6-phosphate dehydrogenase', *Acta Crystallographica Section D: Biological Crystallography,* 61, (5), pp. 495-504.

Krockenberger, M., Honig, A., Rieger, L., Coy, J. F., Sutterlin, M., Kapp, M., Horn, E., Dietl, J. and Kammerer, U. (2007) 'Transketolase-like 1 expression correlates with subtypes of ovarian cancer and the presence of distant metastases', *International Journal of Gynecological Cancer,* 17, (1), pp. 101-106.

Krüger, A., Grüning, N. M., Wamelink, M. M. C., Kerick, M., Kirpy, A., Parkhomchuk, D., Bluemlein, K., Schweiger, M. R., Soldatov, A., Lehrach, H., Jakobs, C. and Ralser, M. (2011) 'The pentose phosphate pathway is a metabolic redox sensor and regulates transcription during the antioxidant response', *Antioxidants & Redox Signaling,* 15, (2), pp. 311-324.

Kumar, D., Abdulovic, A. L., Viberg, J., Nilsson, A. K., Kunkel, T. A. and Chabes, A. (2011) 'Mechanisms of mutagenesis in vivo due to imbalanced dNTP pools', *Nucleic Acids Research,* 39, (4), pp. 1360-1371.

Kumar, D., Viberg, J., Nilsson, A. K. and Chabes, A. (2010) 'Highly mutagenic and severely imbalanced dNTP pools can escape detection by the S-phase checkpoint', *Nucleic Acids Research,* 38, (12), pp. 3975-3983.

Kumari, S., Bugaut, A., Huppert, J. L. and Balasubramanian, S. (2007) 'An RNA G-quadruplex in the 5' UTR of the NRAS proto-oncogene modulates translation', *Nature Chemical Biology,* 3, (4), pp. 218-221.

Lam, C. T., Tang, C. M. C., Lau, K. W. and Lung, M. L. (2002) 'Loss of heterozygosity on chromosome 11 in esophageal squamous cell carcinomas', *Cancer Letters,* 178, (1), pp. 75-81.

Langbein, S., Frederiks, W. M., zur Hausen, A., Popa, J., Lehmann, J., Weiss, C., Alken, P. and Coy, J. F. (2008) 'Metastasis is promoted by a bioenergetic switch: new targets for progressive renal cell cancer', *International Journal of Cancer,* 122, (11), pp. 2422-2428.

Langbein, S., Zerilli, M., Zur Hausen, A., Staiger, W., Rensch-Boschert, K., Lukan, N., Popa, J., Ternullo, M. P., Steidler, A., Weiss, C., Grobholz, R., Willeke, F.,

Alken, P., Stassi, G., Schubert, P. and Coy, J. F. (2006) 'Expression of transketolase TKTL1 predicts colon and urothelial cancer patient survival: Warburg effect reinterpreted', *British Journal of Cancer,* 94, (4), pp. 578-585.

Larochelle, M., Drouin, S., Robert, F. and Turcotte, B. (2006) 'Oxidative Stress-Activated Zinc Cluster Protein Stb5 Has Dual Activator/Repressor Functions Required for Pentose Phosphate Pathway Regulation and NADPH Production†', *Molecular and Cellular Biology,* 26, (17), pp. 6690-6701.

Lawless, C., Wilkinson, D., Young, A., Addinall, S. and Lydall, D. (2010) 'Colonyzer: automated quantification of micro-organism growth characteristics on solid agar', *BMC bioinformatics,* 11, (1), pp. 287.

Lei, M., Podell, E. R., Baumann, P. and Cech, T. R. (2003) 'DNA self-recognition in the structure of Pot1 bound to telomeric single-stranded DNA', *Nature,* 426, (6963), pp. 198-203.

Leonetti, C., Amodei, S., D'Angelo, C., Rizzo, A., Benassi, B., Antonelli, A., Elli, R., Stevens, M. F. G., D'Incalci, M. and Zupi, G. (2004) 'Biological activity of the G-quadruplex ligand RHPS4 (3, 11-difluoro-6, 8, 13-trimethyl-8H-quino [4, 3, 2-kl] acridinium methosulfate) is associated with telomere capping alteration', *Molecular pharmacology,* 66, (5), pp. 1138-1146.

Leonetti, C., Scarsella, M., Riggio, G., Rizzo, A., Salvati, E., D'Incalci, M., Staszewsky, L., Frapolli, R., Stevens, M. F. and Stoppacciaro, A. (2008) 'G-quadruplex ligand RHPS4 potentiates the antitumor activity of camptothecins in preclinical models of solid tumors', *Clinical Cancer Research,* 14, (22), pp. 7284-7291.

Levis, R. W., Ganesan, R., Houtchens, K., Tolar, L. A. and Sheen, F. (1993) 'Transposons in place of telomeric repeats at a Drosophila telomere', *Cell,* 75, (6), pp. 1083-1093.

Levy, D. L. and Blackburn, E. H. (2004) 'Counting of Rif1p and Rif2p on Saccharomyces cerevisiae telomeres regulates telomere length', *Molecular and Cellular Biology,* 24, (24), pp. 10857-10867.

Li, B. and De Lange, T. (2003) 'Rap1 affects the length and heterogeneity of human telomeres', *Molecular Biology of the Cell,* 14, (12), pp. 5060-5068.

Li, B., Oestreich, S. and de Lange, T. (2000) 'Identification of Human Rap1: Implications for Telomere Evolution', *Cell,* 101, (5), pp. 471-483.

Li, Q. and Sham, H. L. (2002) 'Discovery and development of antimitotic agents that inhibit tubulin polymerisation for the treatment of cancer', *Expert Opinion on Therapeutic Patents,* 12, (11), pp. 1663-1702.

Li, Y. F. and Shi, F. (2006) 'Partial Rescue of pos5 Mutants by YEF1 and UTR1 Genes in Saccharomyces cerevisiae', *Acta biochimica et biophysica Sinica,* 38, (5), pp. 293-298.

Lin, J. J. and Zakian, V. A. (1996) 'The Saccharomyces CDC13 protein is a single-strand TG1–3 telomeric DNA-binding protein in vitro that affects telomere behavior in vivo', *Proceedings of the National Academy of Sciences,* 93, (24), pp. 13760.

Lingner, J. and Cech, T. R. (1996) 'Purification of telomerase from Euplotes aediculatus: requirement of a primer 3' overhang', *Proceedings of the National Academy of Sciences,* 93, (20), pp. 10712.

Lingner, J., Cech, T. R., Hughes, T. R. and Lundblad, V. (1997a) 'Three Ever Shorter Telomere (EST) genes are dispensable for in vitro yeast telomerase activity', *Proceedings of the National Academy of Sciences,* 94, (21), pp. 11190.

Lingner, J., Hughes, T. R., Shevchenko, A., Mann, M., Lundblad, V. and Cech, T. R. (1997b) 'Reverse transcriptase motifs in the catalytic subunit of telomerase', *Science,* 276, (5312), pp. 561.

Lipmann, F. (1936) 'Fermentation of phosphogluconic acid', *Nature,* 138, pp. 588.

Longtine, M. S., McKenzie Iii, A., Demarini, D. J., Shah, N. G., Wach, A., Brachat, A., Philippsen, P. and Pringle, J. R. (1998) 'Additional modules for versatile and economical PCR-based gene deletion and modification in Saccharomyces cerevisiae', *Yeast,* 14, (10), pp. 953-961.

Louis, E. J. and Haber, J. E. (1991) 'Evolutionarily recent transfer of a group I mitochondrial intron to telomere regions in Saccharomyces cerevisiae', *Current genetics,* 20, (5), pp. 411-415.

Lundblad, V. and Szostak, J. W. (1989) 'A mutant with a defect in telomere elongation leads to senescence in yeast', *Cell,* 57, (4), pp. 633-643.

Luzzatto, L. (1967) 'Regulation of the activity of glucose-6-phosphate dehydrogenase by NADP+ and NADPH', *Biochimica et Biophysica Acta (BBA)-Enzymology,* 146, (1), pp. 18-25.

Lydall, D. and Weinert, T. (1995) 'Yeast checkpoint genes in DNA damage processing: implications for repair and arrest', *Science,* 270, (5241), pp. 1488-1491.

Ma, J. L., Lee, S. J., Duong, J. K. and Stern, D. F. (2006) 'Activation of the checkpoint kinase Rad53 by the phosphatidyl inositol kinase-like kinase Mec1', *Journal of Biological Chemistry,* 281, (7), pp. 3954-3963.

Mages, G. J., Feldmann, H. M. and Winnacker, E. L. (1996) 'Involvement of the Saccharomyces cerevisiae HDF1 gene in DNA double-strand break repair and recombination', *Journal of Biological Chemistry,* 271, (14), pp. 7910.

Majka, J., Binz, S. K., Wold, M. S. and Burgers, P. M. J. (2006) 'Replication protein A directs loading of the DNA damage checkpoint clamp to 5â€²-DNA junctions', *Journal of Biological Chemistry,* 281, (38), pp. 27855.

Makarov, V. L., Hirose, Y. and Langmore, J. P. (1997) 'Long G tails at both ends of human chromosomes suggest a C strand degradation mechanism for telomere shortening', *Cell,* 88, (5), pp. 657-666.

Marcand, S., Gilson, E. and Shore, D. (1997) 'A protein-counting mechanism for telomere length regulation in yeast', *Science,* 275, (5302), pp. 986-990.

Marcand, S., Pardo, B., Gratias, A., Cahun, S. and Callebaut, I. (2008) 'Multiple pathways inhibit NHEJ at telomeres', *Genes & Development,* 22, (9), pp. 1153-1158.

Maringele, L. and Lydall, D. (2002) 'EXO1-dependent single-stranded DNA at telomeres activates subsets of DNA damage and spindle checkpoint pathways in budding yeast yku70 mutants', *Genes & Development,* 16, (15), pp. 1919.

Martin, S. G., Laroche, T., Suka, N., Grunstein, M. and Gasser, S. M. (1999) 'Relocalization of telomeric Ku and SIR proteins in response to DNA strand breaks in yeast', *Cell,* 97, pp. 621-634.

McElligott, R. and Wellinger, R. J. (1997) 'The terminal DNA structure of mammalian chromosomes', *The EMBO Journal,* 16, (12), pp. 3705-3714.

Meyne, J., Ratliff, R. L. and Moyzis, R. K. (1989) 'Conservation of the human telomere sequence (TTAGGG)n among vertebrates', *Proceedings of the National Academy of Sciences,* 86, (18), pp. 7049.

Miclet, E., Stoven, V., Michels, P. A. M., Opperdoes, F. R., Lallemand, J. Y. and Duffieux, F. (2001) 'NMR spectroscopic analysis of the first two steps of the pentose-phosphate pathway elucidates the role of 6-phosphogluconolactonase', *Journal of Biological Chemistry,* 276, (37), pp. 34840-34846.

Mikami-Terao, Y., Akiyama, M., Yuza, Y., Yanagisawa, T., Yamada, O., Kawano, T., Agawa, M., Ida, H. and Yamada, H. (2009) 'Antitumor activity of TMPyP4 interacting G-quadruplex in retinoblastoma cell lines', *Experimental Eye Research,* 89, (2), pp. 200-8.

Mikami-Terao, Y., Akiyama, M., Yuza, Y., Yanagisawa, T., Yamada, O. and Yamada, H. (2008) 'Antitumor activity of G-quadruplex-interactive agent TMPyP4 in K562 leukemic cells', *Cancer Letters,* 261, (2), pp. 226-34.

Milne, G. T., Jin, S., Shannon, K. B. and Weaver, D. T. (1996) 'Mutations in two Ku homologs define a DNA end-joining repair pathway in Saccharomyces cerevisiae', *Molecular and Cellular Biology,* 16, (8), pp. 4189.

Moore, M. J. B., Schultes, C. M., Cuesta, J., Cuenca, F., Gunaratnam, M., Tanious, F. A., Wilson, W. D. and Neidle, S. (2006) 'Trisubstituted acridines as G-quadruplex telomere targeting agents. Effects of extensions of the 3, 6-and 9-side chains on quadruplex binding, telomerase activity, and cell proliferation', *Journal of Medicinal Chemistry,* 49, (2), pp. 582-599.

Morin, I., Ngo, H. P., Greenall, A., Zubko, M. K., Morrice, N. and Lydall, D. (2008) 'Checkpoint-dependent phosphorylation of Exo1 modulates the DNA damage response', *The EMBO Journal,* 27, (18), pp. 2400.

Moye-Rowley, W. S. (2002) 'Transcription factors regulating the response to oxidative stress in yeast', *Antioxidants & Redox Signaling,* 4, (1), pp. 123-140.

Moyzis, R. K., Buckingham, J. M., Cram, L. S., Dani, M., Deaven, L. L., Jones, M. D., Meyne, J., Ratliff, R. L. and Wu, J. R. (1988) 'A highly conserved repetitive DNA sequence, (TTAGGG)n, present at the telomeres of human chromosomes', *Proceedings of the National Academy of Sciences,* 85, (18), pp. 6622.

Muñoz-Jordán, J. L., Cross, G. A. M., de Lange, T. and Griffith, J. D. (2001) 'T-loops at trypanosome telomeres', *The EMBO Journal,* 20, (3), pp. 579.

Nakamura, T. M., Morin, G. B., Chapman, K. B., Weinrich, S. L., Andrews, W. H., Lingner, J., Harley, C. B. and Cech, T. R. (1997) 'Telomerase catalytic subunit homologs from fission yeast and human', *Science,* 277, (5328), pp. 955.

Neidle, S. and Balasubramanian, S. (2007) 'DNA Quadruplex-Ligand Recognition: Structure and Dynamics', in *Quadruplex Nucleic Acids.* RSC Biomolecular Sciences.

Neidle, S. and Parkinson, G. N. (2008) 'Quadruplex DNA crystal structures and drug design', *Biochimie,* 90, (8), pp. 1184-1196.

Neidle, S. and Read, M. A. (2000) 'G-quadruplexes as therapeutic targets', *Biopolymers,* 56, (3), pp. 195-208.

Niebuhr, E. (1978) 'The cri du chat syndrome', *Human Genetics,* 44, (3), pp. 227-275.

Nkhoma, E. T., Poole, C., Vannappagari, V., Hall, S. A. and Beutler, E. (2009) 'The global prevalence of glucose-6-phosphate dehydrogenase deficiency: a systematic review and meta-analysis', *Blood Cells, Molecules, and Diseases,* 42, (3), pp. 267-278.

Nugent, C. I., Bosco, G., Ross, L. O., Evans, S. K., Salinger, A. P., Moore, J. K., Haber, J. E. and Lundblad, V. (1998) 'Telomere maintenance is dependent on activities required for end repair of double-strand breaks', *Current Biology,* 8, (11), pp. 657-662.

Nugent, C. I., Hughes, T. R., Lue, N. F. and Lundblad, V. (1996) 'Cdc13p: a single-strand telomeric DNA-binding protein with a dual role in yeast telomere maintenance', *Science,* 274, (5285), pp. 249.

Olovnikov, A. M. (1971) 'Principle of marginotomy in template synthesis of polynucleotides', *Doklady Akademii Nauk SSSR,* 201, (6), pp. 1496.

Olovnikov, A. M. (1973) 'A theory of marginotomy. The incomplete copying of template margin in enzymic synthesis of polynucleotides and biological significance of the phenomenon', *Journal of Theoretical Biology,* 41, (1), pp. 181-190.

Paeschke, K., Simonsson, T., Postberg, J., Rhodes, D. and Lipps, H. J. (2005) 'Telomere end-binding proteins control the formation of G-quadruplex DNA structures in vivo', *Nature Structural & Molecular Biology,* 12, (10), pp. 847-854.

Palm, W. and de Lange, T. (2008) 'How shelterin protects mammalian telomeres', *Annual Review of Genetics,* 42, pp. 301-334.

Palmer, A. M. (1999) 'The activity of the pentose phosphate pathway is increased in response to oxidative stress in Alzheimer's disease', *Journal of Neural Transmission,* 106, (3), pp. 317-328.

Panozzo, C., Nawara, M., Suski, C., Kucharczyka, R., Skoneczny, M., Bécam, A. M., Rytka, J. and Herbert, C. J. (2002) 'Aerobic and anaerobic NAD+ metabolism in Saccharomyces cerevisiae', *FEBS Letters,* 517, (1-3), pp. 97-102.

Park, Y. C., Choi, J. H., Bennett, G. N. and Seo, J. H. (2006) 'Characterization of d-ribose biosynthesis in Bacillus subtilis JY200 deficient in transketolase gene', *Journal of biotechnology,* 121, (4), pp. 508-516.

Parkinson, H., Kapushesky, M., Shojatalab, M., Abeygunawardena, N., Coulson, R., Farne, A., Holloway, E., Kolesnykov, N., Lilja, P. and Lukk, M. (2007) 'ArrayExpress--a public database of microarray experiments and gene expression profiles', *Nucleic acids research,* 35, (Database issue), pp. D747.

Perl, A., Qian, Y., Chohan, K. R., Shirley, C. R., Amidon, W., Banerjee, S., Middleton, F. A., Conkrite, K. L., Barcza, M. and Gonchoroff, N. (2006) 'Transaldolase is essential for maintenance of the mitochondrial transmembrane potential and fertility of spermatozoa', *Proceedings of the National Academy of Sciences,* 103, (40), pp. 14813-14818.

Petreaca, R. C., Chiu, H. C., Eckelhoefer, H. A., Chuang, C., Xu, L. and Nugent, C. I. (2006) 'Chromosome end protection plasticity revealed by Stn1p and Ten1p bypass of Cdc13p', *Nature Cell Biology,* 8, (7), pp. 748-755.

Petreaca, R. C., Chiu, H. C. and Nugent, C. I. (2007) 'The role of Stn1p in Saccharomyces cerevisiae telomere capping can be separated from its interaction with Cdc13p', *Genetics,* 177, (3), pp. 1459.

Phan, A. T., Kuryavyi, V., Gaw, H. Y. and Patel, D. J. (2005) 'Small-molecule interaction with a five-guanine-tract G-quadruplex structure from the human MYC promoter', *Nature Chemical Biology,* 1, (3), pp. 167-173.

Phatak, P., Cookson, J. C., Dai, F., Smith, V., Gartenhaus, R. B., Stevens, M. F. G. and Burger, A. M. (2007) 'Telomere uncapping by the G-quadruplex ligand RHPS4 inhibits clonogenic tumour cell growth in vitro and in vivo consistent with a cancer stem cell targeting mechanism', *British Journal of Cancer,* 96, (8), pp. 1223-1233.

Qi, H. and Zakian, V. A. (2000) 'The Saccharomyces telomere-binding protein Cdc13p interacts with both the catalytic subunit of DNA polymerase and the telomerase-associated Est1 protein', *Genes & Development,* 14, (14), pp. 1777.

Rainer, J., Sanchez-Cabo, F., Stocker, G., Sturn, A. and Trajanoski, Z. (2006) 'CARMAweb: comprehensive R-and bioconductor-based web service for microarray data analysis', *Nucleic Acids Research,* 34, (Web Server issue), pp. W498.

Raïs, B., Comin, B., Puigjaner, J., Brandes, J. L., Creppy, E., Saboureau, D., Ennamany, R., Paul Lee, W. N., Boros, L. G. and Cascante, M. (1999) 'Oxythiamine and dehydroepiandrosterone induce a G1 phase cycle arrest in Ehrlich's tumor cells through inhibition of the pentose cycle', *FEBS Letters,* 456, (1), pp. 113-118.

Ralser, M., Heeren, G., Breitenbach, M., Lehrach, H. and Krobitsch, S. (2006) 'Triose phosphate isomerase deficiency is caused by altered dimerization--not catalytic inactivity--of the mutant enzymes', *PLoS One,* 1, pp. e30.

Ralser, M., Wamelink, M. M., Kowald, A., Gerisch, B., Heeren, G., Struys, E. A., Klipp, E., Jakobs, C., Breitenbach, M., Lehrach, H. and Krobitsch, S. (2007) 'Dynamic rerouting of the carbohydrate flux is key to counteracting oxidative stress', *Journal of Biology,* 6, (4), pp. 10.

Read, M., Harrison, R. J., Romagnoli, B., Tanious, F. A., Gowan, S. H., Reszka, A. P., Wilson, W. D., Kelland, L. R. and Neidle, S. (2001) 'Structure-based design of

selective and potent G quadruplex-mediated telomerase inhibitors', *Proceedings of the National Academy of Sciences,* 98, (9), pp. 4844.

Read, M. A., Wood, A. A., Harrison, J. R., Gowan, S. M., Kelland, L. R., Dosanjh, H. S. and Neidle, S. (1999) 'Molecular modeling studies on G-quadruplex complexes of telomerase inhibitors: structure-activity relationships', *Journal of Medicinal Chemistry,* 42, (22), pp. 4538-4546.

Reichard, P. (1988) 'Interactions between deoxyribonucleotide and DNA synthesis', *Annual Review of Biochemistry,* 57, (1), pp. 349-374.

Reichenbach, P., Höss, M., Azzalin, C. M., Nabholz, M., Bucher, P. and Lingner, J. (2003) 'A human homolog of yeast Est1 associates with telomerase and uncaps chromosome ends when overexpressed', *Current Biology,* 13, (7), pp. 568-574.

Ren, J. and Chaires, J. B. (1999) 'Sequence and structural selectivity of nucleic acid binding ligands', *Biochemistry,* 38, (49), pp. 16067-16075.

Richter, T. and Zglinicki, T. (2007) 'A continuous correlation between oxidative stress and telomere shortening in fibroblasts', *Experimental Gerontology,* 42, (11), pp. 1039-1042.

Salvati, E., Leonetti, C., Rizzo, A., Scarsella, M., Mottolese, M., Galati, R., Sperduti, I., Stevens, M. F. G., D Incalci, M. and Blasco, M. (2007) 'Telomere damage induced by the G-quadruplex ligand RHPS4 has an antitumor effect', *Journal of Clinical Investigation,* 117, (11), pp. 3236.

Samland, A. K. and Sprenger, G. A. (2009) 'Transaldolase: from biochemistry to human disease', *The International Journal of Biochemistry & Cell Biology,* 41, (7), pp. 1482-1494.

Sanchez, Y., Bachant, J., Wang, H., Hu, F., Liu, D., Tetzlaff, M. and Elledge, S. J. (1999) 'Control of the DNA damage checkpoint by chk1 and rad53 protein kinases through distinct mechanisms', *Science,* 286, (5442), pp. 1166-1171.

Schaaff-Gerstenschläger, I., Mannhaupt, G., Vetter, I., Zimmermann, F. K. and Feldmann, H. (1993) 'TKL2, a second transketolase gene of Saccharomyces cerevisiae', *European Journal of Biochemistry,* 217, (1), pp. 487-492.

Schaffitzel, C., Berger, I., Postberg, J., Hanes, J., Lipps, H. J. and Plückthun, A. (2001) 'In vitro generated antibodies specific for telomeric guanine-quadruplex DNA react with Stylonychia lemnae macronuclei', *Proceedings of the National Academy of Sciences,* 98, (15), pp. 8572.

Schultes, C. M., Guyen, B., Cuesta, J. and Neidle, S. (2004) 'Synthesis, biophysical and biological evaluation of 3, 6-bis-amidoacridines with extended 9-anilino substituents as potent G-quadruplex-binding telomerase inhibitors', *Bioorganic & medicinal chemistry letters,* 14, (16), pp. 4347-4351.

Seenisamy, J., Rezler, E. M., Powell, T. J., Tye, D., Gokhale, V., Joshi, C. S., Siddiqui-Jain, A. and Hurley, L. H. (2004) 'The dynamic character of the G-quadruplex element in the c-MYC promoter and modification by TMPyP4', *Journal of the American Chemical Society,* 126, (28), pp. 8702-8709.

Sen, D. and Gilbert, W. (1988) 'Formation of parallel four-stranded complexes by guanine-rich motifs in DNA and its implications for meiosis', *Nature,* 334, pp. 364-366.

SGD (2011) *Saccharomyces Genome Database*. Available at: http://pathway.yeastgenome.org/YEAST/NEW-IMAGE?type=PATHWAY&object=PENTOSE-P-PWY&detail-level=2 (Accessed: April 2012).

Shay, J. W., Pereira-Smith, O. M. and Wright, W. E. (1991) 'A role for both RB and p53 in the regulation of human cellular senescence', *Experimental Cell Research,* 196, (1), pp. 33-39.

Shay, J. W. and Wright, W. E. (2005) 'Senescence and immortalization: role of telomeres and telomerase', *Carcinogenesis,* 26, (5), pp. 867-874.

Shay, J. W. and Wright, W. E. (2006) 'Telomerase therapeutics for cancer: challenges and new directions', *Nature Reviews Drug Discovery,* 5, (7), pp. 577-584.

Siddiqui-Jain, A., Grand, C. L., Bearss, D. J. and Hurley, L. H. (2002) 'Direct evidence for a G-quadruplex in a promoter region and its targeting with a small molecule to repress c-MYC transcription', *Proceedings of the National Academy of Sciences,* 99, (18), pp. 11593.

Siegers, K., Waldmann, T., Leroux, M. R., Grein, K., Shevchenko, A., Schiebel, E. and Hartl, F. U. (1999) 'Compartmentation of protein folding in vivo: sequestration of non-native polypeptide by the chaperonin-GimC system', *The EMBO Journal,* 18, (1), pp. 75-84.

Singer, M. S. and Gottschling, D. E. (1994) 'TLC1: template RNA component of Saccharomyces cerevisiae telomerase', *Science,* 266, (5184), pp. 404.

Sinha, H., David, L., Pascon, R. C., Clauder-Münster, S., Krishnakumar, S., Nguyen, M., Shi, G., Dean, J., Davis, R. W. and Oefner, P. J. (2008) 'Sequential elimination of major-effect contributors identifies additional quantitative trait loci conditioning high-temperature growth in yeast', *Genetics,* 180, (3), pp. 1661-1670.

Sjöberg, B. (1997) 'Ribonucleotide reductases - a group of enzymes with different metallosites and a similar reaction mechanism', *Metal Sites in Proteins and Models*, pp. 139-173.

Slekar, K. H., Kosman, D. J. and Culotta, V. C. (1996) 'The yeast copper/zinc superoxide dismutase and the pentose phosphate pathway play overlapping roles in oxidative stress protection', *Journal of Biological Chemistry,* 271, (46), pp. 28831-28836.

Smith, G. and Jackson, S. P. (1999) 'The DNA-dependent protein kinase', *Genes & Development,* 13, (8), pp. 916.

Smith, J. S., Chen, Q., Yatsunyk, L. A., Nicoludis, J. M., Garcia, M. S., Kranaster, R., Balasubramanian, S., Monchaud, D., Teulade-Fichou, M. P., Abramowitz, L., Schultz, D. C. and Johnson, F. B. (2011) 'Rudimentary G-quadruplex-based telomere capping in Saccharomyces cerevisiae', *Nature Structural & Molecular Biology,* 18, (4), pp. 478-485.

Smogorzewska, A. and de Lange, T. (2004) 'Regulation of telomerase by telomeric proteins', *Annual Review of Biochemistry,* 73, (1), pp. 177-208.

Snow, B. E., Erdmann, N., Cruickshank, J., Goldman, H., Gill, R. M., Robinson, M. O. and Harrington, L. (2003) 'Functional conservation of the telomerase protein Est1p in humans', *Current Biology,* 13, (8), pp. 698-704.

Stearns, T., Hoyt, M. A. and Botstein, D. (1990) 'Yeast mutants sensitive to antimicrotubule drugs define three genes that affect microtubule function', *Genetics,* 124, (2), pp. 251-262.

Stellwagen, A. E., Haimberger, Z. W., Veatch, J. R. and Gottschling, D. E. (2003) 'Ku interacts with telomerase RNA to promote telomere addition at native and broken chromosome ends', *Genes & Development,* 17, (19), pp. 2384.

Sun, D., Guo, K., Rusche, J. J. and Hurley, L. H. (2005) 'Facilitation of a structural transition in the polypurine/polypyrimidine tract within the proximal promoter region of the human VEGF gene by the presence of potassium and G-quadruplex-interactive agents', *Nucleic Acids Research,* 33, (18), pp. 6070-6080.

Sun, D., Thompson, B., Cathers, B. E., Salazar, M., Kerwin, S. M., Trent, J. O., Jenkins, T. C., Neidle, S. and Hurley, L. H. (1997) 'Inhibition of human telomerase by a G-quadruplex-interactive compound', *Journal of Medicinal Chemistry,* 40, (14), pp. 2113-2116.

Sun, H., Bennett, R. J. and Maizels, N. (1999) 'The Saccharomyces cerevisiae Sgs1 helicase efficiently unwinds GG paired DNAs', *Nucleic Acids Research,* 27, (9), pp. 1978-1984.

Sun, H., Karow, J. K., Hickson, I. D. and Maizels, N. (1998) 'The Bloom's syndrome helicase unwinds G4 DNA', *Journal of Biological Chemistry,* 273, (42), pp. 27587-27592.

Sundquist, W. I. and Klug, A. (1989) 'Telomeric DNA dimerizes by formation of guanine tetrads between hairpin loops', *Nature,* 342, pp. 825 - 829.

Sweeney, F. D., Yang, F., Chi, A., Shabanowitz, J., Hunt, D. F. and Durocher, D. (2005) 'Saccharomyces cerevisiae Rad9 acts as a Mec1 adaptor to allow Rad53 activation', *Current Biology,* 15, (15), pp. 1364-1375.

Szostak, J. W. and Blackburn, E. H. (1982) 'Cloning yeast telomeres on linear plasmid vectors', *Cell,* 29, (1), pp. 245-255.

Szostak, J. W., Orr-Weaver, T. L., Rothstein, R. J. and Stahl, F. W. (1983) 'The double-strand-break repair model for recombination', *Cell,* 33, (1), pp. 25-35.

Teo, S. H. and Jackson, S. P. (2001) 'Telomerase subunit overexpression suppresses telomere-specific checkpoint activation in the yeast yku80 mutant', *EMBO reports,* 2, (3), pp. 197-202.

Theobald, D. L. and Wuttke, D. S. (2004) 'Prediction of multiple tandem OB-fold domains in telomere end-binding proteins Pot1 and Cdc13', *Structure,* 12, (10), pp. 1877-1879.

Tomlinson, J. E., Nakayama, R. and Holten, D. (1988) 'Repression of pentose phosphate pathway dehydrogenase synthesis and mRNA by dietary fat in rats', *The Journal of Nutrition,* 118, (3), pp. 408-415.

Tong, A. H. Y. and Boone, C. (2005) 'Synthetic genetic array analysis in Saccharomyces cerevisiae', *Methods in Molecular Biology,* 313, pp. 171.

Tsolou, A. and Lydall, D. (2007) 'Mrc1 protects uncapped budding yeast telomeres from exonuclease EXO1', *DNA repair,* 6, (11), pp. 1607-1617.

Tsukamoto, Y., Taggart, A. K. P. and Zakian, V. A. (2001) 'The role of the Mre11-Rad50-Xrs2 complex in telomerase-mediated lengthening of Saccharomyces cerevisiae telomeres', *Current Biology,* 11, (17), pp. 1328-1335.

Tu, B. P., Kudlicki, A., Rowicka, M. and McKnight, S. L. (2005) 'Logic of the yeast metabolic cycle: temporal compartmentalization of cellular processes', *Science,* 310, (5751), pp. 1152-1158.

Tu, B. P., Mohler, R. E., Liu, J. C., Dombek, K. M., Young, E. T., Synovec, R. E. and McKnight, S. L. (2007) 'Cyclic changes in metabolic state during the life of a yeast cell', *Proceedings of the National Academy of Sciences,* 104, (43), pp. 16886.

Tucker, C. L. and Fields, S. (2004) 'Quantitative genome-wide analysis of yeast deletion strain sensitivities to oxidative and chemical stress', *Comparative and functional genomics,* 5, (3), pp. 216-224.

Ufer, C., Wang, C. C., Borchert, A., Heydeck, D. and Kuhn, H. (2010) 'Redox control in mammalian embryo development', *Antioxidants & Redox Signaling,* 13, (6), pp. 833-875.

Van der Knaap, M. S., Wevers, R. A., Struys, E. A., Verhoeven, N. M., Pouwels, P. J. W., Engelke, U. F. H., Feikema, W., Valk, J. and Jakobs, C. (1999) 'Leukoencephalopathy associated with a disturbance in the metabolism of polyols', *Annals of Neurology,* 46, (6), pp. 925-928.

Vander Heiden, M. G., Cantley, L. C. and Thompson, C. B. (2009) 'Understanding the Warburg effect: the metabolic requirements of cell proliferation', *Science's STKE,* 324, (5930), pp. 1029.

Vega, L. R., Mateyak, M. K. and Zakian, V. A. (2003) 'Getting to the end: telomerase access in yeast and humans', *Nature Reviews Molecular Cell Biology,* 4, (12), pp. 948-959.

Veltel, S., Gasper, R., Eisenacher, E. and Wittinghofer, A. (2008) 'The retinitis pigmentosa 2 gene product is a GTPase-activating protein for Arf-like 3', *Nature structural & molecular biology,* 15, (4), pp. 373-380.

Venclovas, C. and Thelen, M. P. (2000) 'Structure-based predictions of Rad1, Rad9, Hus1 and Rad17 participation in sliding clamp and clamp-loading complexes', *Nucleic Acids Research,* 28, (13), pp. 2481.

Verdun, R. E. and Karlseder, J. (2007) 'Replication and protection of telomeres', *Nature,* 447, (7147), pp. 924-931.

Verma, A., Halder, K., Halder, R., Yadav, V. K., Rawal, P., Thakur, R. K., Mohd, F., Sharma, A. and Chowdhury, S. (2008) 'Genome-wide computational and expression analyses reveal G-quadruplex DNA motifs as conserved cis-regulatory elements in human and related species', *Journal of Medicinal Chemistry,* 51, (18), pp. 5641-5649.

Vialard, J. E., Gilbert, C. S., Green, C. M. and Lowndes, N. F. (1998) 'The budding yeast Rad9 checkpoint protein is subjected to Mec1/Tel1-dependent hyperphosphorylation and interacts with Rad53 after DNA damage', *The EMBO Journal,* 17, (19), pp. 5679-5688.

von Zglinicki, T. (2002) 'Oxidative stress shortens telomeres', *Trends in Biochemical Sciences,* 27, (7), pp. 339-344.

Wakil, S. J., Stoops, J. K. and Joshi, V. C. (1983) 'Fatty acid synthesis and its regulation', *Annual Review of Biochemistry,* 52, (1), pp. 537-579.

Walmsley, R. W., Chan, C. S. M., Tye, B. K. and Petes, T. D. (1984) 'Unusual DNA sequences associated with the ends of yeast chromosomes', *Nature,* 310, pp. 157 - 160.

Wamelink, M. M. C., Struys, E. A. and Jakobs, C. (2008) 'The biochemistry, metabolism and inherited defects of the pentose phosphate pathway: a review', *Journal of Inherited Metabolic Disease,* 31, (6), pp. 703-717.

Wang, F., Podell, E. R., Zaug, A. J., Yang, Y., Baciu, P., Cech, T. R. and Lei, M. (2007) 'The POT1–TPP1 telomere complex is a telomerase processivity factor', *Nature,* 445, (7127), pp. 506-510.

Wang, H. and Blackburn, E. H. (1997) 'De novo telomere addition by Tetrahymena telomerase in vitro', *The EMBO Journal,* 16, (4), pp. 866-879.

Wang, Y. and Patel, D. J. (1993) 'Solution structure of a parallel-stranded G-quadruplex DNA', *Journal of molecular biology,* 234, (4), pp. 1171-1183.

Wang, Y. and Patel, D. J. (1994) 'Solution structure of the Tetrahymena telomeric repeat d(T2G4)4 G-tetraplex', *Structure,* 2, (12), pp. 1141-1156.

Wang, Y. and Patel, D. J. (1995) 'Solution Structure of the OxytrichaTelomeric Repeat d[G4(T4G4)3] G-tetraplex', *Journal of molecular biology,* 251, (1), pp. 76-94.

Warburg, O. and Christian, W. (1937) 'Abbau von Robisonester durch Triphospho-Pyridin-Nucleotid', *Biochem. Z,* 292, pp. 287.

Warburg, O., Christian, W. and Griese, A. (1935) 'Wasserstoffübertragendes Co-Ferment, seine Zusammensetzung und Wirkungsweise', *Biochem. Z,* 282, pp. 157-205.

Watson, J. D. (1972) 'Origin of concatemeric T7 DNA', *Nature New Biology,* 239, (94), pp. 197-201.

Wei, C., Jia, G., Yuan, J., Feng, Z. and Li, C. (2006) 'A spectroscopic study on the interactions of porphyrin with G-quadruplex DNAs', *Biochemistry,* 45, (21), pp. 6681-6691.

Wellinger, R. J., Wolf, A. J. and Zakian, V. A. (1993) 'Saccharomyces telomeres acquire single-strand TG1-3 tails late in S phase', *Cell,* 72, (1), pp. 51-60.

Williamson, J. R., Raghuraman, M. K. and Cech, T. R. (1989) 'Monovalent cation-induced structure of telomeric DNA: the G-quartet model', *Cell,* 59, (5), pp. 871-80.

Wong, H. M., Stegle, O., Rodgers, S. and Huppert, J. L. (2010a) *Quadruplex.org*. Available at: http://www.quadruplex.org/?view=quadbaseDownload (Accessed: April 2012).

Wong, H. M., Stegle, O., Rodgers, S. and Huppert, J. L. (2010b) 'A toolbox for predicting G-quadruplex formation and stability', *Journal of Nucleic Acids*.

Wright, W. E., Piatyszek, M. A., Rainey, W. E., Byrd, W. and Shay, J. W. (1996) 'Telomerase activity in human germline and embryonic tissues and cells', *Developmental genetics,* 18, (2), pp. 173-179.

Wright, W. E. and Shay, J. W. (1992) 'The two-stage mechanism controlling cellular senescence and immortalization', *Experimental Gerontology,* 27, (4), pp. 383.

Yang, Q., Xiang, J., Yang, S., Zhou, Q., Li, Q., Tang, Y. and Xu, G. (2009) 'Verification of specific G-quadruplex structure by using a novel cyanine dye supramolecular assembly: I. Recognizing mixed G-quadruplex in human telomeres', *Chemical Communications*, (9), pp. 1103-1105.

Yao, R., Zhang, Z., An, X., Bucci, B., Perlstein, D. L., Stubbe, J. A. and Huang, M. (2003) 'Subcellular localization of yeast ribonucleotide reductase regulated by the DNA replication and damage checkpoint pathways', *Proceedings of the National Academy of Sciences,* 100, (11), pp. 6628.

Zahler, A. M., Williamson, J. R., Cech, T. R. and Prescott, D. M. (1991) 'Inhibition of telomerase by G-quartet DNA structures', *Nature,* 350, (6320), pp. 718-20.

Zaug, A. J., Podell, E. R. and Cech, T. R. (2005) 'Human POT1 disrupts telomeric G-quadruplexes allowing telomerase extension in vitro', *Proceedings of the National Academy of Sciences,* 102, (31), pp. 10864.

Zhang, A., Zheng, C., Hou, M., Lindvall, C., Li, K. J., Erlandsson, F., Björkholm, M., Gruber, A., Blennow, E. and Xu, D. (2003) 'Deletion of the telomerase reverse transcriptase gene and haploinsufficiency of telomere maintenance in Cri du chat syndrome', *The American Journal of Human Genetics,* 72, (4), pp. 940-948.

Zhang, W. and Durocher, D. (2010) 'De novo telomere formation is suppressed by the Mec1-dependent inhibition of Cdc13 accumulation at DNA breaks', *Genes & Development,* 24, (5), pp. 502.

Zhao, X., Georgieva, B., Chabes, A., Domkin, V., Ippel, J. H., Schleucher, J., Wijmenga, S., Thelander, L. and Rothstein, R. (2000) 'Mutational and Structural Analyses of the Ribonucleotide Reductase Inhibitor Sml1 Define Its Rnr1 Interaction Domain Whose Inactivation Allows Suppression of mec1 andrad53 Lethality', *Molecular and Cellular Biology,* 20, (23), pp. 9076-9083.

Zhao, X., Muller, E. G. D. and Rothstein, R. (1998) 'A suppressor of two essential checkpoint genes identifies a novel protein that negatively affects dNTP pools', *Molecular Cell,* 2, (3), pp. 329-340.

Zhao, X. and Rothstein, R. (2002) 'The Dun1 checkpoint kinase phosphorylates and regulates the ribonucleotide reductase inhibitor Sml1', *Proceedings of the National Academy of Sciences,* 99, (6), pp. 3746.

Zhou, Z. and Elledge, S. J. (1993) 'DUN1 encodes a protein kinase that controls the DNA damage response in yeast', *Cell,* 75, (6), pp. 1119-1127.

Zou, L. and Elledge, S. J. (2003) 'Sensing DNA damage through ATRIP recognition of RPA-ssDNA complexes', *Science's STKE,* 300, (5625), pp. 1542.

Zubko, M. K., Guillard, S. and Lydall, D. (2004) 'Exo1 and Rad24 differentially regulate generation of ssDNA at telomeres of Saccharomyces cerevisiae cdc13-1 mutants', *Genetics,* 168, (1), pp. 103.

Zubko, M. K., Maringele, L., Foster, S. S. and Lydall, D. (2006) 'Detecting repair intermediates in vivo: effects of DNA damage response genes on single-stranded

DNA accumulation at uncapped telomeres in budding yeast', *Methods in Enzymology,* 409, pp. 285.